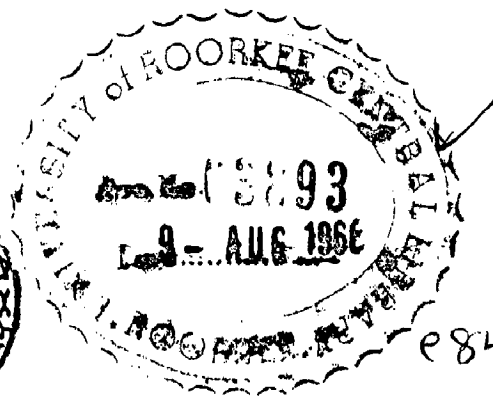


INVESTIGATION OF THE EFFECT OF ROTOR BAR SKEW ON THE PERFORMANCE OF AN INDUCTION MOTOR

By
OM PRAKASH GARG

A Dissertation
submitted in partial fulfilment
of the requirements for the Degree
of
MASTER OF ENGINEERING
in
ADVANCED ELECTRICAL MACHINES



DEPARTMENT OF ELECTRICAL ENGINEERING
UNIVERSITY OF ROORKEE
ROORKEE
1966




CERTIFICATE

CERTIFIED that the dissertation entitled "Investigation of the Effect of Rotor Bar Skew on the Performance of an Induction Motor" which is being submitted by Shri O.P.Garg in partial fulfilment for the award of the Degree of Master of Engineering in 'Advanced Electrical Machines' of the University of Roorkee is a record of student's own work carried out by him under my supervision and guidance. The matter embodied in this dissertation has not been submitted for the award of any other Degree or Diploma.

This is further to certify that he has worked for a period of 5-months from November 1965 to March 1966 for preparing this dissertation for Master of Engineering Degree at University of Roorkee, Roorkee.

Roorkee
Dated 5.4.1966.


(J.L.Jothi)
Reader,
Electrical Engineering
Department,
University of Roorkee,
Roorkee (U.P)

ACKNOWLEDGEMENTS

The author wishes to acknowledge his profound sense of gratitude to Shri J. L. Jethi, Reader in Electrical Engineering, University of Roorkee, for his expert guidance and continued encouragement without which it would have been impossible for the author to bring the work to this stage. He has been very kind in devoting much of his valuable time in helping at every stage of the work and in giving valuable suggestions in the experimental work.

The author wishes to thank Prof. C.S. Ghosh, Head of Electrical Engineering Department, University of Roorkee, Roorkee, for various facilities offered in the Department in connection with the work.

The author also thanks his colleague Mr. Shri Hari Aggarwal for rendering his help in computer programming.

Sincere thanks are also due to the members of the Laboratory Staff of the Electrical Engineering Department for their valuable help.

SYNOPSIS

Harmonic effects on skewed Induction machine are analysed by means of digital computer using punched card technique. Analytical methods are developed to ascertain the effect of skew over current, power factor, torque and other undesirable features like dead points, crawling, cogging etc., resulting from wide variety of harmonics of machine . In addition to the conventional space harmonics, permeance harmonics which are likely to produce appreciable effects are also considered.

Attention has also been paid to the influence of space harmonics on noise too.

It is shown here that, the skewing improves the performance and reduces the noise to appreciably very low degree.

I N T R O D U C T I O N

Harmonics have been known to be the source of trouble in electrical machines for many years.

For almost as long as Engineers have been designing induction machines, they have attempted to suppress harmonics to make it trouble free. The interest has given rise to large number of articles on the subject. Most of the significant articles appearing before 1947 are limited to phase belt harmonics only.

A review of the literature of the subject shows, the wide acceptance of the view that slot ripples in the electrical machines are caused by the interaction of rotor permeance harmonics with those set up by non-sinusoidal distribution of stator winding, non-uniformity of air gap and slotted surfaces of stator and rotor. It is shown for that very high slot frequency currents are induced in rotor circuit, but these high frequency currents are not the problem as the magnitude of such currents is not generally appreciable so these can be overlooked easily. The old reasoning of non-integral number of slots being the cause of higher harmonics was based on incomplete understanding and has been ruled out by Carter, Kron⁽²⁵⁾, Hearty⁽¹⁶⁾, Walker⁽¹⁹⁾, supported by mathematical theory.

Attempts have been made by Alger^(17,18), to study the effects of principal harmonics of the air gap field neglecting saturation and saturation harmonics by means of equivalent circuit. The harmonics deteriorate the performance in respect of current, torque, power factor. Not so much so but sometimes, it is impossible to start the

motor due to stand still locking (dead points). Even if the motor starts, it fails to come to speed due to harmonic parasite torque and soon gets heated up due to poor power factor and high currents. Therefore, the problem of reduction or elimination of harmonics have gathered large attention and, one of these suggestions in addition to others frequently advocated for squirrel cage rotor is skewing of rotor bars. The interest in the subject is being revived at present by the need for precision electric machines free from magnetic⁽³²⁾ noise and starting torque trouble etc.

The phenomena of harmonics in 3 phase induction machines can be better understood by Block diagram showing, the relations of harmonic fluxes and voltages. The block diagram (see adjacent page) shows considerable similarity with induction machine free from harmonics when operating, in the balanced steady state. The diagram gives a diagrammatic representation of quantitative equations, where the relationship between the quantities such as flux, emf, current etc., are treated as cause and effect sequence. Quantities which react back to modify earlier quantities are treated as cases of feed back.

The generality of the concepts used here has the important advantage that by a process of physical reasoning, it provides a means of arriving quickly at a qualitative understanding of the machine harmonic phenomena, which arises to predetermine the exact behaviour of the machine. The machine is further assumed to work in unsaturated region.

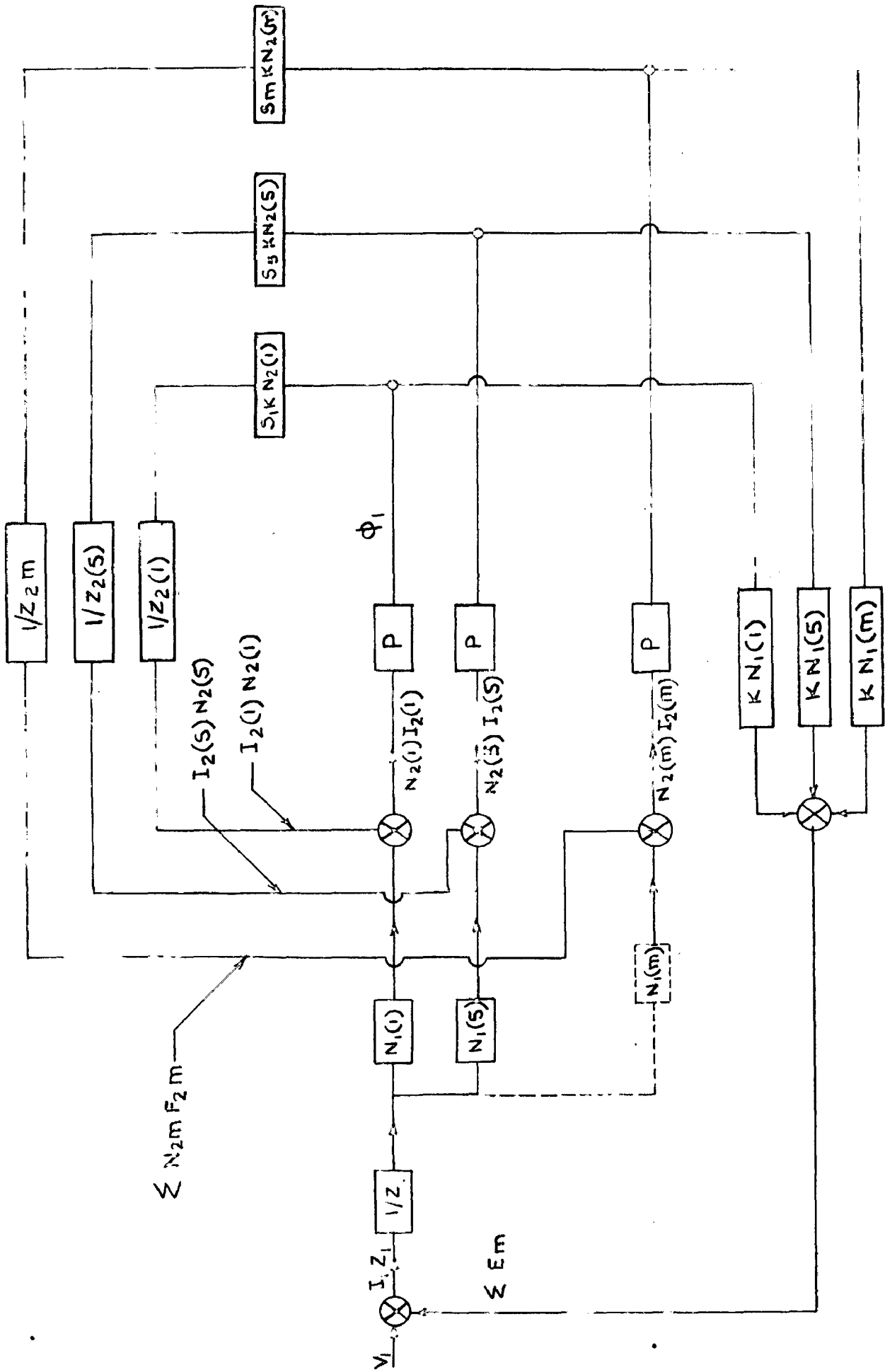
The recent developments in computing techniques over computer have made possible large scale computations pertaining to

machines which otherwise would be out of the question. These techniques make a frontal assault on long standing problems feasible; this work is a report of such an investigation. The basic purpose of this work is to present qualitative as well as quantitative approach to the behavioural complexity of harmonics.

Performance curves for useful torque, parasitic torque due to a number of harmonics, currents, power factor and speed have been computed for full range of the skewed rotor machine. Similar calculations are also performed, neglecting the skew of the rotor. The results so obtained draws attention to the improvements which the skewing can introduce in starting as well as in running conditions.

Noise⁽³⁰⁾ in electrical machines is also equally retrograde effects of space harmonics. All the harmonics produce air gap forces and there by contribute to noise and vibration. The author has attempted to predict the noise level of the machine inspite of the voluminous calculation involved. Noise spectrum and sound intensity curves have been computed.

And lastly, the influence of further skewing of rotor bar over parasitic torque starting torque, etc., is analytically studied and thus criteria for most proper skew angle in general and for the 'test - model' is suggested.



BLOCK DIAGRAM OF HARMONIC FLUXES

C O N T E N T S

	Certificate	1
	Acknowledgements	11
	Synopsis	111
	Introduction	iv
	List of Symbols	ix
CHAPTER I	HARMONIC ANALYSIS OF INDUCTION MACHINE	
	1.1. Space belt harmonics	2
	1.2. Formance Harmonics	3
	1.3. Amplitude of harmonic mfs	13
	1.4. Stator-Rotor Harmonics	19
	1.5. A model of the space harmonics	17
	1.6. Machine winding and their interaction with the general flux density component	17
CHAPTER II	GENERAL EQUIVALENT CIRCUIT FOR SKINNED AND UNSKINNED ROTOR INDUCTION MACHINE AND DETERMINATION OF CIRCUIT CONSTANTS	
	2.1 General Equivalent circuit	20
	2.2 Self Inductance of coil	23
	2.3 Voltage equations	29
	2.4 Analogy with coupled circuits	27
	2.5 Harmonic slip	29
	2.6 Equivalent circuit of formance harmonics	30
	2.7 Determination of circuit constants	31
	2.8 Skin factors for harmonic stator and rotor resistances	37
	2.9 Specifications of test machine and tests	39
	2.10 Calculation of circuit constants of general equivalent circuit with and without skew angle	41
CHAPTER III	COMPUTATION OF ASYNCHRONOUS PARASITIC TORQUE OF INDUCTION MACHINE WITH ROTOR SKINNED AND UNSKINNED.	
	3.1 Production of Asynchronous torque	51
	3.2 Magnitude of Asynchronous torque	53

	3.3 Pull out slip and Pull out torque	55
	3.4 Determination of current slip curve	56
	3.5 Determination of Harmonic Avg. torques	56
CHAPTER IV	SYNCHRONOUS PARASITIC TORQUES AND DEAD POINTS OF SQUIRREL CAGE INDUCTION MACHINE WITH AND WITHOUT ROTOR SKEWED.	
	4.1. Synchronous Crawling torque	60
	4.2. Dead points in T/s curve	69
	4.3. Relation of Parasitic torques with slots	70
	4.4. Calculation of synchronous torques	72
	4.5. Determination of Dead points	73
CHAPTER V	ELECTROMAGNETIC NOISE AND MAGNETIC RADIAL FORCES OF SQUIRREL CAGE POLYPHASE INDUCTION MOTOR	
	5.1 Qualitative Analysis of noise	77
	5.2. Utility of noise measurement	80
	5.3. Sources of noise in motors	83
	5.4. Mathematical Analysis of magnetic noise in Poly phase Induction motor	88
	5.5. Magnitudes of force waves	93
	5.6. Deflection of frame and sound intensity	93
CHAPTER VI	SONANCE CALCULATION OF SQUIRREL CAGE INDUCTION MACHINE WITH AND WITHOUT SKEW.	
	6.1. Procedure	97
	6.2. Calculations	98
	6.3. Natural frequency	100
	6.4. Reduction of parasitic torques and Noise of induction machine with rotor skewing	109
CHAPTER VII	EXPERIMENTAL RESULTS	
	7.1 Measurement of Resistance	115
	7.2. Torque - speed curve	116
	7.3. Recording of current characteristics	116
	CONCLUSIONS	119
	APPENDIX I	121
	APPENDIX II	123
	APPENDIX III	128
	REFERENCES	131

LIST OF SYMBOLS

F, f	Magneto motive force
I, i	Current.
$(A)_i$	mf. constant.
θ	Space angle
m_b, m_f	Forward, backward harmonic (mth)
m	Order of space harmonic
m_p	order of permeance harmonic
m_s	Order of slot harmonic
ω	Radians / sec.
t	Time.
γ	Slot angle
k	number of phase
g_0, l_g	air gap length
B, b	flux density
R	number of rotor slots
S	Number of stator slots
p	Pair of poles
P	Number of Poles
P_s	Stator permeance factor
P_r	Rotor permeance factor
v_1, v_2	Order of permeance wave.
e_s, e_r	Ratio of R.M.S. to average values of stator and Rotor resp.
K	Constant
ϕ	Flux
\mathcal{L}	Flux linkage
c'	Integral number
K_1, K_2	Average Mean Permeance.

Nomenclature

x

s	Slip
T_p	Number of stator turn per phase.
k_{w1}	Primary winding factor
k_{w2}	Secondary winding factor
D	Diameter of stator
D_n	Damping factor for n th harmonic (primary currents)
$G(m)$	Damping factor for m th harmonic (Rotor current)
K_1, K_2	Average mean permeance.
$k /$	Integral constant
\bar{n}, N	Number of turns
X_M	magnetising reactance
X_{l2}, X_2	Secondary leakage reactance referred to primary
X_{l1}, X_1	Primary leakage reactance.
L	Length of Stator Core
y	Distance along y - axis
$\alpha, \sigma, \theta_{sk}$	Skew angle
m_1, m_2	Number of stator and rotor phases
λ_g	Air gap flux linkage
β	Coil span
K_s	Skew factor
μ	Permeability factor
L_{11}, L_{22}	Self inductances
M_{12}, M_{21}	Mutual inductance
\mathcal{E}, E	Induced emf
v, V	Applied voltage
ω_n	Speed of n th harmonic
X_z	Zig Zag leakage reactance

$K_{(m)}$	Skin factor for mth harmonic resistance.
$J_{(m)}$	Reactance, skin factor
CSC	Cosec
n	Order of rotor harmonics
\sqrt{c}	Coil span angle
$P(\theta)$	Permeance
r_1, R_1	Stator resistance per phase
r_2, R_2	Rotor resistance per phase (refer to primary)
X_c	Coil end leakage
X_d	skew leakage flux
K_R	$\frac{\beta}{2 - \beta}$
α_s	Slot angle
h_1, h_2, h_3, h_4	Height of sections of slots.
w_s	Width of slot
w_o	Opening of slot
λ	Slot pitch cms.
C	Constant defined by equation (4.26)
P_d	Power developed (syn watts)
$T_{(m)}$	Torque developed of mth harmonic (Syn Watts).
N_s	Synchronous speed (Syn. r.p.m.)
N_m	Speed of mth harmonic
$s_{MP.o}$	Full out slip (for mth harmonics)
V_{ina}	Speed of nth harmonic
F_m	X_2/X_M
T	POLE pitch
q	Number of phase belts

Part II

p	r.m.s. pressure in dynes /cm ²
d'	Density of air
v	Velocity of sound in air cms/sec.
w	Watts/cm ²
h	Radial depth of the stator core behind the slot in inches.
D_s	Mean diameter of the stator core
W	Load in lbs.
k_{ro}	Correction factor.
F_r, f_r	Radial force lbs.
d	Deflection in micro inch
I_d	Sound intensity (abs)
f	Frequency
p'	Force wave poles
E	Modulus of Elasticity
r	Phase number.

CHAPTER I

HARMONIC ANALYSIS OF INDUCTION MACHINE.

Since induction motors were the first built, it has been noticed that some motors behave erratically, some do not go up to full speed but 'crawl' at a lower speed or are noisy in certain regions and are useless for all commercial application. This behaviour was attributed to the presence of harmonic in the air gap but the conclusions drawn from these analysis were at variance with the observed facts. The slot openings have also been suggested as a possible cause of these irregularities. However, in the analysis of slot openings either one of the surfaces was assumed to be smooth as emphasis is paid only on the change in the fundamental flux due to the presence of slots.

Analysts arrived at some empirical relations for the selection of rotor and stator slots some of which were mathematically supported⁽²⁵⁾ at a latter stage. By using such empirical or semi-empirical rules they were reasonably safe from unpleasant surprises.

The present chapter presents the review of what has been achieved till now in the field of treatment of harmonics of non-salient electrical machines. For our purpose of determining the different types of parasitic torques e.g., synchronous, crawling torques, dead points, vibrating forces and other desirable effects produced by harmonics, we will consider all the possible harmonics of desirable orders and magnitudes likely to effect the normal performance of the machine to an appreciable degree.

Figures written in paranthesis denotes the serial number of references given at the end.

The possible harmonics are:

1. Space Harmonics produced by the non-sinusoidal distribution of the winding known as phase belt harmonics.
2. Space Harmonics due to slotting of stator and rotor surfaces.
3. Permeance Harmonics introduced by the non-uniform air gap of the machine. As these harmonics are produced in collusion of air gap variance harmonics and higher order harmonics of stator and rotor, these harmonics are also function of number of slots of both sides. Generally permeance harmonics are of very low amplitude.
4. And lastly the time harmonics present in the supply wave and which consequently give rise to other higher order of space and time harmonics. But for our purpose we will assume the supply a sinusoidal free from any time harmonics.

1.1. PHASE BELT HARMONICS

1.1.1. Order of Harmonics

It is shown that each distribution of winding may be resolved into space harmonics, beginning with a fundamental and the higher harmonics.

Fig. (1.1) represents the third and fifth harmonics in addition to fundamental of a winding in which number of slots per pole per phase $q = 4$. slot angle $\gamma = 15^\circ$ with no chording.

Taking 0 as reference point, the space distribution of any harmonic mmf due to current i_1 in phase I may be represented by

$$F_1 = (A)_1 \cos(m\theta)$$

where $i_1 = I_m \cos(\omega t)$

$$\therefore F_1 = (A)_1 \cos(\omega t) \cos(m\theta)$$

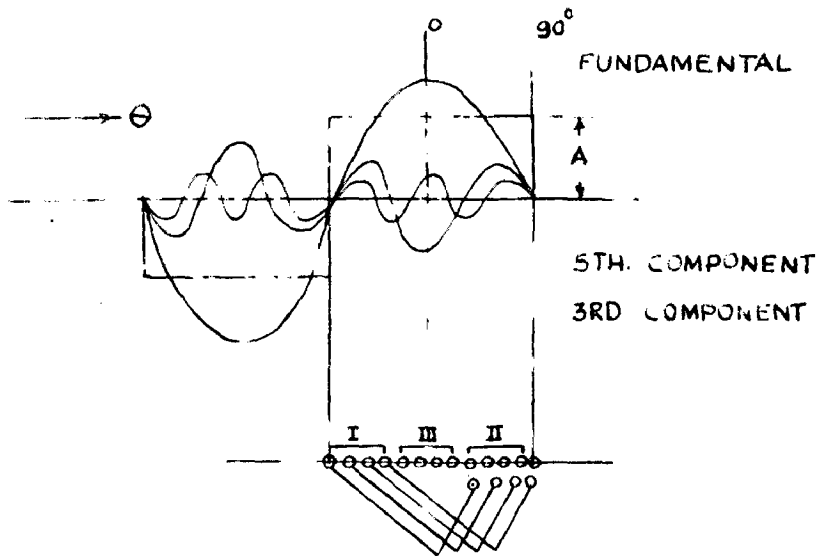


FIGURE 1.1

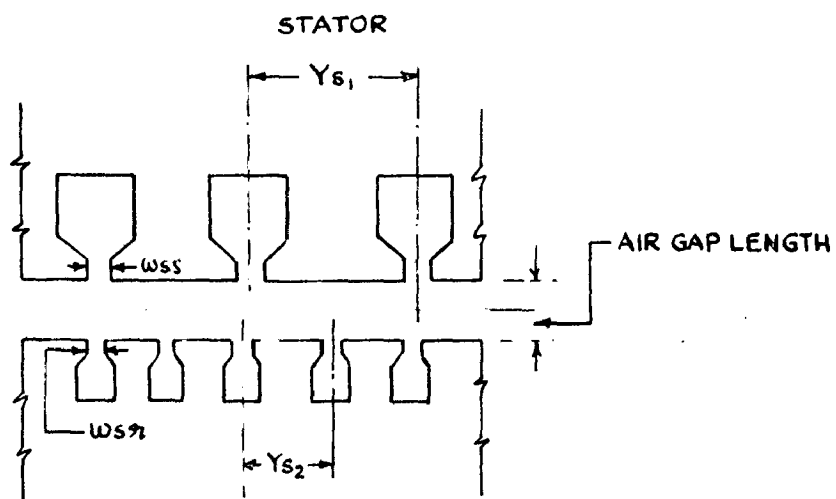


FIGURE 1.2

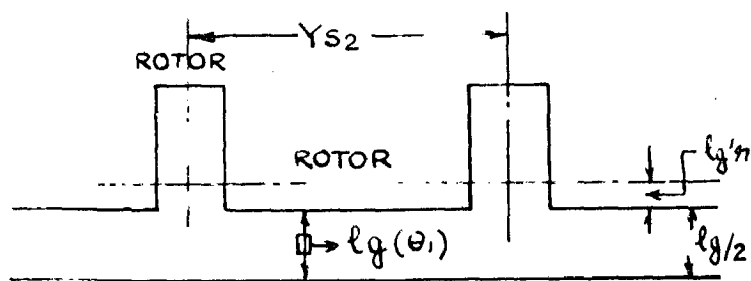


FIGURE 1.3

Similarly

$$f_2 = A_1 \cos \left(m\theta - \frac{2\pi}{k} \right) \cos \left(\omega t + \frac{2\pi}{k} \right)$$

$$f_3 = A_2 \cos \left(m\theta + \frac{2\pi}{k} \right) \cos \left(\omega t - \frac{2\pi}{k} \right)$$

The resultant distribution for mth harmonic is

$$F(m) = A_m \sum_{r=1}^{r=k} \left\{ \cos \left[m\theta + \omega t - (r-1)(m+1) \frac{2\pi}{k} \right] + \cos \left[m\theta + \omega t - (r-1)(m-1) \frac{2\pi}{k} \right] \right\}$$

Summing it up for 'k' phases

$$F = \frac{A_m}{2} \left\{ \frac{\sin(m+1)\pi}{\sin(m+1)\frac{\pi}{k}} \cos \left[m\theta + \omega t - \frac{(k-1)(m+1)\pi}{k} \right] \right\} + \frac{A_m}{2} \left\{ \frac{\sin(m-1)\pi}{\sin(m-1)\frac{\pi}{k}} \cos \left[m\theta - \omega t - \frac{(k-1)(m-1)\pi}{k} \right] \right\} \dots(1-1)$$

Where

m = order of space harmonic due to distributed winding.

k = number of phases

θ = space angle

A_m = Maximum magnitude of mth harmonic

Finding the limiting conditions of the equation (1-1)

$$\frac{\sin(m-1)\pi}{\sin(m-1)\frac{\pi}{k}} = \frac{0}{0} = k \dots\dots(1-2)$$

If (m-1) is multiple of k

Similarly $\frac{\sin(m+1)\pi}{\sin(m+1)\frac{\pi}{k}} = \frac{0}{0} = k \dots\dots(1-3)$

If $(m+1)$ is multiple of k .

1.1.2. Velocity and Direction of rotation of Harmonics.

Differentiating the angular function of cosine terms of equation (1-1)

$$m \frac{d\theta}{dt} = -w \quad \therefore \frac{d\theta}{dt} = -\frac{w}{m} \quad (1-4)$$

$$m \frac{d\theta}{dt} = +w \quad \frac{d\theta}{dt} = \frac{w}{m} \quad (1-5)$$

Therefore the first cosine term of equation (1-1) gives only Backward rotations and second cosine term gives 'forward rotating' harmonics. Tabulating the possible harmonics thus produced in space with $k = 3$ (number of phase) with respective speeds and direction of rotation.

Table (1-1) Speeds and Directions of Rotation of Components of Armature ~~and~~ of 3 Phase windings.

Order of space Harmonics	Speed & Direction.	Order of space Harmonic	Speed & Direction
1	+1	29	$-\frac{1}{29}$
5	$-\frac{1}{5}$	31	$+\frac{1}{31}$
7	$+\frac{1}{7}$	35	$-\frac{1}{35}$
11	$\frac{1}{11}$	37	$+\frac{1}{37}$
13	$+\frac{1}{13}$	41	$-\frac{1}{41}$
17	$-\frac{1}{17}$	43	$+\frac{1}{43}$
19	$+\frac{1}{19}$	47	$-\frac{1}{47}$
23	$-\frac{1}{23}$	49	$+\frac{1}{49}$
25	$+\frac{1}{25}$	53	$-\frac{1}{53}$

1.2. PERMEANCE HARMONICS

1.2.1. Order of Stator Permeance Harmonics

First it is assumed that both the stator and rotor teeth are removed. The permeance of the resulting gap is P_0 (constant) and is represented on figure by unit height.

Let the stator teeth be introduced. At certain places the length of the gap is decreased and permeance increased. This change of permeance can be considered as if an additional permeance P_s consisting of *sharp* angles had been introduced with the stator teeth. Similarly let now the stator teeth be removed and revolving rotor teeth be introduced. This is equivalent to introducing an additional revolving permeance P_r .

If both teeth are introduced, at those points along the circumference where no stator teeth exist, permeance due to the rotor teeth is the same as P_r but at those points where both the teeth exist the permeance would be much different. The net permeance is given by the product of two permeance functions. Writing for the mmf F as $f(\theta, t)$ as it is function of θ and time. Assuming unsaturated conditions, the air gap flux density at the stator surface is

$$b(\theta_1, \theta_2, t) = f(\theta_1, t) P(\theta_1, \theta_2) = \frac{f(\theta_1, t)}{l_g(\theta_1, \theta_2)} \quad (1-6)$$

Where

$b(\theta_1, \theta_2, t)$ = flux density which is function of rotor position

θ_2 , stator position θ_1 and time t .

$l_g(\theta_1, \theta_2)$ = length of the airgap which is a function of rotor position and stator position.

The permeance function (a term chosen by the author to avoid using the longer term 'reciprocal air gap length function') is defined as $1/l_g(\theta_1, \theta_2)$

The exact solution to the equation (1-6) is very complex involving three variables θ_1 , θ_2 and t . $P(\theta_1, \theta_2)$ permeance function itself consist of infinite series terms, but the function can be simplified by introducing an assumption. The assumption is that there exists in the air gap of any machine a magnetic equipotential surface of cylindrical fasion. This assumption is well founded in machines with semi-closed slots, it may not hold good for salient machines.

If this postulate is permitted, ⁽¹⁶⁾ all of the effects of stator slots may be measured with respect to the equipotential surface without reference to sotor and all of the sotor effects without reference to the stator. Thus it may be written

$$l_g(\theta_1, \theta_2) = l_{gs}(\theta_1) + l_{gr}(\theta_2)$$

when

$l_{gs}(\theta_1)$ = length of the air gap from equipotential surface to the stator and a function of θ_1 alone.

$l_{gr}(\theta_2)$ = length of the air gap from equipotential surface to the rotor and a function of θ_2 alone as represented in Fig. (1-5).

Each of these terms l_{gs} and l_{gr} may be expanded as infinite series.

$$l_g(\theta_1, \theta_2) = l_{g0} + \sum_{p=1}^{\infty} l_{gsr} \cos p\theta_2 + l_{gsr}' \sin p\theta_2 + l_{gsp} \cos p\theta_1 + l_{gsp}' \sin p\theta_1 \quad (1-7)$$

Where

l_{go} = mean effective air gap length.

$l_{gpr}^1, l_{gpr}^2, l_{gpr}^3, l_{gpr}^4$ = harmonic coefficients of air gap length.

$R \ \& \ S$ = number of rotor and stator slots respectively.

By means of binomial theorem it can be shown that

$$P(\theta_1, \theta_2) = P_0 + P_r + P_s \quad (1-8)$$

where

P_0 = mean effective permeance.

P_r = additional permeance due to rotor slotting.

P_s = additional permeance due to stator slotting.

If P_1 = permeance of the air gap assuming the rotor smooth and stator slotted with S slots.

P_2 = Permeance of the air gap assuming the stator smooth and rotor slotted with R slots.

The two permeance equations derived with the help of conformal - Transformation (see Appendix I) Theory are:-

$$P_1 = k_1 \left[1 + \sum_{v_1=1}^{\infty} \frac{eR}{v_1} \cos(v_1 \theta) \right] \quad (1-9)$$

$$P_2 = k_2 \left[1 + \sum_{v_2=1}^{\infty} \frac{eR}{v_2} \cos(v_2 R \theta') \right] \quad (1-10)$$

Where,

v_1 = order of permeance harmonic with rotor smooth or in brief stator permeance harmonic order.

v_2 = Rotor permeance harmonic order.

e, e_r = Ratio of R.M.S to average values of stator and rotor respectively.

$$r(\theta_1, t) = \frac{1}{2} A_m \sum \cos (m\theta_1 \mp \omega t)$$

defining a new space variable angle in terms of number of pair of poles (p) as

$$\theta_1 = p\theta$$

$$\text{then } r(\theta, t) = \frac{1}{2} A_m \sum \cos (mp\theta \mp \omega t) \quad (1-11)$$

$$\beta_s = r(\theta, t) \times P_1$$

$$\beta_s = \frac{1}{2} A_m k_1 \sum \cos [mp\theta \mp \omega t] \left[1 + \sum_{v_1=0}^{\infty} \frac{2S}{v_1} \cos(v_1 S\theta) \right]$$

$$\begin{aligned} \beta_s &= \frac{1}{2} A_m k_1 \sum_m \cos (mp\theta \mp \omega t) \\ &+ \frac{1}{2} A_m k_1 \frac{2S}{v_1} \sum_m \sum_{v_1} \cos (mp\theta \mp \omega t) \cos (v_1 S\theta) \end{aligned}$$

$$\beta_s = \beta_0 + \beta_{Ps}$$

$$\therefore \beta_{Ps} = \sum_m \sum_{v_1} \frac{1}{2} \left\{ \cos (mp\theta \mp \omega t - v_1 S\theta) + \cos (mp\theta \mp \omega t + v_1 S\theta) \right\}$$

$$\beta_{Ps} = \sum_m \sum_{v_1} \frac{1}{2} \left\{ \cos \left[\left(\frac{v_1 S}{p} - m \right) p\theta \mp \omega t \right] + \cos \left[\left(\frac{v_1 S}{p} + m \right) p\theta \mp \omega t \right] \right\}$$

.....(1-12)

∴ mth phase-belt harmonic when combined with v₁th permeance harmonic give rise to two new space harmonics which we will call as 'Permeance travelling wave' of the order of

$$\left(\frac{v_1 S}{p} \mp m \right) \quad \text{travelling at the speed of}$$

$$\frac{\pm \omega}{\frac{v_1 S}{p} - m} \quad \text{and} \quad \frac{\mp \omega}{\frac{v_1 S}{p} + m} \quad \text{i.e., one in forward direction}$$

and other in backward direction.

The permeance travelling waves will influence the magnitude of flux density of m th belt harmonic (b_m) with respect to which they are stand still. These are the stator slot harmonics. To each stator harmonic b_m there corresponds a series of permeance travelling waves.

The order of the slot harmonics of stator is given by the relation

$$m_s = \pm C \left(\frac{S}{P} \right) + 1 \quad \text{where } C = 1, 2, 3, \dots \quad (1-13)$$

and permeance travelling wave order is

$$m_p = v_1 \left(\frac{S}{P} \right) \pm 1 \quad \text{or} \quad \pm v_1 \left(\frac{S}{P} \right) + 1 \quad (1-14)$$

Comparing equations (1-13), (1-14) it is seen that the permeance waves of first order ($v_1 = 1$) are at stand still with respect to slot harmonics of first order ($C=1$) and similarly second order permeance wave are stand still with 2nd order slot harmonics ($C = 2$).

The table (1-2) gives the order of stator permeance harmonics produced by air gap permeance harmonics ($v_1 = 1, 2, \dots$). For our purpose we will limit ourselves to $v_1 = 1, 2$ i.e. first and second order air gap permeance components and the resultant stator permeance harmonics are listed in Table (1-2).

TABLE (1-2)

v_1	m	m_p	Speed of m_p
1	1	23	-1/23
		25	+1/25
2	1	47	-1/47
		49	+1/49
1	5	19	+1/19
		25	-1/25

Table (1-2) Contd..

v_1	m	m_p	Speed of m_p
		43	+1/43
2	5	55	+1/55
		17	-1/17
1	7	31	+1/31
		41	-1/41
2	7	55	+1/55
		13	+1/13
1	11	35	-1/35
		35	+1/35
2	11	59	-1/59
		11	-1/11
1	13	37	+1/37
		7	+1/7
1	17	41	-1/41
		5	-1/5
1	19	43	+1/43
		1	+1
1	23	47	-1/47

1.2.2. Rotor Permeance Harmonics

While finding the rotor permeance harmonics, more accurately rotor permeance travelling waves, it is assumed that only rotor surface is slotted and stator surface is smooth, then permeance equation is:

$$P_2 = K_2 \left[1 + \sum_{v_2} \frac{2R}{v_2} \cos \left(\frac{v_2}{p} p\theta - w_2 t \right) \right] \quad (1-15)$$

Where

- R = number of rotor slots.
- w_2 = Radians/sec.
- v_2 = order of permeance component.

The mmf at the stator surface is

$$f(\theta, t) = \frac{3}{2} A_m \sum_m \cos(p\theta \mp wt)$$

$$\begin{aligned} \therefore \phi(r) &= P_2 \times f(\theta, t) = \frac{3}{2} K_2 A_m \sum \cos(p\theta \mp wt) \\ &\quad + \frac{3}{2} K_2 A_m \frac{2R}{v_2} \cos(p\theta \mp wt) \cos\left(\frac{v_2 R}{p}(p\theta - w_2 t)\right) \\ &\quad \dots\dots(1-16) \end{aligned}$$

$$\phi_r = \phi_{ro} + \phi_{rp}$$

$$\therefore \phi_{rp} = K \cos(p\theta \mp wt) \cos\left[\frac{v_2 R}{p}(p\theta - w_2 t)\right]$$

Substituting

$$\frac{w - w_2}{w} = s \text{ (slip)}$$

$$w_2 = w - w s$$

Simplifying it

$$\begin{aligned} \phi_{rp} &= \frac{K}{2} \cos \left\{ p\theta \left(\frac{v_2 R}{p} + s \right) \mp wt \left[\frac{v_2 R}{p}(1-s) \pm 1 \right] \right\} \\ &\quad + \frac{K}{2} \cos \left\{ p\theta \left(\frac{v_2 R}{p} - s \right) \pm wt \left[\frac{v_2 R}{p}(1-s) \mp 1 \right] \right\} \quad (1-17) \end{aligned}$$

$$P_2 = K_2 \left[1 + \sum_{v_2} \frac{2R}{v_2} \cos \left(\frac{v_2 R}{p} p\theta - w_2 t \right) \right] \quad (1-15)$$

Where

- R = number of rotor slots.
 w_2 = Radians/sec.
 v_2 = order of permeance component.

The mmf at the stator surface is

$$f(\theta, t) = \frac{3}{2} A_m \sum_m \cos(p\theta \mp wt)$$

$$\begin{aligned} \therefore \phi(r) &= P_2 \times f(\theta, t) = \frac{3}{2} K_2 A_m \sum \cos(p\theta \mp wt) \\ &\quad + \frac{3}{2} K_2 A_m \frac{2R}{v_2} \cos(p\theta \mp wt) \cos\left(\frac{v_2 R}{p}(p\theta - w_2 t)\right) \\ &\quad \dots (1-16) \end{aligned}$$

$$\phi_r = \phi_{ro} + \phi_{rp}$$

$$\therefore \phi_{rp} = K \cos(p\theta \mp wt) \cos\left[\frac{v_2 R}{p}(p\theta - w_2 t)\right]$$

Substituting

$$\frac{w - w_2}{w} = s \text{ (slip)}$$

$$w_2 = w - ws$$

Simplifying it

$$\begin{aligned} \phi_{rp} &= \frac{K}{2} \cos \left\{ p\theta \left(\frac{v_2 R}{p} + m \right) \mp wt \left[\frac{v_2 R}{p} (1-s) \pm 1 \right] \right\} \\ &\quad + \frac{K}{2} \cos \left\{ p\theta \left(\frac{v_2 R}{p} - m \right) \pm wt \left[\frac{v_2 R}{p} (1-s) \mp 1 \right] \right\} \quad (1-17) \end{aligned}$$

Giving the following values to equation (1-17)

$$R = 68 \quad p = 2 \quad v_2 = 1, 2$$

and $m =$ order of stator belt harmonic

The equation (1-17) shows that rotor permeance harmonics are function of rotor slots and order of air gap permeance. It also shows that each space belt harmonic will produce a series of permeance harmonics. The permeance harmonics are sometimes also called sub-harmonics too. Tabulating the useful rotor permeance harmonics likely to produce an appreciable effect. Rotor permeance Harmonic is given by

$$v_2(R/p) \pm m$$

or $\pm v_2(R/p) + m$ (1-18)

Plus sign for forward rotating and minus sign for backward rotating.

Table (1-3)

v_2	m	order of Harmonic	Speed & direction
		35	1/35
1	1	33	-1/33
		69	1/69
2	1	67	-1/67
		39	+1/39
1	5	29	-1/29
		41	+1/41
1	7	27	-1/27
		69	+1/69
1	35	1	-1

Contd...

Table (1-5) contd..

v_2	m	order of Harmonics	Speed & direction
1	31	65	+1/65
		5	-1/5
1	29	63	+1/63
		5	-1/5

1.3. AMPLITUDES OF HARMONIC ⁽¹⁹⁾

1.3.1. Amplitude of Belt Harmonics

The equation (1-1) gives the amplitude as

$$F_m = \frac{A_m}{2} \frac{\sin (m-1) \pi}{\sin (m-1) \pi / k} \quad (1-18)$$

while finding the mathematical limit of the function.

$$F_m = \frac{A_m}{2} \frac{k}{P} \quad \text{where } k = \text{number of phases} = 3$$

$$\therefore F_m = 3/2 A_m ; A_m = 4/\pi \cdot \frac{1}{m} \cdot K_{wm} T_p \frac{I_m}{P}$$

Where

T_p = Turns per phase.

I_m = Max. current of fundamental time harmonic.

K_{wm} = Distribution factor for m th harmonic.

$$\begin{aligned} \therefore F_m &= \frac{6}{\pi} \frac{1}{m} \frac{K_{wm}}{P} T_p I_m \\ &= 0.9 \frac{k}{m} \frac{(T_p K_{wm})}{P} I_1 \quad (\text{mf per pole}) \dots (1-19) \end{aligned}$$

(1-19) gives the amplitude of mth harmonic in air gap. For stator mth

$$I_{1m} + I_{2m} = I_1$$

$$\therefore F_{(m)s} = 0.9 \frac{k}{m} \left(\frac{\tau_p K_{wm}}{P} \right) I_1'$$

$$= 0.9 (k/m) \left(\frac{\tau_p K_{wm}}{P} \right) D_m I_1 \quad (1-20)$$

When $D_m = I_1' / I_1 =$ damping factor per mth harmonic.

Similarly if $1 - D_m = G_m$ (Damping factor for rotor currents)

then $F_{(m)r} = 0.9 \left(\frac{k}{m} \right) \left(\frac{\tau_p K_{wm}}{P} \right) G_m I_1 \quad (1-21)$

1.3.2 Amplitude of Permeance Harmonics

Equations (1-12) and (1-16) gives the amplitude of permeance waves as $3/4 K_1 \frac{\Sigma \Sigma}{v_1} A_m$ and $3/4 K_2 \frac{\Sigma \Sigma}{v_2} A_m$ for stator and rotor respectively.

Amplitude of permeance harmonics is function of e_s and K_1, K_2 and v_1, v_2 .

$$F_{mp(s)} = \frac{3}{4} K_1 \frac{\Sigma \Sigma}{v_1} \frac{A_{mp}}{P} \quad (\text{Stator permeance harmonic per pole})$$

.....(1-22)

$$F_{mp(r)} = \frac{3}{4} K_2 \frac{\Sigma \Sigma}{v_2} \frac{A_{mp}}{P} \quad \text{.....(1-23)}$$

As defined earlier

$$e_s \text{ and } e_r = \frac{R_{\Sigma \Sigma}}{\text{AVG.}} \quad \text{value of permeance waves.}$$

$$K_1 \text{ \& } K_2 = \text{Average mean permeances.}$$

The above factors are investigated in detail in Chapter 2. .

1.3.3. Amplitude of Slot Harmonics:

For slot harmonics, the fundamental mmf of the stator when sets with non-uniform permeance produced by stator slotting gives rise to slot harmonic is the same as of fundamental. Therefore mmf of slot harmonics can be written

$$F_{ms}(s) = 0.9 \frac{k}{ms} \left(\frac{F_p K_{w1}}{p} \right) \frac{1}{2} \dots\dots\dots (1-24)$$

$$F_{ms}(s) = \frac{F_1(s)}{ms} \dots\dots\dots (1-25)$$

1.4. STATOR AND ROTOR HARMONICS

Summing up the harmonic phenomena we have

1. Phase Belt harmonic tabulated in Table 1-1
2. Stator permeance Harmonics given by $\pm k (S/P) + m$
3. Rotor permeance Harmonics given by $\pm k (R/p) + m$
4. Stator slot harmonics given by $\pm k (S/P) + 1$
5. Rotor slot harmonics given by $\pm k (R/p) + 1$.

For our purpose we will consider all these. The harmonics of importance of stator and rotor are listed below:

Table (1-4) Stator Rotor Harmonics:

STATOR	R O T O R				
	$v_2 = 0$	$v_2 = +1$	$v_2 = -1$	$k = +2$ $v_2 = +2$	$v_2 = -2$
+1	1	+35P	-33	+69	-67
-25	5	+29P	-39	+63	-73
+37	7	+41P	-27	+75	-61

Contd..

Table (1-4) Contd..

STATOR	R O T O R				
	$v_2 = 0$	$v_2 = +1$	$v_2 = -1$	$k' = +2$ $v_2 = +2$	$v_2 = -2$
-11	11	+25P	-45	+57	-79
+13	13	+47P	-21	81	-55
-17	17	+17P	-51	51	-85
+19	19	+53P	-15	87	-49
-23	23	+11P	-57	45	-91
+25	25	+59P	- 9	93	-43
-29	29	+ 5P	-63	39	-97
+31	31	+65P	- 3	99	-37
-35	35	-1P	-69	33	-103
+37	37	+31	+ 3	105	-31
-41	41	-7 P	-75	27	-109
-43	43	+77	+ 9	111	-25
-47	47	-13P	-81	21	-115
+49	49	+83	+15	117	-19
-53	53	-19P	-87	15	-121
+55	55	+89	+21	123	-13
-59	59	-25P	-93	9	-127
+61	61	+95	+27	129	- 7
-65P	65	-31P	-99	3	-133
+67	67	+101	+33	135	- 1
-71	71	-37P	-105	- 3	-139
+73	73	+107	+39	141	+ 5
-77	77	-43P	-111	- 9	-145
+79	79	+113	+45	147	11
-83	83	-49P	-117	-15	-151
+85	85	+119	+51	153	17
-89	89	-55P	-123	-21	-157
+91	91	+125	+57	159	23
-95	95	-61P	-129	-27	-163
+99	99	+131	+63	165	29

P indicates the combination for parasitic loops.

1.5. A MODEL OF THE SPACE HARMONICS

The model shown in the Fig (1-4) is based on the following assumptions ⁽⁴⁾.

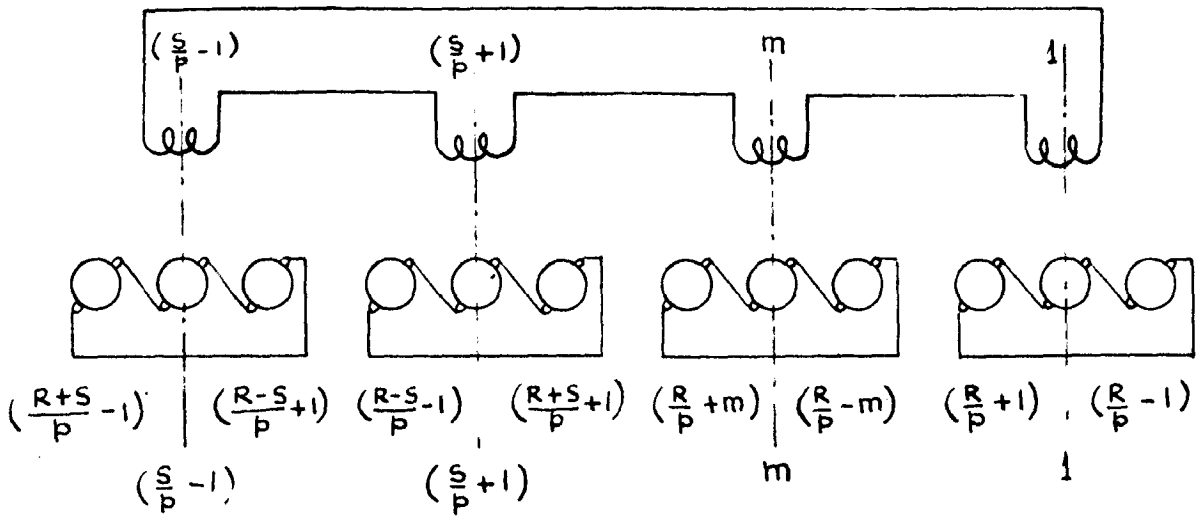
1. Harmonic fluxes having different numbers of pairs of poles do not interfere with each other, they may be assumed to exist in different induction motor structures.
2. Each such motor has different mutual and leakage inductances, also resistances (The resistances are different for each motor because of the skin effect due to the currents of different frequencies). There is no mutual linkage between harmonics.

Since one current in stator produces a series of fluxes is represented on the model by connecting a group of stators or rotors in series. These series connected structures have the same number of pairs of poles as the fluxes produced by the current.

A model for the first stator, m th stator and first slot harmonic of stator and rotor group of harmonics is represented in Fig. (1-4). Rotor sub harmonics are not indicated.

1.6 MACHINE WINDINGS AND THEIR INTERACTION WITH THE GENERAL FLUX DENSITY COMPONENT.

1.6.1. As explained earlier, one finds, on examining a variety of harmonic, phenomena in rotating machines, that all have in common the fact that the air gap flux density cannot be expressed as a simple rotating wave function, sinusoidal in space and time but contains in general a combination of such rotating waves, harmonically related in space or in time. Attention is directed initially to the general



MODEL OF THE STATOR AND ROTOR HARMONICS

FIGURE 1.4

FIGURE 1.5

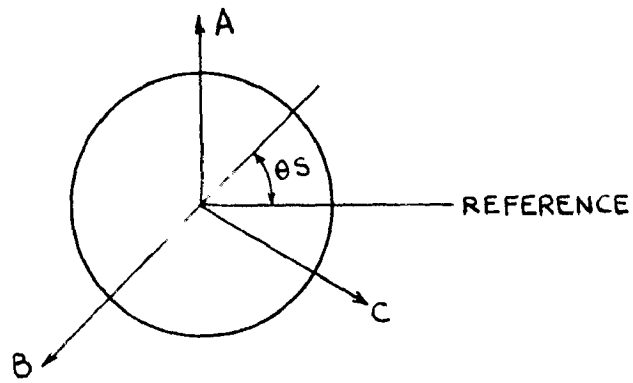
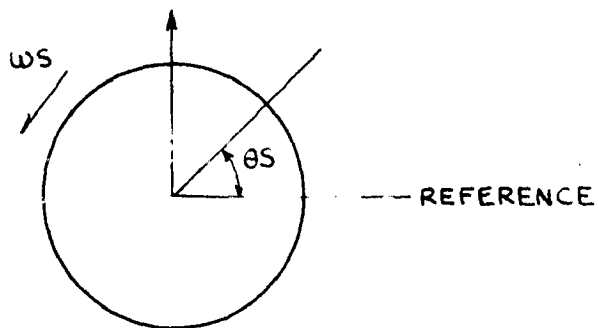


FIGURE 1.6



form of the flux density components as follows :

It is assumed that the air gap flux density is uniform in axial direction and end effects are ignored. Thus flux density b , can be written $\theta_r = \theta_s - \omega r t$ (taking two references winding at time zero).

$$b = B \sin (m\theta_s \pm \omega r t + \phi)$$

The method of approach here is that instead of considering a non-sinusoidal current in space, machine winding will be considered as sum of the harmonic component each varying sinusoidally in space.

Taking \bar{n} a periodic function of space angle θ , it can be expanded in Fourier series -

$$\bar{n} = \sum_{j=1,5} N_j \sin j \theta_s$$

If $i = i(t)$

$$f = \bar{n}i = i \sum_{j=1,5} N_j \sin j \theta_s.$$

In this respect, therefore, the actual winding can be considered as equivalent to series connection of windings having conductor distribution $N_1 \sin \theta_s$, $N_5 \sin 5 \theta_s$ etc. when

$$N_j = N \times K_{wn}$$

1.6.2. Voltage Induced in Winding

The voltage $v = \frac{d\psi}{dt}$ when ψ is the flux linkage in wb time.

$$\psi = K \int_0^{2\pi} \bar{n} b d\theta_s$$

$$\psi = \int_0^{2\pi} \left(\sum N_j \sin j \theta \right) B \sin (m\theta + k\omega t + \beta) d\theta$$

evaluation of this integral shows that $\psi_j = 0$ if $j \neq m$
 $\psi_j = \psi_m$ if $j = m$

Therefore there is induced voltage only when m th harmonic flux links with m th harmonic winding distribution.

$$v = v_m = - \frac{d\psi}{dt} = K \omega^m N_m B \sin (k\omega t + \beta)$$

We reach to same result by winding distribution approach. This approach the outline of which is presented here will be further utilized in next Chapters for finding out general equivalent circuit and harmonic torque phenomena of non-salient pole electrical machine.

CHAPTER II

GENERAL EQUIVALENT CIRCUIT FOR SKEWED ROTOR INDUCTION MACHINE AND DETERMINATION OF CIRCUIT CONSTANTS

2.1. THE GENERAL EQUIVALENT CIRCUIT

There are two general types of harmonic fields besides the fundamental magnetising field, namely the permeance harmonic fields and mmf harmonic fields. The equivalent circuit consists of the following series parallel connected impedances (17).

1. Primary as stator winding resistance R_1 .

Primary leakage reactance X_1 resulting from all the leakage flux that does not cross the air gap.

2. X_M = Fundamental magnetising reactance corresponding to the fundamental air gap flux wave of winding.

3. X_2 = Secondary leakage reactance.

R_2 = Secondary resistance.

4. A Magnetising reactance and secondary impedance corresponding to the stator permeance harmonic fields at $(n_1 \pm 1)$ the harmonic frequencies, where $n_1 = \frac{S_1}{p}$

4. B Magnetising reactance and secondary impedance corresponding to the rotor permeance harmonic fields at $(n_2 \pm 1)$ the harmonic frequencies where $n_2 = \frac{S_2}{p}$

5. A Magnetising reactance $X_M(mb)$ resulting from stator behaviour mmf harmonic field at mb th harmonic frequency in parallel

with rotor impedance consisting of reactance.

$X_2(mb)$, and resistance $R_2(mb) / S(mb)$ where $S(mb)$ represents backward harmonic slip.

- 5B Magnetising reactance $X_M(mf)$, resulting resulting down stator forward m th harmonic field at m th harmonic. Frequency in parallel with rotor impedance and resistance $\frac{R_2(mf)}{S(mf)}$ when $S(mf)$ is harmonic slip.
- 6 There is still another type of harmonics under stator m th harmonics, which is produced due to the m th across slot openings and these are known as slot harmonics. The steps in the m th were due to the concentration of the stator m th across the slot openings produce $(S-p)$ and $(S+p)$ harmonic fields also.
- 7 And lastly the- these space harmonics produced by the higher order of time harmonics. The order of the space harmonics produced time harmonics will be determined by combinational equations, but the effect being too meager, therefore such harmonics are neglected.

2.1.1. Induction Motors in Series

As analysed in Chapter I, there are various order and type of harmonics in m th wave of a smooth rotor machine, to establish equivalent circuit for their study, it will be assumed that each particular set of space harmonics exists in a separate machine and so as many separate machines of the same type have to be interconnected as there are space harmonics to be considered. But these machines, though

identical in structure differ in following respect.

1. Each has a different number of pairs of poles.
2. They are connected through either stator windings or rotor windings OR both.

Hence the problem of space harmonics consists of the inter-connection of several similar machines running at the same speed and having a different number of pairs of poles.

The physical picture presented by Kuon⁽⁴⁾ as shown in Fig. (2-1) four space harmonics with P_1, P_2, P_3, P_4 pairs of poles respectively are connected in series on stator side, and each with its own similar virtual rotor rotating at the same speed v in the same direction. Kuon derived the equivalent circuit for such cases from physical consideration of flux linkage etc. As the Fig (2-1) indicates, the stator mmf is the sum of the space harmonic mmfs connected in series and for each harmonic flux linking to its corresponding virtual rotor induces harmonic rotor emf causing to circulate rotor harmonic amount as $i_{r1}, i_{r2}, i_{r3}, i_{r4}$ etc to balance the stator harmonic flux.

When the rotor windings 2.1.1(b) are connected in series (Fig. 2-2) then the absolute frequencies in their stator windings are different. This case is for sub harmonics, induced back by rotor harmonic currents in stator, as n th rotor current induced by n th stator induces back in stator k th order with different frequency.

The physical concept presented by Kuon has been utilised by the author to formulate the results so obtained. The same results have been tried with conventional flux linkage theorem for harmonics of air gap mmf. The full effect of skewing of slots is also included

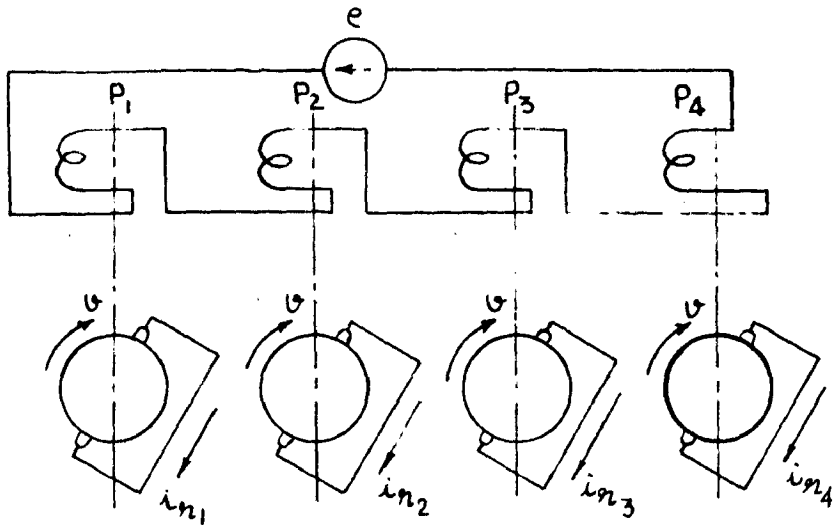


FIGURE 2.1

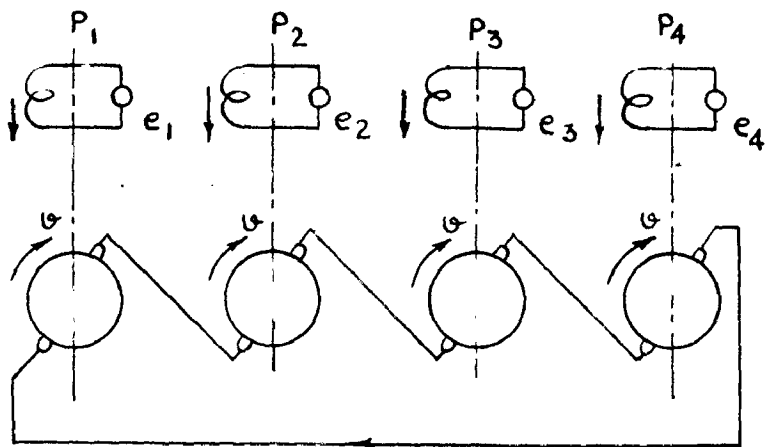


FIGURE 2.2

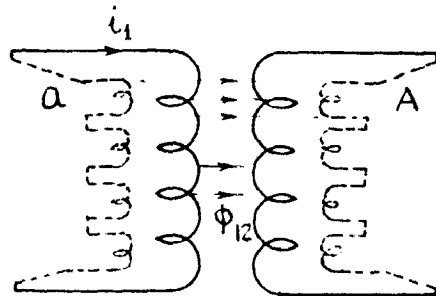


FIGURE 2.3

in analysis.

2.2. SELF INDUCTANCE OF COIL

The phase group coil 'a' and 'A' of stator and rotor respectively can be considered equivalent to harmonic coil connected in series. The total flux produced by the coil due to current

$$i_1 \text{ is if } \phi_a = \phi_{ar} + \phi_{aA}$$

$$\phi_{1a} = \phi_a - \phi_{aA}$$

$$(\phi_{11} + \phi_{22} + \dots + \phi_{mm}) = (\phi_1 + \phi_2 + \dots + \phi_m) - (\phi_{11'} + \phi_{22'} + \phi_{33'} + \dots + \phi_{mm'})$$

.....(2-1)

$$x_{1a} = \phi_{aa} - \phi_{aA} = (\phi_{11} - \phi_{11'}) + (\phi_{22} - \phi_{22'}) + \dots + (\phi_{mm} - \phi_{mm'})$$

$$= x_{11} + x_{12} + x_{13} + \dots + x_{1m}$$

$$= x_{1a} \quad \dots \quad \dots \quad (2-2)$$

The equation (2-1) is based on the assumption that there is a mutual coupling between same order of stator and rotor harmonics only

2.3 VOLTAGE EQUATION

The stator mmf equation as given by equation (1.11)

$$r(\theta, t) = \frac{3}{2} A_m \sum \cos (mp\theta_1 \mp \omega t)$$

stator mmf is :

$$r(\theta, t) = \frac{3}{2} A_m \sum \cos (mp\theta_1 \mp \omega t) \quad (2-3)$$

Rotor mmf is

$$r(\theta, t) = \frac{3}{2} A'_m \sum \cos (mp\theta_2 \mp \omega_2 t) \quad (2-4)$$

From equations (2-3) and (2-4), the net mmf acting across the air gap is the algebraic sum of these two expressions ⁽¹⁰⁾, neglecting saturation hysteresis and eddy currents, permitting superposition to be applied. The effect of parallel leakage paths prominence only in terms of voltage drops will be taken into account in this manner.

$$\text{mmf (air gap)} = \text{mmf (stator)} - \text{mmf (rotor)}$$

$$f_g(\theta, t) = f_s(\theta, t) - f_r(\theta, t) \quad (2-5)$$

$$\theta_2 = \theta_1 - (1-s)wt \quad (\text{If rotor not skewed})$$

θ_{sk} = angle of skew is defined as the difference in total angular displacement in electrical radians between θ_2 and θ_1 at the two ends of the rotor stack. The origin of the coordinates is taken at the centre of the stack.

$$y_R' = y_R = y \quad \dots \quad (2-6)$$

$$\theta_2 = \theta_1 = \theta_{sk} \frac{y}{L} - (1-s)wt \quad (2-7)$$

Air gap mmf in terms of stator coordinates

$$f_g(\theta, t) = \frac{N_1 N_2}{2\pi} \sum I_{2m} K_{w2m} \cos \left[\frac{p\theta_1 \pm wt [1+(n-m)]}{(1-s)} \right]$$

$$\frac{N_1 I_{1m}}{2\pi} \sum K_{w1m} \cos (p\theta_1 \pm wt)$$

Considering only slot harmonics and belt harmonics then

$$n = m$$

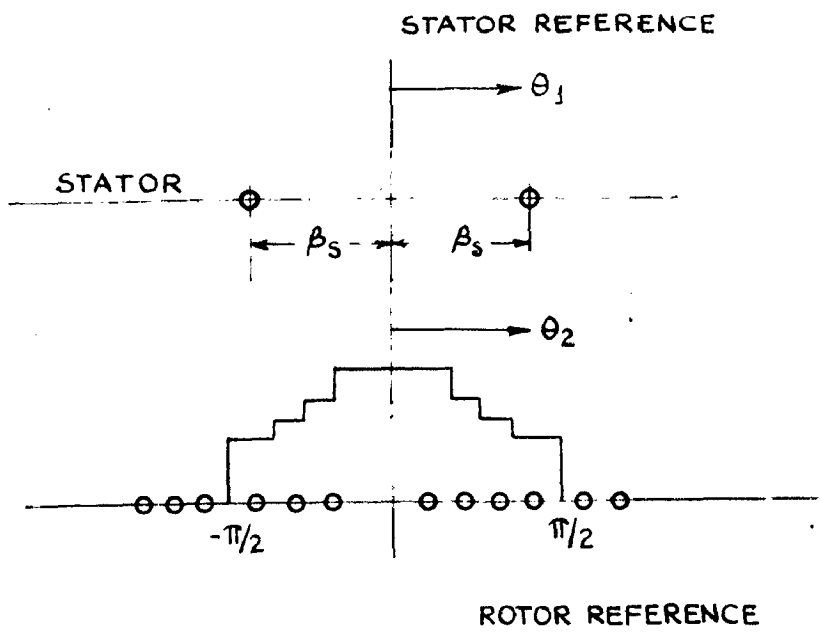


FIGURE 2.4

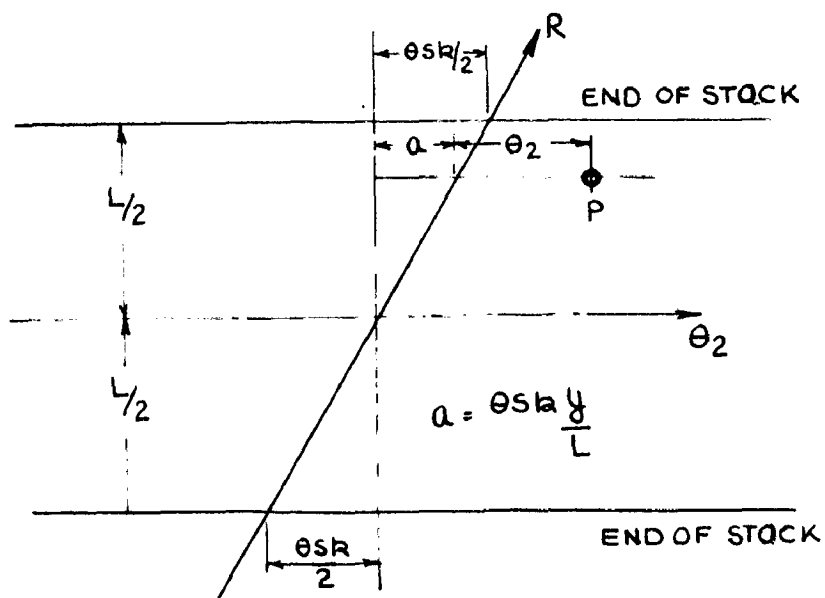


FIGURE 2.5

$$\begin{aligned}
 \phi_g(\theta, t) &= \frac{N_2 m_2}{m} \sum F_2 n K_{w2m} \cos(p\theta_1 \pm \omega t \pm \theta_{sk} \frac{p}{L}) \\
 &+ \frac{N_1 I_1 m_1}{m} \sum k_{w1m} \cos(p\theta_1 \pm \omega t) \quad (2-8)
 \end{aligned}$$

The flux linkage of a single rotor coil turn is obtained by integrating the air gap density referred to the rotor over the area spanned by the rotor coil turn.

$$\lambda_g(s) = \int_{-\beta}^{+\beta} \int_{-L/2}^{+L/2} \frac{D}{P} \frac{\Delta}{\epsilon_0} \phi_g(\theta, t) d\theta ds \quad (2-9)$$

Where β = coil span

Substituting the following in simplifying equation (2-9)

$$k_{w1m} = k_{p(m)} k_{d(m)}$$

$$\theta_{sk} = p \theta_{sk} \quad (\text{Elect. Skew}) \quad (2-10)$$

$$k_{sk(m)} = \frac{\sin m\theta_{sk}/2}{m \theta_{sk}/2} \quad (\text{skew factor}) \quad (2-11)$$

$$\begin{aligned}
 \lambda_g(s) &= \frac{2D/\mu L}{w \mu_0} N_2 m_2 \sum \frac{I_2(m)^{k_{w1(m)}} k_{w2(m)} k_{sk(m)} \cos \omega t}{m^2} \\
 &- \frac{2D/\mu L}{w \mu_0} N_1 I_1 m_1 \sum \frac{(k_{w1(m)})^2}{m^2} \cos \omega t \quad (2-12)
 \end{aligned}$$

Total flux linking phase I

$$\lambda_1(s) = \lambda_g(s) \cdot N_1$$

$$\lambda'_g(s) = \frac{2D^{\mu}L}{\pi P_{g0}} N_1 N_2 m_2 \sum \frac{I_{2(m)}^k k_{w1(m)} k_{w2(m)} K_s(m) \cos wt}{m^2}$$

$$= \frac{2 D^{\mu}L}{\pi P_{g0}} N_1^2 I_{1m_1} \sum \frac{k_{w1(m)}^2}{m^2} \cos wt \quad (2-13)$$

Since $e = -\frac{d\phi}{dt}$ (per turn)

$e = -\frac{d\lambda_1}{dt}$ (per phase)

Differentiating:

$$e_1(s) = \frac{2D^{\mu}}{\pi P_{g0}} N_2 N_1 m_2 \sum \frac{k_{w2(m)} k_{w1(m)} I_{2(m)} K_s(m) \omega \sin(\omega t)}{m^2}$$

$$+ \frac{2D^{\mu}}{\pi P_{g0}} N_1^2 m_1 I_1 \sum \left(\frac{k_{w1(m)}}{m}\right)^2 \omega \sin(\omega t) \quad (2-14)$$

Similarly when air gap mmf is referred to rotor side using the following coordinate transformation

$$\theta_2 = \theta_1 + \theta_{sk} \frac{r}{L} \quad (2-15)$$

and since rotor w.r. to stator is rotating at slip speed.

$$f_2(\theta, t) = \frac{3}{2} A'_m (m p \theta_2 - s_m \omega t)$$

where s_m = slip harmonic

$$s_m = 1 \pm m(1-s) \quad (2-16)$$

In incorporating equation (2-15) and (2-16) in equation (2-5) and (2-6) the voltage induced in the rotor circuit turns out

$$e_1(r) = \frac{2D^{\mu}}{\pi P_{g0}} N_2^2 m_2 \sum \left(\frac{k_{w2m}}{m}\right)^2 I_{2m}(s_m) \sin[(s_m \omega t)]$$

$$= \frac{2 D^{\mu}}{\pi P_{g0}} I_1 N_1 N_2 m_1 \sum \frac{(k_{w1m})(k_{w2m}) K_s(m) s_m \sin \omega t}{m^2} \dots (2-17)$$

Substituting -

Total self inductance of stator phase = L_{11}

Total self inductance of rotor phase = L_{22}

and M_{12} or M_{21} is the mutual inductance

When

$$L_{11(m)} = \frac{2 D^2 \mu L}{\pi g_0} N_1^2 m_1 \left(\frac{k_{w1m}}{m} \right)^2 \quad (2-18)$$

$$L_{22(m)} = \frac{2}{\pi} \frac{D^2 \mu L}{g_0} N_2^2 m_2 \left(\frac{k_{w2m}}{m} \right)^2 \quad (2-19)$$

$$M_{12(m)} = \frac{2}{\pi} \frac{D^2 \mu L}{g_0} N_2 N_1 m_1 k_{w1m} k_{w2m} K_{sm} \quad (2-20)$$

$$M_{21(m)} = \frac{2}{\pi} \frac{D^2 \mu L}{g_0} N_2 N_1 m_2 k_{w1m} k_{w2m} K_{sm} \quad (2-21)$$

$$M_{21} = M_{12} \quad (2-22)$$

Equations (2-18) through (2-22) in equation (2-19) and (2-17)

$$e_1(s) = w \sin(wt) \sum M_{21(m)} I_{2m} - w \sin(wt) I_1 \sum L_{11(m)} \quad (2-23)$$

$$e_1(r) = e_m \sin(wt) \sum L_{22(m)} I_{2m} - e_m \sin(wt) I_1 \sum L_{22(m)} \quad (2-23b)$$

2.4 ANALOGY WITH COUPLED CIRCUITS

The well known coupled circuit equations are, for the differential equation form

$$\begin{aligned} L_{11} \frac{di_1}{dt} - M \frac{di_2}{dt} &= e_1 \\ -L_{22} \frac{di_2}{dt} + M \frac{di_1}{dt} &= e_2 \end{aligned}$$

As far a.c. steady state form

$$j\omega L_{11} I_1 - j\omega M I_2 = E_1 \quad (2-24)$$

$$j\omega M I_1 - j\omega L_{22} I_2 = E_2 \quad (2-25)$$

Equations (2-22) and (2-25) does not take into account the voltage drop due to ohmic resistance of stator and rotor.

If r_1 = Stator resistance.

r_{2m} = Harmonic rotor resistance.

The rotor resistance r_{2m} will vary as per higher harmonics, skin effects predominates as considered further in this chapter.

If drops are taken into account, the equations for applied voltage V_1 becomes

$$V_1 = e_1(m) + \text{stator drop.}$$

$$V_1 = I_1 r_1 + j\omega I_1 L_{11(m)} - j\omega M \sum I_{2m} \quad (2-26)$$

$$E_R = I_{2m} r_{2m} - j\omega \sum a_m L_{22(m)} I_{2(m)} + j\omega I_1 \sum a_m M_m \quad (2-27)$$

As the whole mmf of rotor is consumed in circulating current $I_{2(m)}$ therefore E_R is zero.

$$0 = \frac{I_{2m} r_{2m}}{a_m} - j\omega L_{22(m)} I_{2(m)} + j\omega I_1 M_m \quad (2-28)$$

Modifying (2-26) and (2-27) with (2-1) and (2-2)

$$V_1 = I_1 r_1 + I_1 \sum j\omega L_{11(m)} + \sum (I_1 - I_{2(m)}) j\omega M_m \quad (2-29)$$

$$0 = I_{2m} \frac{r_{2m}}{a_m} + j\omega \sum I_{2m} L_{22(m)} + j\omega \sum (I_1 - I_{2m}) M_m \quad (2-30)$$

Equations (2-29) and (2-30) gives the conventional general

circuit (Fig. 2-6). This presents equivalent circuit for harmonics induced in rotor by non-sinusoidal winding distribution and due to the presence of slots on rotor and stator surfaces. This does not account the harmonics produced by rotor currents which are termed as 'sub-harmonics'.

2.5 HARMONIC SLIP

2.5.1. Harmonic Slip of Rotor Currents Directly Induced by Stator mfs.

For m th harmonic revolving forward per unit synchronous speed is

$$N_{sm} = 1/m$$

Rotor per unit speed is $= 1-s$

$$\therefore \text{Harmonic slip is } S_m = \frac{(1/m) - (1-s)}{1/m} = 1-m(1-s)$$

(for forward rotations)

$$= 1 + m(1-s) \text{ (for backward rotations)}$$

2.5.2. Harmonic Slip of Rotor permeance Harmonics

1. For example, considering k th forward rotor harmonic due to the rotor current induced by the m th backward stator harmonic field, the speed with respect to the stator m of this m th harmonic stator field

is $= -1/m$ and its speed with respect to the rotor is

$$-1/m - (1-s) = 1/m [ms - (m+1)]$$

The speed of the k th forward rotor harmonic of this field with respect to the rotor is

$$\frac{1}{mk} [ms - (m+1)]$$

and the speed of mk th harmonic with respect to the stator is

$$\frac{1}{mk} [ms - (m+1)] + (1-s) = \frac{1}{mk} [m(k-1)(1-s) - 1] \quad (2-31)$$

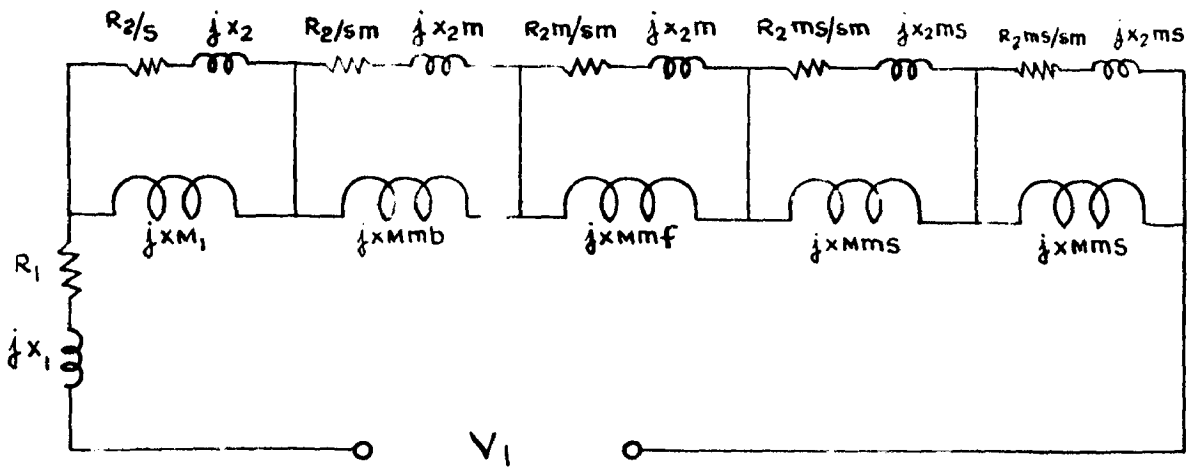


FIGURE 2.6

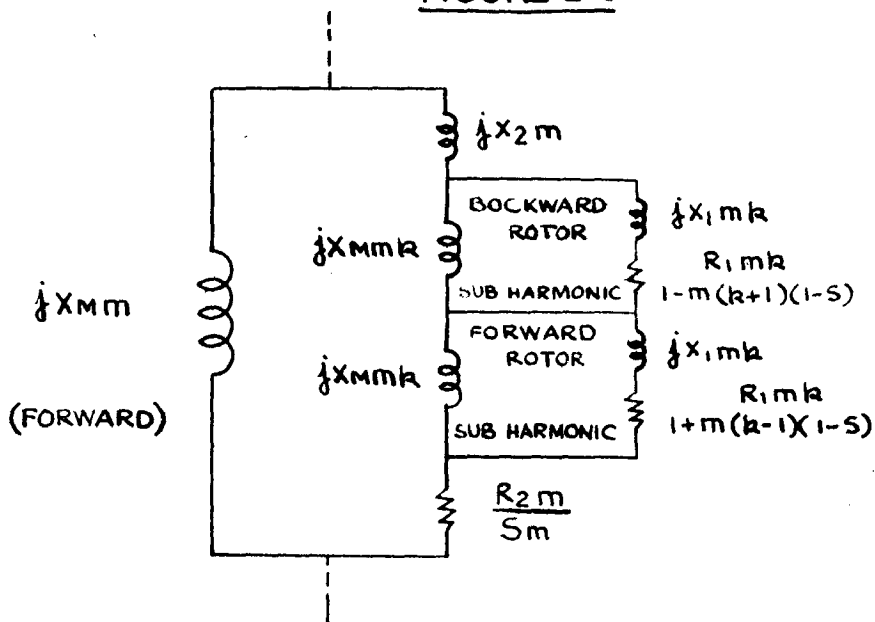


FIGURE 2.7

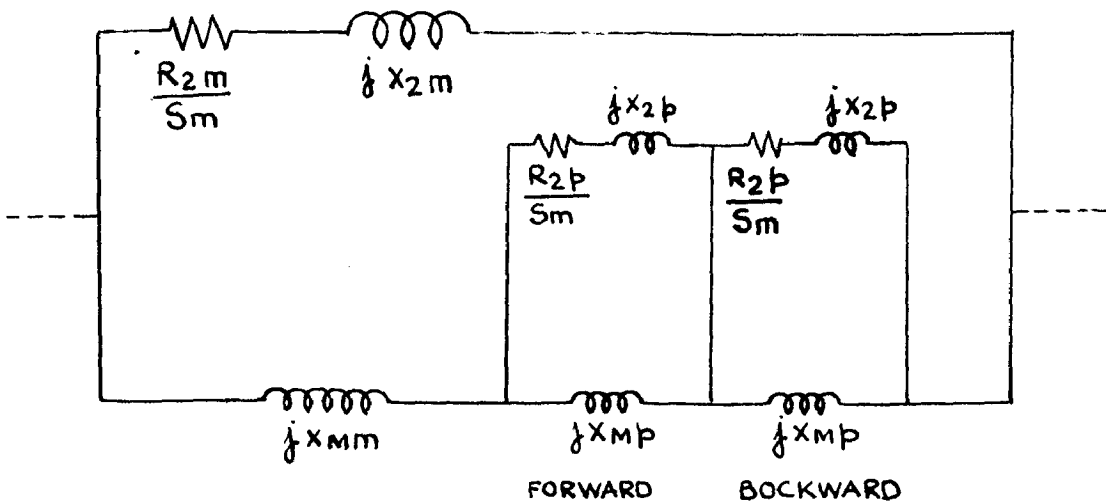


FIGURE 2.8

at $s = 1$ Speed of field in = $\frac{1}{nk}$ giving harmonic slip

$$s_{nk} = 1 - n(k-1)(1-s)$$

This per unit speed appears as the denominator of the stator resistance term in the k th forward field circuit of the n th backward stator harmonic field in Fig. (2-7).

(11) The case (1) has been considered for particular set of harmonics. Taking n and k as general order of any direction of rotation, then

$$s_{nk} = 1 \pm n(k \mp 1)(1-s) \quad (2-32)$$

2-6. EQUIVALENT CIRCUIT OF PERMEANCE HARMONICS

As discussed under Chapter I, effect of slot openings is to introduce permeance travelling waves of order

$$\pm v_1 \frac{R}{p} + n \quad \text{in case of stator}$$

$$\pm v_2 \frac{R}{p} + n \quad \text{in case of Rotor}$$

As they are produced by stator and rotor harmonic including fundamental currents, such permeance fluxes have the same frequency as the mmf producing them when viewed from the stator side. Hence, the effect of the slot openings is to introduce a double set of inductors in series with stator as rotor inductor respectively as the case may be.

2.6.1 First Considering Rotor Permeance Waves

Alger puts them in equivalent form like Fig. (2-7).

2.6.2. Equivalent Circuit for Stator Permeance Waves

If exciting field is from stator of m th order then frequency of stator permeance travelling waves would be same as of m th harmonic. They are included in circuit as shown by Alger⁽¹⁷⁾ (Fig. 2.8) where p stands for order of permeance wave produced by m th mmf wave p includes effect of both stator and rotor slot openings, for clarity sake only, general terms forward and backward are shown over the diagram.

2.7. DETERMINATION OF CIRCUIT REACTANCES

2.7.1. Primary and Secondary Leakage Fluxes of Belt Harmonics

Conventionally the leakage reactance takes into account of

1. Primary slot leakage.
2. Coil end leakage.
3. Zig Zag and phase belt leakage.
4. Skew leakage flux.

The zig zag reactance includes the magnetising reactances of all mmfs. Since some of the mmf harmonics are to be considered separately in the harmonic circuit, the magnetising reactances of these harmonics would not be included in the primary (stator) leakage. To facilitate calculations, the coil end leakage reactance will be assumed to contribute equally to the primary and secondary sides.

$$\text{Total primary leakage reactance is} \\ X_1 = X_{s1} + \left[X_{st} - \sum X_{M(m)} \right] + \frac{X_0}{2} + X_d \quad (2-33)$$

Where

X_{s1} = Primary or stator leakage reactance.

X_{st} = Primary zig zag leakage reactance.

X_{Mh} = Magnetising reactance of harmonics.

X_0 = Coil and leakage reactance.

X_{α} = Skew reactance.

The secondary leakage reactance for the fundamental is

$$X_2 = X_{s2} + X_{m2} + \frac{X_0}{2} + X_{\alpha} \quad (2-34a)$$

where

X_{s2} = Secondary slot leakage reactance of secondary.

X_{m2} = Secondary Harmonic leakage reactance.

and for m th harmonic

$$X_{2(m)} = X_{s2(m)} + X_{m2(m)} + X_{\alpha}(m) \quad (2-34b)$$

There is no practically coil and leakage reactance. For higher harmonics only sig sag leakage reactance predominates.

Slot Leakage Reactance

As well known

$$X_{s1} = \frac{2 f m_1 L N^2 P_{s1}}{8 \times 10^7} \quad \text{Ohm / Phase} \quad (2-35)$$

$$X_M = \frac{6.38 m_1 N^2 (k_{w1})^2 DL}{l_{go} p^2 10^8} \quad \text{Ohms/Phase} \quad (2-36)$$

Where z = number of conductors in series per phase.

S = Number of stator slots.

P_{s1} = permeance constant of slot.

l_{go} = effective air gap length.

L = Base length in inches.

N = Number of turns per phase.

D = Bore diameter in inches.

m_1 = *Prism. No of Phases.*

other of Adams, considers first time correctly the air gap leakage i.e. harmonic fluxes as source of leakage. Alger treats it as two separate (zig zag and belt) leakages. This segregation makes Adam's⁽²¹⁾ theory in applicable to harmonics. More over this theory does not consider any damping by squirrel cage winding in the rotor of stator fluxes. Further no due consideration is given for slots. The influence of slots is two fold as already discussed in Chapter I. Slot Openings may considerably decrease or increase the amplitude of permeance waves.

Here the results are reproduced of the analysis presented by Liewchits - Garik. These results are dealt in detail under Appendix II.

$$X_{s2(m)} = \left\{ \left[\frac{\frac{mp^2}{R}}{K_{sm}} \quad C_{so} \left(\frac{m w p}{R} \right) \right]^2 - 1 \right\} X_H(m) \quad (2-40)$$

The skin effect factor for leakage reactance of slots is to be considered. The slot leakage position is considerably affected by high frequencies as shown by curve (Fig. II-2) of Appendix II. The skin effect factor for reactances is given by

$$J(m) = \frac{1.5}{1.68 \left[\frac{(1 \pm m) 50}{60} \right]^{\frac{1}{2}}} \quad (2-41)$$

for m - forward use negative sign.
 m - backward use positive sign.

Therefore total leakage reactance for m th phase harmonic by substituting 2-35 to 2-41 in (2-34b)

$$X_{2(m)} = \left(\frac{K_{sm}}{K_{w1}} \right)^2 \left[\frac{X_{s2}(J_m)}{K_{sm}^2} + \left\{ \left(\frac{\frac{mp^2}{R}}{K_{sm}} \right)^2 C_{so}^2 \frac{mp^2}{R} - 1 \right\} X_H + \frac{X_{\sigma}}{m^2} \right] \quad (2-42)$$

2.7.2. Primary and Secondary Leakage Reactances of Slot Harmonics

The differential leakage reactance for slot harmonics is substituting in 2-40.

$$X_{s2}(n_s) = \left[\frac{\left(\frac{v_1 B}{p} \pm 1\right)^2}{K_{sm}^2} \cos^2 \frac{\left(\frac{v_1 B}{p} \pm 1\right) p^n}{R} - 1 \right] X_{M1} \dots(2-43)$$

The other leakage components would be the same as given by (2-42)

2.7.3. Primary and Secondary Leakage Reactance for Permeance Harmonics

On the similar lines as equation (2-40), a mathematical form for the differential reactance can be got for permeance Harmonics. Since as pointed out earlier too, permeance harmonic mmfs are of very low order. So total leakage reactance can be taken with sufficient accuracy equal to zig zag reactance, because as equation 2-40 indicates, zig zag reactance increases with increased order of harmonics.

Writing

n_p = order of permeance harmonic.

$$X_{2P} = X_{2}(n_p) = X_{s2}(n_p) = \left[\frac{p^2 w^2}{K_{sm}^2 R^2} \cos^2 \frac{p w n_1}{R} - 1 \right] \frac{X_{M}(n)}{n_1^2} \dots(2-44)$$

$$n_1 = \left(v_2 \frac{B}{p} \pm n \right) \dots(2-45)$$

2.7.4. Magnetizing Reactance of Phase Belt Harmonics

From equation 2-29, 2-21 and current transformation

$$X_{M(m)} = \frac{X_{M1}}{m^2} \left(\frac{k_{wm1}}{k_{w1}} \right)^2 \quad (2-45)$$

When X_{M1} = magnetizing reactance of primary.

2.7.5. Magnetizing Reactance of slot harmonic and permeance Harmonics

$$X_{M(ms)} = \frac{X_{M1}}{\left(\frac{v_1 s}{p} + 1 \right)^2} \quad (2-47)$$

As the winding distribution for slot harmonic is the same as of fundamental so factor $\left(\frac{k_{wm}}{k_{w1}} \right)^2$ does not appear for slot

harmonics.

and

Permeance Harmonic Magnetizing Reactance

From equation 1-9, 1-10 it is seen that factor k_1, k_2 affects the permeance and since k_1, k_2 are function of slot openings and air gap, these slot openings have a turbulent effect over permeance harmonic magnetizing motive force. It is directly reduced in proportional to factor $K(R)$

where $K_R = \frac{\text{Single amplitude of the permeance pulsation}}{\text{Average permeance}} \dots\dots(2-48)$

(arrived on the assumption that permeance is sinusoidal over the slot)

$$K_R = \frac{\beta}{2-\beta} = \frac{\beta/2}{1-\beta/2} \quad (2-49)$$

$$\text{Where } \beta = \frac{\text{Double amplitude variation}}{\text{maximum permeance.}} \quad (2-50)$$

If exciting harmonic for m th permeance wave is n th phase harmonic where $m_p = \left(\frac{v_2 R}{p} \pm n \right)$

$$\text{then } X_{M(p)} = \frac{K_{R2} X_{M(m)}}{2v_2 \left(\frac{v_2 R}{p} \pm n \right)} \quad (2-51)$$

(for rotor permeance)

$$\text{and } X_{M(p)} = \frac{K_{R1} X_{M(m)}}{2v_1 \left(\frac{v_1 R}{p} \pm n \right)} \quad (2-52)$$

(for stator permeance)

3.8. SKIN FACTOR FOR HARMONIC STATOR AND ROTOR RESISTANCES

3.8.1. For Rotor bar Resistance:

The rotor resistance is composed of ⁽¹⁵⁾

$$R'_2 = R_{2\text{bar}} + R_{2(\text{wing})} \text{ (effective)}$$

$$R'_2 = R_{2b} + R_{2r(\text{eff.})}$$

$$R'_2 = R_{2b} + \frac{R_{2r}}{2 \sin^2(\alpha'_s/2)} \quad (2-53)$$

Where α'_s = Angle between two bars by which bar currents are displaced.

$$\alpha'_s = \frac{w F}{R} \text{ (Elect. degree).}$$

Equation (2-53) applied to main wave. Considering n th the skin effect has to be taken into account in term R_{2b} . For n th the slot angle becomes :-

$$\alpha'_{s(m)} = n \alpha'_s$$

$$\therefore R'_{2(m)} = \frac{k_{wm}^2}{k_w^2} \left[R_{2b} (km) + \frac{R_r}{2 \sin^2 (c_s/2)} \right] \dots(2-54)$$

For higher order of harmonics, Ring resistance does not form any appreciable part of resistance in comparison with bar resistance which increases very fast due to skin effect at high frequencies of harmonics. Therefore

$$R'_{2(m)} \approx R_{2(b)} \cdot K(m) \quad (2-55)$$

Where $K(m)$ = skin factor for mth harmonic dealt in detail in Appendix II.

As in case of slot harmonics, the exciting field is fundamental therefore skin factor is not important to them and slot harmonics will experience the same resistance as of fundamental i.e.,

$$R_{2(ms)} \approx R_2$$

Where $R_2 = \frac{R'_2 \times 4 m_1 (N_1 k_{wm})^2}{R_2 K_{sm}^2} \quad (2-56)$

and $\frac{4 m_1 (N_1 k_{wm})^2}{R_2 K_{sm}^2} = \text{Reduction factor (RF)} \quad (2-57)$

2.8.2. Rotor Resistance of Rotor permeance Waves:

$$R_{2(mp)} = R_{2p} = R_{2(m)}$$

Where m is the exciting field for m th permeance field. Similarly for stator permeance waves.

All the results, determined under section 2.7 and 2.8 holds good only when the fundamental and harmonic flux paths are assumed

unsaturated. This assumption is valid to a greater extent as the locked rotor performance curve of the machine under test (Fig. 1-5) indicates. From this fig, we can safely assume the machine working in unsaturated region without any appreciable error creeping in.

2.9. SPECIFICATIONS OF INDUCTION MACHINE UNDER TEST AND EXPERIMENTAL

DETERMINATION OF CIRCUIT CONSTANT:

2.9.1. Specifications:

The experimental skewed rotor induction machine was put to some tests and measurement to know certain relevant data necessary for further analysis and calculations.

1. Measurements : The following figures were collected after careful measurements of the 5 ϕ , 3 H.P. , 1500 RPM , rotor skewed induction machine.

Angle of skew = 6° (Elect)

Length of Rotor = 7.1 Cms.

Length of Rotor bar = 7.5 Cms.

Diameter at the air gap = 17.0 cms.

Length of armature = 7.5 cms.

2. Stator: Number of slots = 48

Number of Poles = 4

No. of turns per phase = 256.

Chording = full pitch coils.

Phase spread = 60° (4 slots)

speed = 1500 (asynchronous)

slot width = 5.5 mm

Slot pitch = 11.1 mm.

Slot depth = 21.0 mm.

slot opening = 2.5 mm.

3. <u>Rotor:</u> No. of slots	= 68
Ring size	= 2.3 x 0.5 cms.
Mean dia. of Ring	= 15.8 cms.
Width of rotor slot	= 0.65 cms.
Rotor slot opening	= 1.5 mm.
Slot pitch	= 0.785 cms.

2.9.2. Tests:

(a) Test for Windage Friction loss:

The conventional method of variable voltage test and then determining friction windage loss by extra plotation procedure.

Results are plotted in Fig. (2-9) giving windage friction loss (wf)

$$= 185 \text{ watts.}$$

(b) Magnetising reactance:

The magnetising reactance was determined at rated voltage, machine running at synchronous speed by means of external drive in current direction of rotation.

$$I = 2.20 \text{ Amps} \quad V = 440 \text{ Volts} \quad W = 910 \text{ Watts.}$$

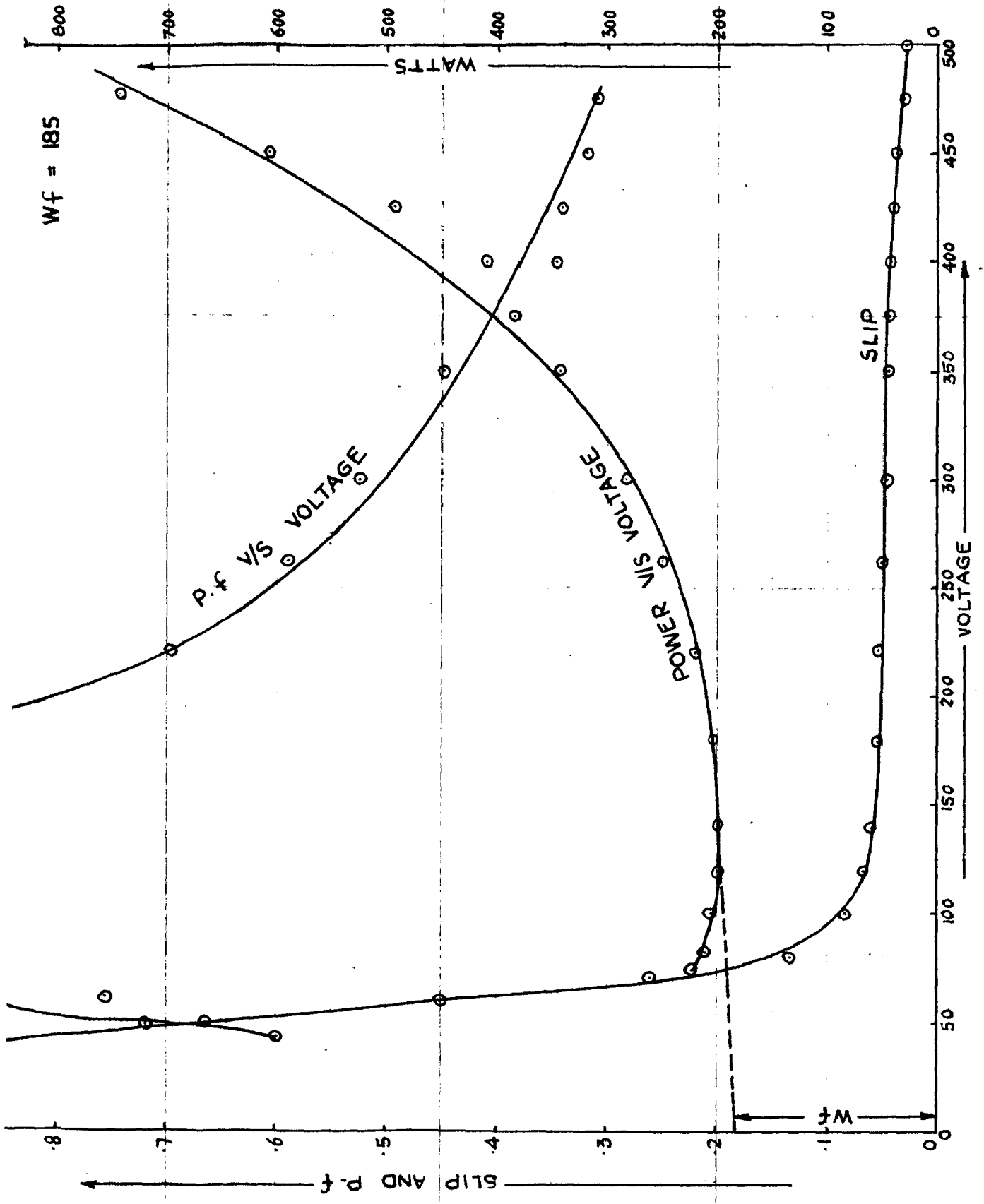
$$X_M = 138.0 \text{ Ohms} \quad , \quad R_1 = 5.7 \text{ Ohms} \quad , \quad X_1 = 3.5 \text{ Ohms}$$

$$X_2 = 3.1 \text{ Ohms, (Rotor resistance referred to primary)} \quad R_2' = 1.93 \text{ Ohms.}$$

(c) Stray Load Loss Test over Induction Machine

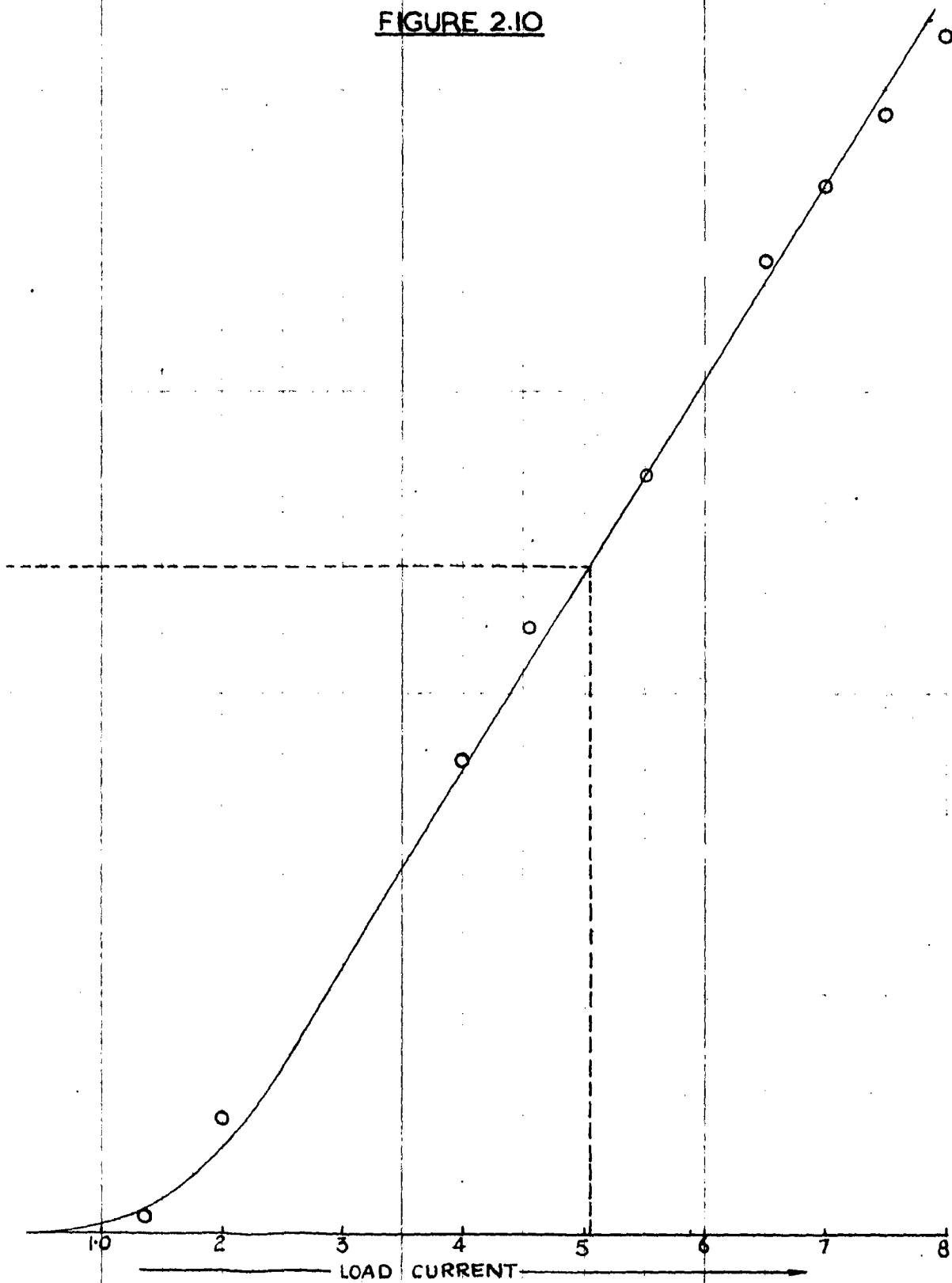
A stray load loss curve against loss (Fig. (2-10) is drawn.

Results are obtained when a reverse rotations test is performed over induction machine.



STRAY LOSS CURVE

FIGURE 2.10



**2.10. CALCULATION OF CIRCUIT CONSTANTS OF GENERAL EQUIVALENT CIRCUIT
WITH AND WITHOUT SKEW ANGLE OF THE ROTOR**

2.10.1 Calculation of Constant Factors:

Before going over to actual calculation of circuit constants, it is essential to find out certain factors required in further calculations.

(a) Distribution Factor

$$k_{w1}(m) = k d_1(m) \quad (\text{as coils are full pitched})$$

$$k_{w1}(m) = \frac{\text{Sin } \frac{m \sigma_c}{2}}{g \text{ Sin } \frac{m \sigma_c}{2g}} \quad (2-58)$$

Where g = no. of slots per pole per phase = 4.

σ_c = coil span angle = 60°

Results are tabulated in Table 2.1

Table 2.1 A.

m	1	5	7	11	13	17	19	23	25	29	31	35	37
k_{w1m}	.955	.205	.157	.126	.126	.157	.205	.955	.955	.205	.157	.126	.126

Table 2.1 B.

m	41	43	47	49	53	55	59	61	65	67	71	73	77
k_{w1m}	.157	.205	.955	.955	.205	.157	.126	.126	.157	.205	.955	.955	.205

(b) Stator slot permeance factor

From well known relation

$$P_s = \frac{h_1}{3w_s} + \frac{h_2}{w_s} + \frac{2h_3}{w_s + w_o} + \frac{h_4}{w_o}$$

$$y_g = 0.85 \text{ cm} , h_1 = 16.0 \text{ mm} , h_2 = 2.0 \text{ mm} , h_3 = 2.0 \text{ mm}$$

$$h_4 = 1.0 \text{ mm} \quad w_g = 5 \text{ mm} , w_o = 2.6 \text{ mm}$$

$$\therefore P_g = 2.2$$

(c) Stator slot opening factors:

Fig. (2-16) shows the dip caused in the flux density curve due to the presence of slot opening w ,

$$\text{mf} = P_o \left[1 + K_R \cos (\delta x) \right] \dots\dots\dots (2-59)$$

$$K_R = \frac{\beta}{2 - \beta}$$

Equation 1-9 is
$$P = K + \frac{K_{sg}}{v_1} \cos \delta \theta + \frac{K_{sg}}{2} \cos 2 \delta \theta + \dots\dots\dots$$

Considering only 1st and 2nd order of permeance wave.

If

P_g = permeance with smooth surfaces.

P'_g = Effective permeance with effective air gap length.

$P_o = K$ = constant permeance.

P_s = half amplitude of 1st order permeance wave = $\frac{K_{sg}}{v_1}$

The maximum value which the stepped permeance can take is P_g

$$\therefore P_g = P + \frac{P_s}{2} + P_s$$

$$\therefore P_o = P_g - 1.5 P_s \dots\dots\dots (2-60)$$

Taking same δ value

$$P(\text{ms}) = P_o(\text{ms}) + P_s \cos \theta(\text{ms}) + \frac{P_s}{2} \cos 2\theta(\text{ms})$$

$$P'_g = P_o + \frac{P_s}{2} + \frac{P_s}{2(2)^2}$$

$$P'_g = P_g - 0.44 P_s \dots\dots\dots (2-61)$$

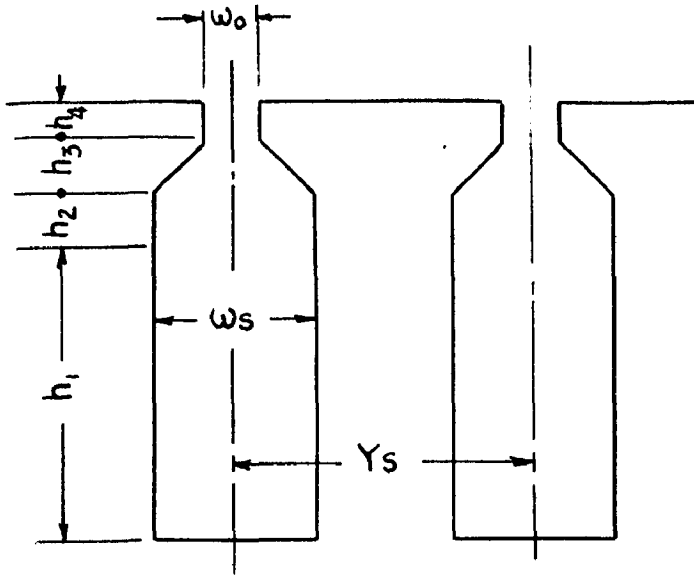


FIGURE 2.16 A

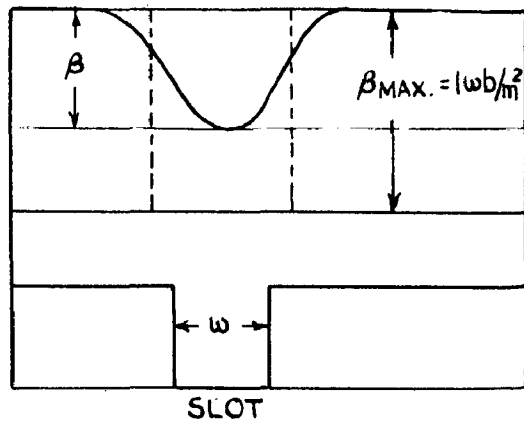


FIGURE 2.16 B

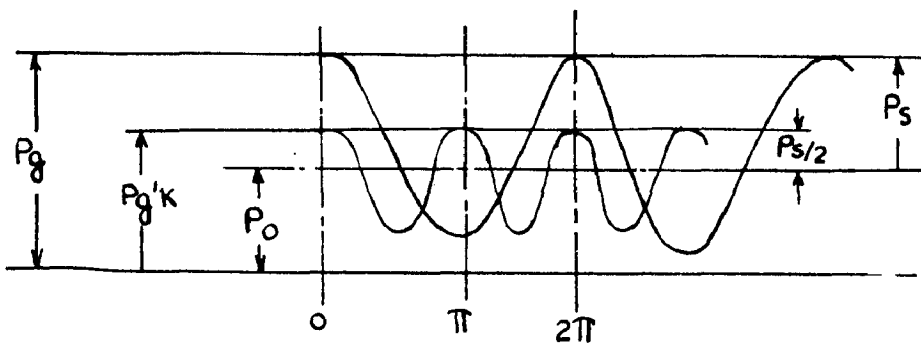


FIGURE 2.16 C

Taking permeance $P \propto \frac{1}{\text{air gap length}}$

$$A = \text{Const.}$$

$$P_g = \frac{A}{l_g} = 2.5 A \quad l_g = 0.04 \text{ cm.}$$

and P'_g (222) = A/l'_g when l'_g = Effective air gap with Carter Coefficient.
= 1.99 A.

$$l'_g = .048 \text{ cm.}$$

From (2-61) $P_g = 0.91$

$$\therefore P_o = 1.135$$

$$\therefore P = 1.135 + 0.91 \cos 8\theta + 0.455 \cos 28\theta$$

from equation (2-59)

$$K_{R1} = \frac{P_g}{P_o} = 0.809 \quad (2.62)$$

(For stator)

Similarly finding factor K_{R2} for Rotor taking effective air gap length $l''_g = 0.424 \text{ mm.}$

After using Carter's coefficient for rotor slots.

the permeance equation with rotor slotted and stator smooth

becomes:

$$P_2 = 2.023 + 0.518 \cos R(\theta - w_{2t}) + 0.159 \cos 2R(\theta - w_{2t})$$

$$\therefore K_{R2} = \frac{0.518}{2.023} = 0.156 \quad (2.63)$$

Comparing these results with those computed by Robinson in the form of curves

In our case, width of slot $S = 0.5 \text{ cm.}$ (stator)

$$\lambda = 0.85 \text{ cm.}$$

$$s/\lambda = 0.59$$

$$l_g = 0.04 \text{ cm.}$$

$$s/l_g = .9/.04 = 12.5$$

From Fig. (1-4) Mean flux density = 0.49

From Fig. (1-5) $V = K_{R1} = 0.9$

For Rotor slot width = 0.2 cms.

$$\lambda = 0.65 \text{ cms.}$$

$$s/\lambda = 0.31 \quad \text{and} \quad s/l_g = 5.0 \quad \text{from Fig. I-5) } \quad V = K_{R_2} = 0.2$$

The values of these factors K_{R_1} and K_{R_2} are coinciding too a fair degree.

(d) Skew leakage flux and Skew Factor:

Designers have long recognised that the space fundamental air gap flux varies with axial position because of the skewing the rotor slots with respect to stator slots, here an quantitative data are presented to demonstrate its effect, showing how much this flux may vary. It is important that variation in flux is taken into account to know the exact performance of induction machine. As Fig. (2-17) shows the skew flux path, though it crosses air gap, but it does not produce any useful torque, the skew flux simply adds to the leakage (equ. 2-35).

The skew flux is produced by inequality of stator and rotor mmf brought in by skewing of rotor bars.

Fig. (2-15) shows the stator bore surface and the rotor outside surface developed into the plane of the paper. The figure shows the stator - rotor and resultant mmf's at the ends of the stack. In the centre ($y = 0$) the resultant mmf is zero. Considering only fundamental.

$$\text{Skew factor} = \frac{\text{If } \sigma = \text{Total electrical skew angle (See Fig. 2.17)} = \alpha}{\text{Eaf induced in skewed bar}} \\ \text{Eaf induced in straight bar.}$$

$$K_s = \frac{E_{sk}}{E} \quad (2-65)$$

The element of voltage induced in a short⁽³⁾ length of the conductor at point x is $\frac{E dx}{l} \angle x$, where E is the total voltage

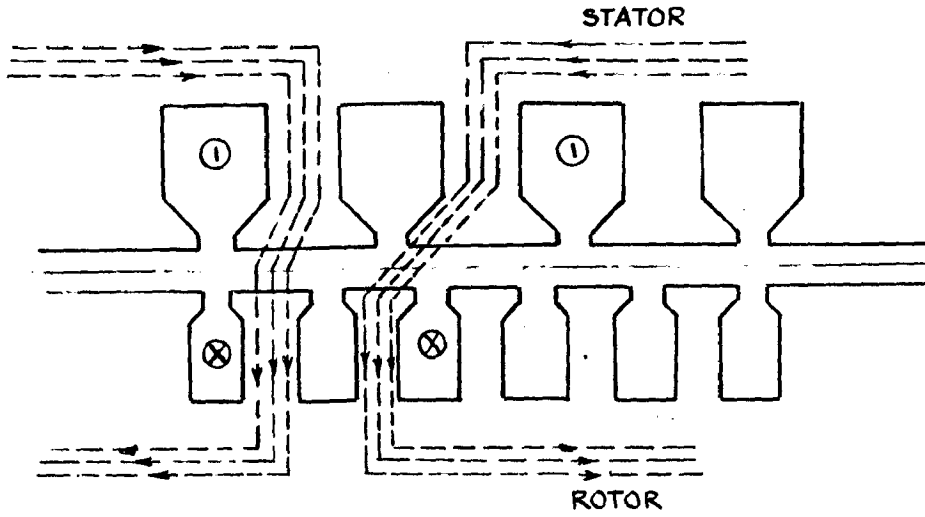


FIGURE 2.17

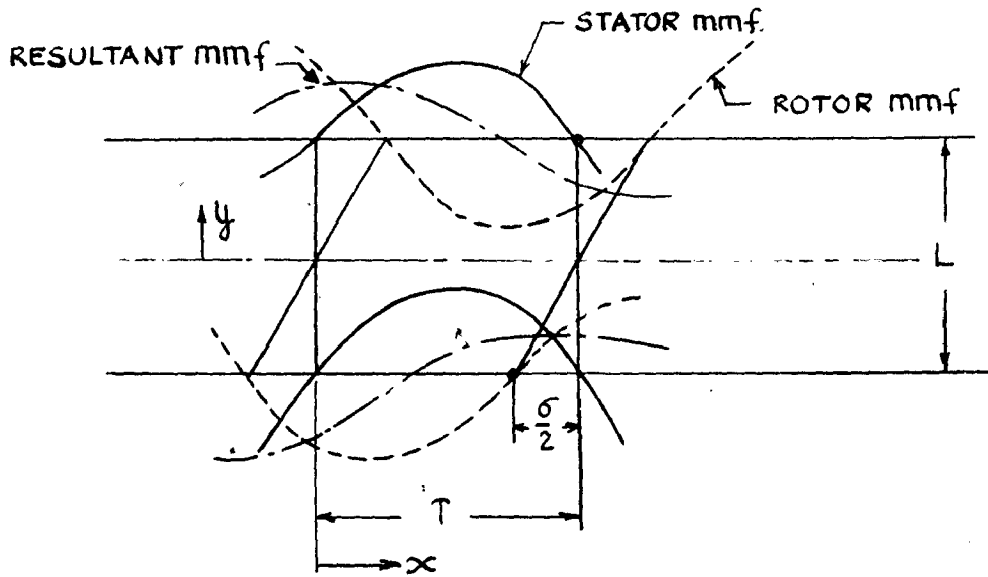


FIGURE 2.18

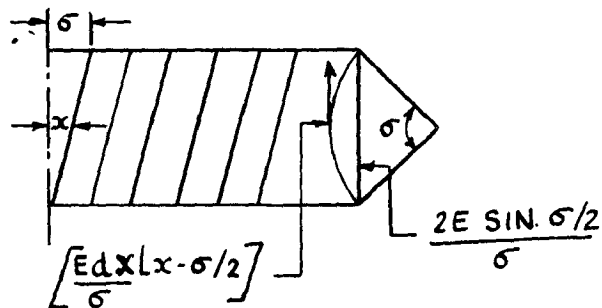


FIGURE 2.19

induced in a straight conductor. The net voltage across the bar is the sum of the projections of the elementary voltages on the mid point value

$$E = \int_0^{\sigma} \frac{E}{\sigma} \cos \left(x - \frac{\sigma}{2} \right) dx = \frac{2 E \sin \sigma / 2}{\sigma}$$

$$\therefore K_B = \frac{2 \sin \sigma / 2}{\sigma}$$

Similarly for mth harmonic

$$K_{B(m)} = \frac{2 \sin m\sigma / 2}{m \sigma} \tag{2-66}$$

Skew factor for harmonics are tabulated in Table 2-10 with $\sigma = 60^\circ$ (Elect)

Table 2.10 HARMONIC SKEW FACTORS

m	1	5	7	11	13	17	19	23	25	29	31
$K_{B(m)}$.998	.987	.98	.946	.925	.873	.845	.79	.74	.657	.616
m	35	37	41	43	47	49	53	55	59	61	65
$K_{B(m)}$.527	.482	.591	.546	.256	.212	.129	.09	.017	.06	.076

Table (2.2) MAGNETISING REACTANCE OF PHASE BELT HARMONICS WITH AND WITHOUT SKEW

m	1	-5	7	-11	13	-17	19	-23	25	-29
$X_{M(m)}$ ohm	138.0	0.256	.077	.02	.0144	.0132	.0176	.261	.221	.0076
m	31	-35	37	-41	43	-47	-71	73	-95	97
$X_{M(m)}$ ohms	.004	.002	.002	.002	.0034	.0625	.0274	.0258	.015	.0146

Table 2.3 MAGNETISING REACTANCE OF SLOT HARMONICS WITH AND WITHOUT SKEW

m	-25	25	-47	49	-71	73	-95	97
$X_M(m)$ (ohms)	.26	.221	.0625	.0575	.0274	.0256	.0153	.0147

Table 2.4 MAGNETISING REACTANCE OF PERMEANCE HARMONICS WITH AND WITHOUT SKEW

	M	$(v_1 \frac{R}{p} \pm m)$	$X_M(p)$	Direction of Rotation.
Stator $X_M = 138$ Ohms.	1	25	2.67	Backward
		25	2.46	Forward
		47	1.30	Backward
		49	1.25	Forward
	m	$(v_1 \frac{R}{p} \pm m)$	$X_M(p)$	Direction of Rotation.
Rotor $X_M = 138$ Ohms.	1	35	.31	Forward
		35	.326	Backward
		69	.078	Forward
		67	.08	Backward

Table 2.5 LEAKAGE REACTANCE OF PHASE BELT HARMONICS

n	K_{sk}	β (m)	$X_M(m)$	with skew				without skew		
				X'_{2m}	X''_{2m}	$X_{d.m}$	X_{2m}	X_{2m}	X_{2m}	X_{2m}
1	.998	.895	138	2.46	.392	.21	3.1	2.44	.392	2.83
5	.987	.360	.256	1.02	.71	.003	.083	.045	.018	.054
7	.98	.36	.077	1.04	.565	.001	.044	.026	.012	.038
11	.946	.258	.02	.784	.685	.001	.026	.012	.008	.02
13	.925	.258	.014	.825	.75	.001	.028	.0123	.009	.022
17	.873	.21	.0132	.755	1.11	.002	.051	.016	.02	.035
19	.845	.21	.0176	.805	1.34	.003	.11	.031	.039	.07
23	.775	.186	.261	.845	2.36	.058	3.25	.51	1.37	1.88
25	.74	.186	.221	.93	3.72	.058	4.70	.51	1.97	2.48
29	.657	.163	.007	1.1	13.9	.002	.692	.02	.278	.298
31	.616	.163	.004	1.17	40.5	.001	1.13	.012	.42	.43
35	.527	.149	.002	1.48	5550	.03	1.97	.071	1.88	1.887
37	.482	.149	.0017	1.73	710	.032	12.5	.007	.248	.255
31	.591	.138	.002	2.46	256	.035	7.05	.01	.066	.096
43	.346	.138	.0034	3.13	246		11.5	.017	.096	.114
47	.256	.129	.0625	5.4	334		339.4	.352	1.27	1.62
49	.212	.129	.0575	7.8	470		477.8	.352	1.15	1.5

Table 2.6 SLOT HARMONIC LEAKAGE REACTANCE WITH AND WITHOUT SKEW FACTOR

(mm)	$X_{2(mm)}$	
	with skew	without skew
23	1.38	4.60
25	1.990	1.97
47	1.36	1.32
49	1.16	1.11
71	15.5	15.2
73	5.74	5.6
95	3.40	3.20
97	10.28	10.1

Table 2.7 PERMEANCE HARMONIC LEAKAGE REACTANCE WITH AND WITHOUT SKEW FACTOR

m	$X_{M(m)}$	$v_1 \frac{S}{P} \pm m$	$\frac{\sin^2 \left(v_1 \frac{S}{P} \pm m \right) p \pi}{R}$	$X_{2(mp)}$
Stator		25	0.75	1.30
Fundamental.	138	25	0.537	1.97
		47	0.675	1.27
		49	.975	1.14

m	$X_{M(m)}$	$v_1 \frac{R}{P} \pm m$	$\frac{\sin^2 \left(v_1 \frac{R}{P} \pm m \right) p \pi}{S}$	$X_{2(mp)}$
Rotor Fundamental.	138	35	0.99	2.28
		35	0.85	2.65
		69	0.154	15.3
		67	0.415	5.28

Table 2.8 ROTOR RESISTANCE OF SLOT HARMONICS WITH AND WITHOUT SKEW

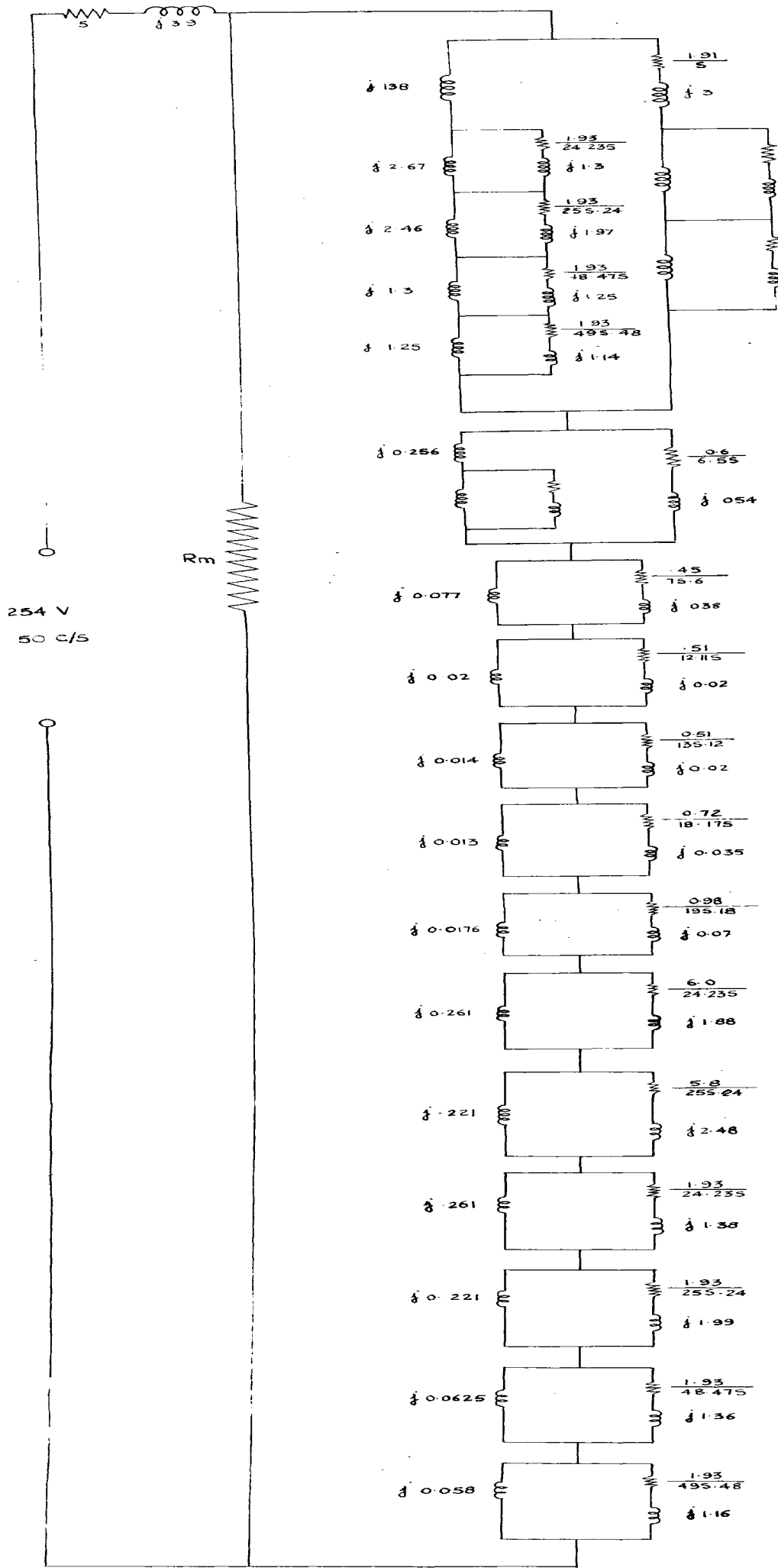
m	23	25	47	49	71	73	95	97
$R_{2(mp)}$ ohms	1.93	1.93	1.93	1.93	1.93	1.93	1.93	1.93

Table 2.9 ROTOR RESISTANCE OF PERMEANCE HARMONICS

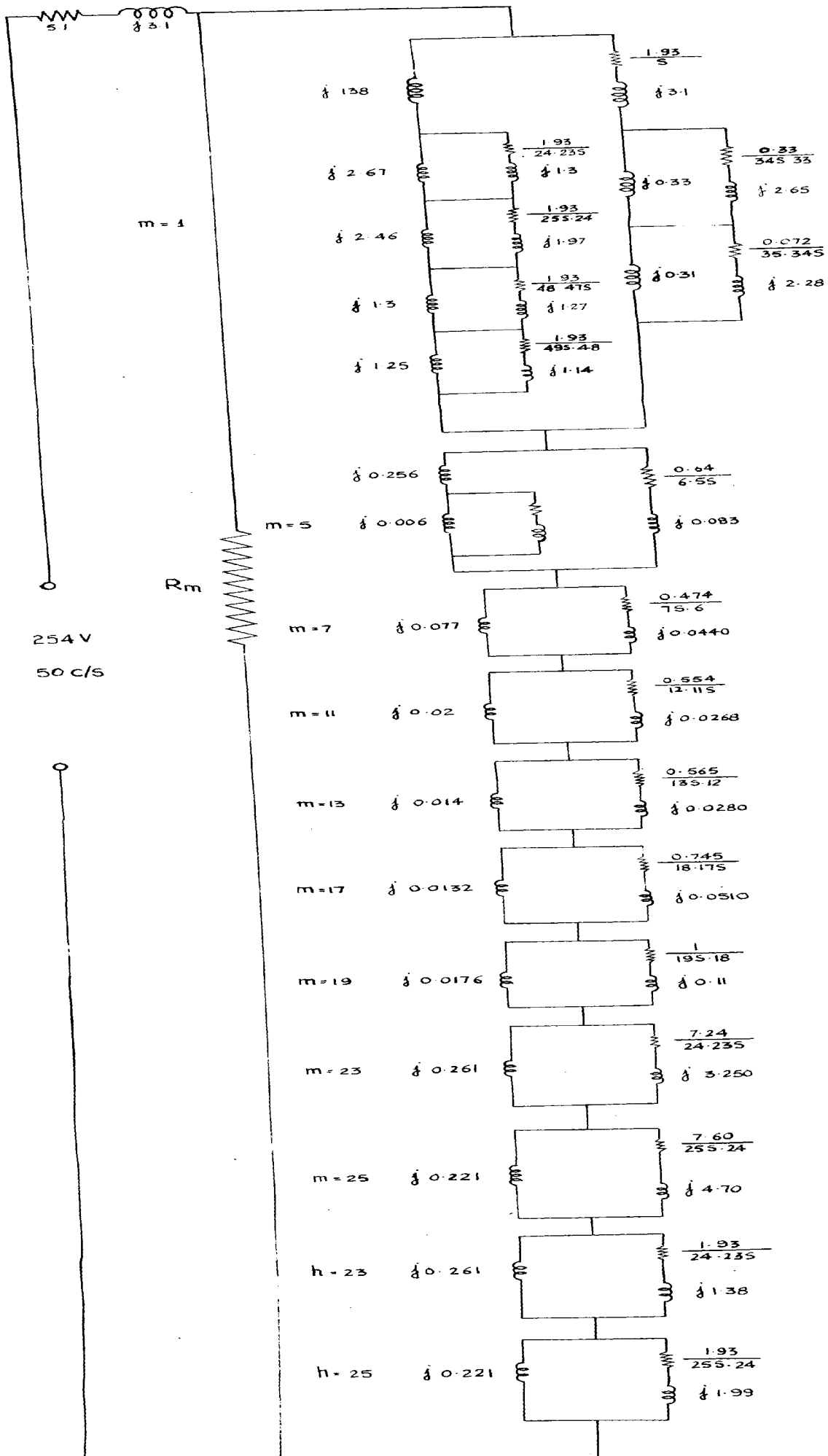
	mp	R_{2mp}		$\frac{R}{S} \pm m$
		with skew	without skew	
Stator	23	1.93	1.91	24-238
	25	1.93	1.91	25a-24
	47	1.93	1.91	48-47a
	49	1.93	1.91	49a-48
Rotor	35	0.072	0.072	34-35a
	35	0.33	0.33	35a-34

Table 2.10 ROTOR RESISTANCE OF PHASE BELT HARMONICS WITH AND WITHOUT ROTOR SKEWED

n	α_{2n} (deg.)	$28 \sin^2 \alpha_{2n} / 2$	R_{2n}	K_{2n}	$R_2^2 (n)$		a_n	Direction of rotation.
					with skew ohms	without skew ohms		
1	10.6	.717	1.025	.998	1.93	1.91	a	+
5	53	.0307	2.523	.981	.64	.60	6-5a	-
7	74.2	.0169	2.523	.98	.474	.45	7a-6	+
11	116.6	.0085	3.56	.945	.554	.515	12-11a	-
13	137.8	.0062	3.56	.925	.565	.51	13a-12	+
17	181	.0064	4.35	.873	0.8	.72	18-17a	-
19	202	.00635	4.35	.845	1.2	0.99	19a-18	+
23	244	.0085	5.05	.77	7.24	6.0	24-23a	-
25	266	.0115	5.05	.74	7.60	5.8	25a-24	+
29	308	.0318	5.61	.657	2.04	1.0	30-29a	-
31	330	.0915	5.61	0.616	1.69	0.65	31a-30	+
35	372	.56	6.15	0.527	1.87	0.64	36-35a	-
37	394	.0717	6.15	.482	1.89	0.50	37a-36	+
41	416	.0278	6.65	.391	3.1	0.50	42-41a	-
43	457	.0109	6.65	.346	4.6	0.58	43a-42	+
47	500	.0069	7.14	.256	31.0	2.0	48-47a	-
49	521	.0065	7.14	.212	37.4	2.0	49a-48	+
53	564	.0064	7.55	.129	13.9	0.20	54-53a	-
55	585	.0072	7.55	0.09	15.25	0.13	55a-54	+
59	626	.0115	7.92	0.0169	21.0	.018	60-59a	-
61	648	.0178	7.92	.0164	21.7	.020	61a-60	+
65	690	.0915	8.24	.076	20.0	.12	66-65a	-



GENERAL EQUIVALENT CIRCUIT OF INDUCTION MACHINE
 (ROTOR UNSKEWED PARAMETERS)
 FIGURE 2.15



GENERAL EQUIVALENT CIRCUIT OF INDUCTION MACHINE
(ROTOR SKEWED PARAMETERS)

FIGURE 2.14

CHAPTER III

COMPUTATION OF ASYNCHRONOUS PARASITIC TORQUES OF INDUCTION MACHINE WITH ROTOR SKEWED AND UNSKEWED

The term parasitic torques includes all those torques produced by mmf wave except that of fundamental. As investigated (Chapter I) superimposed upon the currents due to the fundamental sine wave field of an induction machine, there are smaller harmonic currents produced by the myriad of harmonic fields.

In the induction motor, the rotor is not connected to the line. The main mmf wave (fundamental) of the stator produces an mmf waves in the rotor which has the same number of poles as the stator wave and which is at stand still with respect to the stator wave at any speed of the rotor and so also the other harmonics. Fundamental produces the useful torque of the machine whereas the torque produced of this kind by harmonics is called Asynchronous Parasitic torques.

In addition to asynchronous torque, there are other torques too, e.g. Synchronous torques and stray torques which will be discussed under separate heads.

As the harmonic fields have more poles, therefore asynchronous torques occur at sub-synchronous speed. As the motor accelerates through the asynchronous speed of one of these harmonic fields the harmonic torque reverses causing a dip in the resultant torque-speed curve. Unless minimized by good design, the consequent asynchronous crawling may seriously impair the motor's starting ability. As discussed further in detail,

the skew reduces the asynchronous torque to some extent.

As discussed under Chapter II, the harmonic fields are equivalent to low-power motors connected to the same shaft and electrically connected in series (Fig. 2-15). The asynchronous torque increase the motor heating too much. Theoretical approach to the problem is directed here and then based upon these conventional results, extensive calculation has been undertaken to verify the results.

3.1. PRODUCTION OF ASYNCHRONOUS TORQUE

The stator mmf equation from (1-11):

$$f_s(\theta, t) = F_m \sum \cos (m p \theta \mp \omega t) \quad \dots (3-1)$$

$$f_r(\theta, t) = F'_m \sum \cos \left[\pm \left\{ 1 + (n-m)(1-s) \right\} \omega t + n p \theta \right] \quad (3-2)$$

Power developed in air gap is $\propto B^2$ (by Kelvin's Law)

$$P_d = \bar{C} f_s(\theta, t) \times f_r(\theta, t)$$

$$P_d = \int_0^{2\pi} p_d d\theta = \int_0^{2\pi} \bar{C} F_m \sum \cos (m p \theta \mp \omega t) F'_m \sum \cos \left\{ n p \theta \pm \left[1 + (n-m)(1-s) \right] \omega t \right\} \dots (3.3)$$

where $\bar{C} = \text{constant}$.

$P_d = 0$ If $m \neq n$
 $P_d = \text{definite value}$ If $m = n$

Equation 3.3. reflects that torque can be produced by harmonics of the same order existing separately in stator and rotor respectively. There is no torque possible between two harmonics of unequal order.

Since $n = \text{rotor harmonic order.} = \pm \frac{R}{p} + n \quad \dots (3-4)$

Equation 3-4 (determined under Chapter I) gives rise to two cases viz:

Case 1 : When $v_2 = 0$

then $n = m$ i.e every stator harmonic induces in rotor circuit the equal order of harmonic rotating in the same direction. The torque produced by locking of such two harmonics is named as Asynchronous torque.

Case 2 : When $v_2 = k_2$ (any integer excluding zero)

then $n = \pm v_2 \frac{R}{p} \pm m_1$ (3.5)

When $n = m_2$

Thus there is torque when n is given by (3.5) locks with stator harmonic m_2 . The torque of this kind as already stated is marked as 'asynchronous torque and will be dealt with fully in next Chapter.

Taking up Case 1 when $n = m$ substituting it in equation 3.1 and 3.2, Power developed is

$$P_d \propto F'_n F'_m \cos^2 (n\theta \pm \omega t) \quad (3.6)$$

Equation 3.6 shows, Asynchronous torque thus produced by first order stator and first order ($v_2 = 0$) rotor harmonics is independent of slip. It will be there at every speed of the motor. The nature of Harmonic Asynchronous torque is approximately the same as of fundamental torque / speed curve.

The harmonic (equation 2-31) s_m is :

$$s_m = 1 \pm m (1-s)$$

When harmonic slip becomes zero

$$1 \pm m(1-s) = 0$$

$$\text{then Slip} = 1 \pm 1/m = \frac{N_s - N_r}{N_s} = 1 - \frac{N_r}{N_s}$$

$$\therefore N_r = \mp N_s (1/m) \tag{3.7}$$

i.e., harmonic slip is zero when rotor attains 1/m th of synchronous then torque produced by harmonic 'm' becomes zero and for speed greater than 1/m the torque reverses its direction (See Fig. 3-1).

3.2. MAGNITUDES OF HARMONIC ASYNCHRONOUS TORQUES

The general equivalent circuit for the squirrel cage induction machine dealt under Chapter II, in author's view will be the correct approach to the determination of complex phenomena of torque developed by individual harmonics in certain speed range. Adnan Odok⁽¹¹⁾, simplifies the general equivalent circuit like Fig. (3-2)

$$V_1 = \bar{I}_1 (R_1 + jX_1) + \bar{V}_F + \sum_{m=1}^{\infty} \bar{V}_{1m} \tag{3.8}$$

The torque of mth harmonic

$$T_{(m)} = \frac{R_{2m} (\bar{I}_1 \bar{V}_{1m}^*)}{\omega_{sm}}$$

When

ω_{sm} = Angular velocity of the mth harmonic.

$$\bar{V}_{1m} = \bar{I}_1 \frac{j X_{M2m} (R_{2m}/s_m + j X_{2m})}{\frac{R_{2m}}{s_m} + j (X_{M2m} + X_{2m})} \tag{3.9}$$

He assumes I_1 (current) to be constant, and then by finding the locus diagram of the voltage, torque at different speed is determined. In author's view it is over simplification of the equation (3.9) since current I_1 varies with rotor speed too much as clear from circle locus of the

When harmonic slip becomes zero

$$1 \pm m(1-s) = 0$$

then Slip = $1 \pm 1/m = \frac{N_s - N_r}{N_s} = 1 - \frac{N_r}{N_s}$

$$\therefore N_r = \mp N_s (1/m) \tag{3.7}$$

i.e., harmonic slip is zero when rotor attains 1/m th of synchronous then torque produced by harmonic 'm' becomes zero and for speed greater than 1/m the torque reverses its direction (See Fig. 3-1) .

3.2. MAGNITUDES OF HARMONIC ASYNCHRONOUS TORQUES

The general equivalent circuit for the squirrel cage induction machine dealt under Chapter II , in author's view will be the correct approach to the determination of complex phenomena of torque developed by individual harmonics in certain speed range. Adnan Odok⁽¹¹⁾ , simplifies the general equivalent circuit like Fig. (3-2)

$$V_1 = \bar{I}_1 (R_1 + jX_1 + \bar{V}_P + \sum_{n>1}^{\infty} V_{1n} \tag{3.8}$$

The torque of nth harmonic

$$T_{(n)} = \frac{K_n (\bar{I}_1 \bar{V}_{1n}^*)}{\omega_{2n}}$$

When

ω_{2n} = Angular velocity of the nth harmonic.

$$\bar{V}_{1n} = \bar{I}_1 \frac{j X_{Mn} (R_{2n}/s_n + j X_{2n})}{\frac{R_{2n}}{s_n} + j (X_{Mn} + X_{2n})} \tag{3.9}$$

He assumes I_1 (current) to be constant, and then by finding the locus diagram of the voltage, torque at different speed is determined. In author's view it is over simplification of the equation (3.9) since current I_1 varies with rotor speed too much as clear from circle locus of the

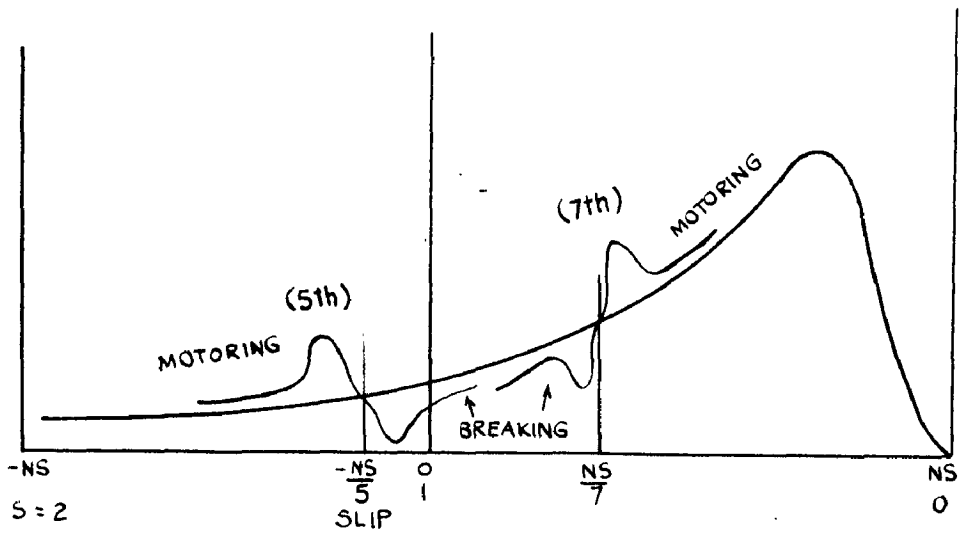


FIGURE 3.1

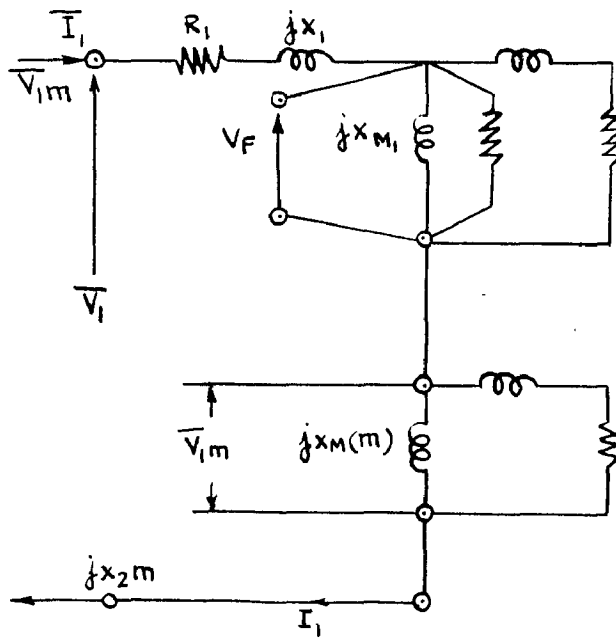


FIGURE 3.2

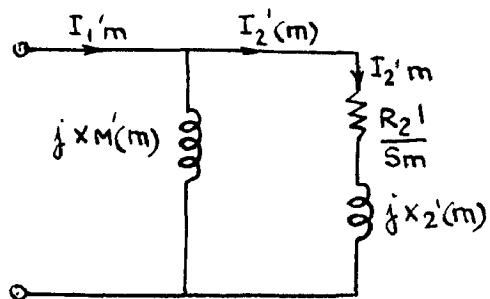


FIGURE 3.3

induction machine. Therefore the author takes the more complicated but more dependable way of finding the harmonic asynchronous torque. The method of attack can be outlined as:

1. Solution of the General equivalent circuit for different slips.
2. Then using the currents so computed for different slips to get harmonic torques.

The torque of the main wave is :

$$T_1 = \frac{I_2^2 R_2}{s}$$

↑

(Referred to primary) $T_1 = I_2' \frac{R_2'}{s}$ watts (3.10)

The squirrel cage rotor does not distinguish between the main wave and the harmonics therefore (3-10) must also apply to the harmonic torques, substituting harmonic values

$$T_{(m)} = \frac{I_{2m}'^2 R_{2m}'}{s_m} \text{ watts} \quad (3.11)$$

Where all the secondary values subscripted with dash and for per bar.

If

I_{1m}' Primary current referred to secondary per bar.

I_{2m}' = Bar current (secondary)

Then from Fig. (3.3)

$$I_{2(m)}' \left[\frac{R_{2m}'}{s_m} + j X_{2(m)}' \right] - \left[I_{1m}' - I_{2(m)}' \quad j X_{M(m)}' \right] = 0$$

$$I_{2(m)}' = \frac{1}{(1 + \tau_{2m}') - j \left(\frac{R_{2m}'}{s_m} \right) / X_{M(m)}'} I_{1m}' \quad (3.12)$$

But $I_{1m}' = \left(\frac{2m_1 N_1 k_{w1m}}{R K_{sm}} \right) I_1$ (3.13)

and reduction factor for impedance from per bar to 'total secondary referred to Primary' value is ⁽⁵⁾

$$RF = \frac{4n_1(N_1 k_{w1m})^2}{R K_{sm}^2} \quad \text{with respect to any wave } (\bar{m}) \quad (3.14)$$

Substituting (3-12) in equation (3.11), and (3.13)

$$T_{(m)} = R_{2m} \left(\frac{s_m X_M^2(m)}{R_{2(m)}^2 + s_m^2 (1 + T_{2m})^2 X_M^2(m)} \right) n_1 I_1^2 \quad \text{watts} \quad (3.15)$$

3.3. FULL OUT SLIP AND FULL OUT TORQUE DEVELOPED

I_1 is complicated function of harmonic slip (s_m), but since the parasitic torque occur at high slips and at high slips primary current can be assumed constant ⁽⁵⁾ to a fair degree of accuracy. In order to find maximum torque (pull out torque) of m th wave, differentiate equation (3.15) taking I_1 constant. Then

$$s_{m \text{ p.o.}} = \frac{R_{2(m)}}{(1 + T_{2m}) X_M(m)} \quad (3.16)$$

and maximum asynchronous torque:

$$T_{m(max)} = \frac{X_M(m)}{(1 + T_{2m})} I_1^2 \quad \text{watts per phase} \quad (3.17)$$

Full out slip defined in terms of fundamental slip is

$$s_{p.o.(m)} = \frac{(m-1)(1 + T_{2m}) X_M(m) + R_{2(m)}}{m(1 + T_{2m}) X_M(m)} \quad (3.18)$$

Neglecting $R_{2(m)}$

$$s_{p.o.(m)} \approx (1 - 1/m) \quad (3.19)$$

3.4. DETERMINATION OF CURRENT SLIP CURVE

The general equivalent circuit of Fig. (2-14) and (2-15) is solved for different values of slip in the range of slip zero to slip two (motoring and braking regions). The calculated results with partial calculations are included in Table (3.1) to Table (3.2). Calculated results are plotted in Figure (3.5) curve 2, Fig. 3.4 curve 2. Curves are found taking into account the skew, and another set considering rotor unskewed.

3.5. DETERMINATION OF HARMONIC ASYNCHRONOUS TORQUE

Calculations for relevant harmonics, which are likely to affect the performance considerably are calculated with the equations dealt 3.1. through 3.19. The calculated results so obtained are plotted on graph and partial calculations carried out are tabulated. Curves of slip, speed, power factor, current developed torque are given in Fig. 3.4 to Fig. 3.10 and Tabulation of Table (3.3) to Table (3.6) shows the results of harmonic torque. Pull out torque and pull out slip for harmonics.

Table 3.1 - DETERMINATION OF CURRENT POWER FACTOR OF GENERAL E UNVALUED CIRCUITS FOR DIFFERENT SLIPS

Slip	Z_{eq}	Z/θ	I	cos θ	Fundamental torque	Total torque	Total harmonic torque
0.0	5.05+j143.17	143.4/87.9	1.77	0.04	0	0	0
0.1	23.35+j9.46	25.0/22.2	10.15	0.93	1935.0	193.0	-5.0
0.2	24.31+j9.29	17.0/32.7	15.0	0.845	2081.0	207.0	-11.0
0.3	11.21+j 8.28	14.0/36.4	18.1	0.80	2028	201.0	-18.0
0.4	9.70+j 8.21	12.65/40.3	20.0	0.765	1887	186.0	-17.0
0.5	8.58+j 8.14	11.8/43.5	21.50	0.735	1731	170.0	-31.0
0.6	8.16+j 8.11	11.6/41	22.0	0.727	1528	149.0	-38.0
0.7	7.71+j 8.22	11.3/46.8	22.5	0.685	1377	133.5	-44.0
0.8	7.42+j 8.28	11.15/48.2	22.8	0.67	1346	128.5	-61.0
0.9	7.16+j 8.34	11.0 / 49.2	23.0	0.65	1193	113.5	-58.0
1.0	6.95+j 8.20	10.75/ 49.7	23.6	0.65	1105	105.0	-50.0
1.1	6.73+j 8.23	10.6 / 50.7	24.0	0.625	1003	96.6	-37.0
1.2	6.55+j 8.23	10.5 / 51.5	24.2	0.675	920	90.5	-15.0
1.3	6.32+j 8.2	10.34/ 52.3	24.6	0.59	844	86.0	+16.0
1.4	6.25+j 8.16	10.3 / 52.6	24.6	0.59	763	80.0	+37.0
1.5	6.14+j 8.12	10.2 / 53.0	24.8	0.6	719	76.5	+ 46.0
1.6	6.06+j 8.07	10.0/ 53.1	25.4	0.6	695	75.0	+55.0
1.7	5.9 +j 8.08	10.0/ 54.0	25.4	0.59	652	70.0	+48.0
1.8	5.95+j 8.0	10.0/ 53.4	25.4	0.6	622	66.5	+33.0
1.9	5.96+j 8.0	9.95/ 53.2	25.5	0.6	605	63.5	+30.0
2.0	5.86+j 8.0	9.91/ 53.7	25.6	0.59	580	60.5	+30.0

Table 3.2 SOLUTION OF GENERAL EQUIVALENT CIRCUIT WITHOUT SKIN

βl	$X + Y$	I	$\cos \theta$
0.05	39.65 + j 17.07	5.8824	.91
0.10	23.27 + j 10.24	9.98	.91
0.15	17.31 + j8.9	13.04	.88
0.2	14.28 + j8.43	15.31	0.86
0.25	12.45 + j8.21	17.02	0.83
0.3	11.22 + j8.1	18.3	0.81
0.35	10.35 + j8.03	19.3	0.79
0.4	9.69 + j 7.9	20.2	0.77
0.45	9.18 + j 7.9	20.87	0.75
0.5	8.78 + j 7.9	21.4	0.74
0.55	8.45 + j 7.95	21.89	0.72
0.6	8.17 + j 7.9	22.2	0.71
0.65	7.9 + j 7.9	22.59	0.70
0.7	7.74 + j 7.9	22.8	0.69
0.75	7.57 + j7.9	23.29	0.68
0.8	7.43 + j7.9	23.45	0.68
0.85	7.29 + j 7.9	23.45	.67
0.9	7.18 + j 8.0	23.58	0.66
0.95	7.08 + j 8.07	23.64	0.66
1.0	7.0 + j8.0	23.7	0.65

Contd..

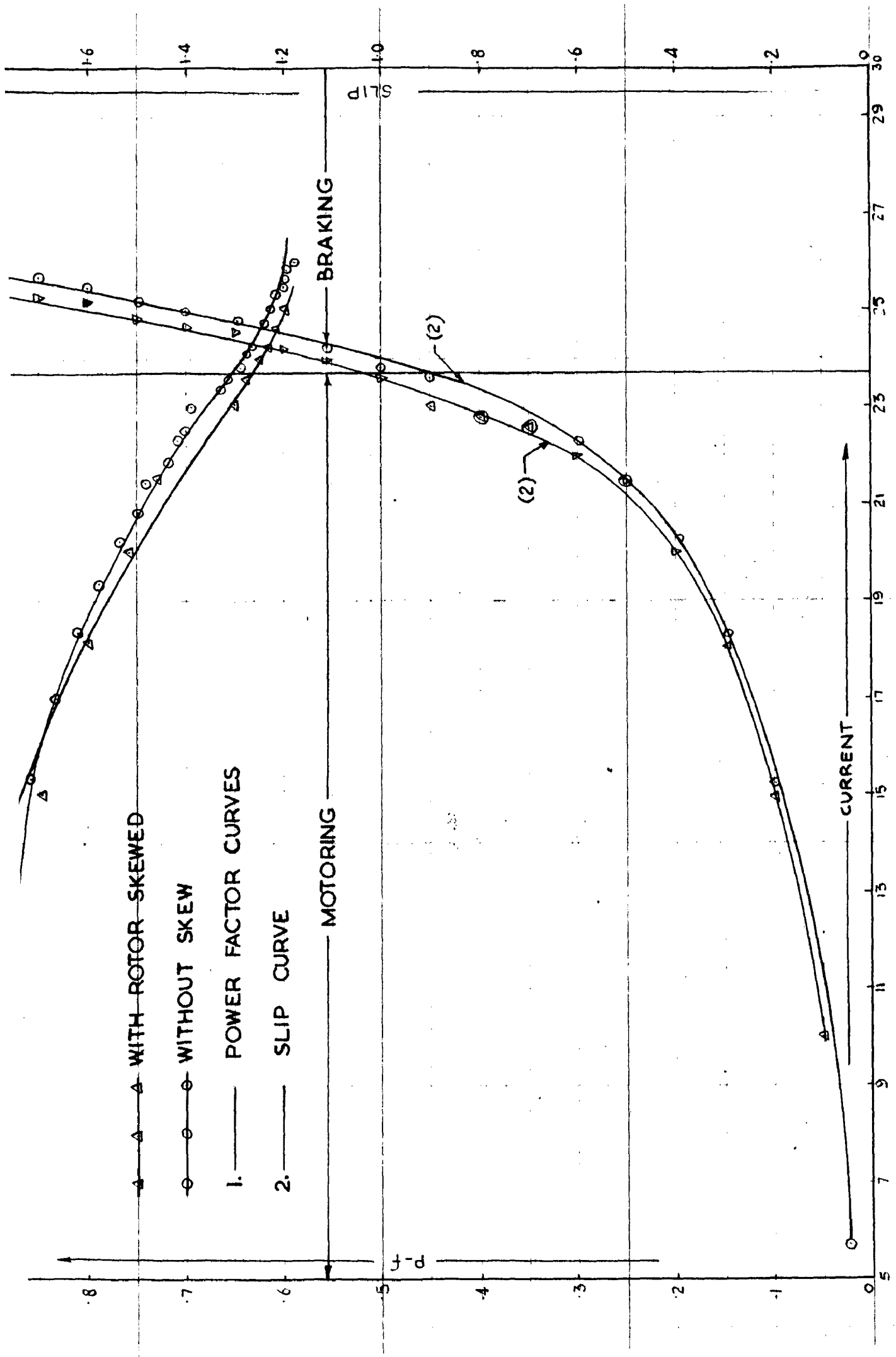
Slip	X + Y	I	Cos θ
1.05	6.866 + j 8.1	23.89	.64
1.1	6.73 + j 8.0	24.12	.64
1.15	6.64 + j 8.0	24.29	0.63
1.25	6.46 + j 8.0	24.6	.62
1.3	6.38 + j 8.0	24.75	.62
1.35	6.31 + j 8.0	24.9	.61
1.4	6.25 + j 7.9	25.0	.61
1.45	6.19 + j 7.9	25.2	.61
1.5	6.14 + j 7.9	25.3	.61
1.55	6.1 + j 7.9	25.39	.61
1.6	6.0 + j 7.9	25.49	.6
1.65	6.03 + j 7.8	25.57	.60
1.7	6.0 + j 7.8	25.65	.6
1.75	5.9 + j 7.8	25.7	.6
1.8	5.9 + j 7.8	25.78	.6
1.85	5.9 + j 7.8	25.84	.6
1.9	5.9 + j 7.8	25.89	.6
1.95	5.8 + j 7.8	25.94	.6
2.0	5.8 + j 7.8	25.99	.59

Table 3.3 HARMONIC ASYN. TORQUES (ROTOR SKEWED)

Slip	5th	7th	11th	13th	17th	23rd belt	25th belt	23rd slot	25th slot
0.0	-17	-	-	-	-	-	-	-2	-
0.1	-6.75	-2.42	-2	-	-.14	-	-	+.56	-.24
0.2	-14.8	-5.5	-1.3	-	-.3	-	-	-.9	-.4
0.3	-22.2	-8.0	-1.4	-	-.44	-	-	-1.3	-.55
0.4	-30.5	-9.6	-2.0	-.7	-.55	-	-.4	-1.8	-
0.5	-38.5	-10.1	-1.7	-	-6.1	-	-	-2.2	-
0.6	-43.6	-9.0	-1.6	-.7	-.60	.2	-.8	-3.1	-1.0
0.7	-48.0	-6.5	1.4	-	-	-.3	-	-4.3	1.5
0.8	-54.0	-1.0	-1.0	-.3	-.5	-3.75	1.75	-7.0	-2.4
0.9	-51.5	-.5	-.75	-	-	-5.1	-2.6	-11.3	-5.6
1.0	-45.0	7.95	.3	.2	.1	-4.4	+2.5	+11.9	+6.1
1.1	-28.4	10.5	-	-	-	5.5	2.2	7.2	2.9
1.2	0	13.4	-	.73	.3	5.5	1.4	4.9	1.8
1.3	29.4	14.4	.53	-	.86	4.0	-	3.6	1.3
1.4	48.5	15.0	1.0	-	.65	-	.8	3.2	1.0
1.5	59.0	14.8	1.4	-	-	-	-	2.5	.9
1.6	67.4	15.2	1.73	1.37	.9	-	.6	2.1	.8
1.7	61.5	14.6	2.1	-	-	-	-	1.8	.6
1.8	58.0	14.0	2.2	-	.9	-	.5	1.6	.6
1.9	53.5	13.5	2.4	-	-	-	-	1.4	.5
2.0	50.0	12.7	3.0	1.64	.85	.13	.35	1.3	.5

Table 3.4. HARMONIC ASYN. TORQUES WITHOUT SKEW

lp	Fund.	5th	7th	11th	23rd belt	25th belt	23rd slot	25th slot	Total torque	Total H. torque
1	1196.7	-2.23	-.84	-.17	-.13	0.0	0.0	0.0	1193.0	-5.7
	1818.6	-6.6	-2.47	-.49	-.4	-.2	-.2	0.0	1808	-10.6
	2164.2	-16.8	-6.0	-1.13	-1.0	-.5	-.6	-.2	2143	-21.0
	2075.5	-26.0	-8.6	-1.5	-1.7	-.8	-1.0	-.4	2030	-45.5
	1890.0	-34.2	-10.2	-1.78	-2.4	-1.1	-1.3	-.5	1839	-61.0
	1702	-41.6	-10.6	-1.84	-3.1	-1.5	-1.8	-.7	1641	-61.0
	1532	-48.5	-9.5	-1.7	-4.0	-2.1	-2.3	-1.0	1464	-68.0
	1385.4	-54.3	-6.9	-1.5	-5.2	-2.9	-3.1	-1.5	1310	-75.0
	1258.0	-58.4	-2.77	-1.2	-7.0	-4.1	-4.5	-2.5	1178	-80.0
	1146	-58.1	2.14	-.8	-8.7	-4.6	-7.3	-5.4	1063	-84.0
	1042.5	-49.5	6.82	-.4	-5.6	3.8	-11.5	6.18	992	-50.0
	980	-30.0	10.8	0	7.0	4.7	-13.0	3.0	972	13.0
	935	0.0	13.7	0.5	9.3	3.5	-7.9	1.9	963	28.0
	884.5	+33.4	15.5	1.0	7.7	2.7	-4.9	1.4	947	63
	839.3	56.4	16.3	1.5	6.1	2.2	-3.7	1.1	923	84
	797.1	67.5	16.5	2.0	5.1	1.8	-2.96	-.9	894	97
	757.9	70.2	16.3	2.4	4.4	1.6	-2.47	-.8	854	97
	721.7	68.6	15.8	2.7	3.7	1.4	-2.13	.7	816	95
	688	64.9	15.2	2.9	3.3	1.2	-1.89	.6	776	88
	656	60.7	14.6	3.1	3.0	1.0	-1.66	.5	738	82



▲ WITH ROTOR SKEWED

○ WITHOUT SKEW

1. ——— POWER FACTOR CURVES

2. ——— SLIP CURVE

MOTORING

BRAKING

CURRENT

1.6

1.4

1.2

1.0

0.8

0.6

0.4

0.2

0

0.8

0.7

0.6

0.5

0.4

0.3

0.2

0.1

0

30 29 27 25 23 21 19 17 15 13 11 9 7 5

P.F.

SLIP

(2)

(2)

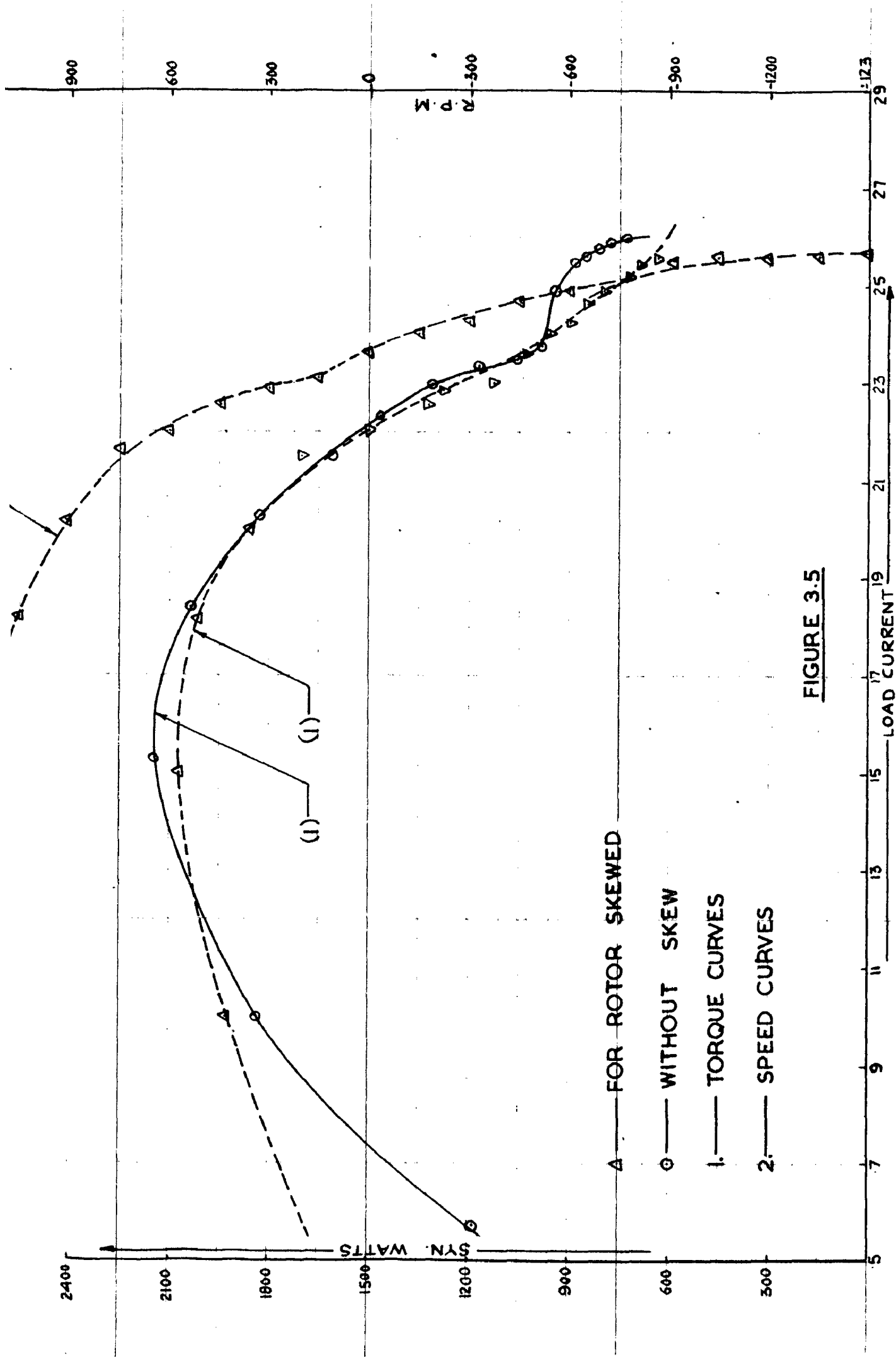
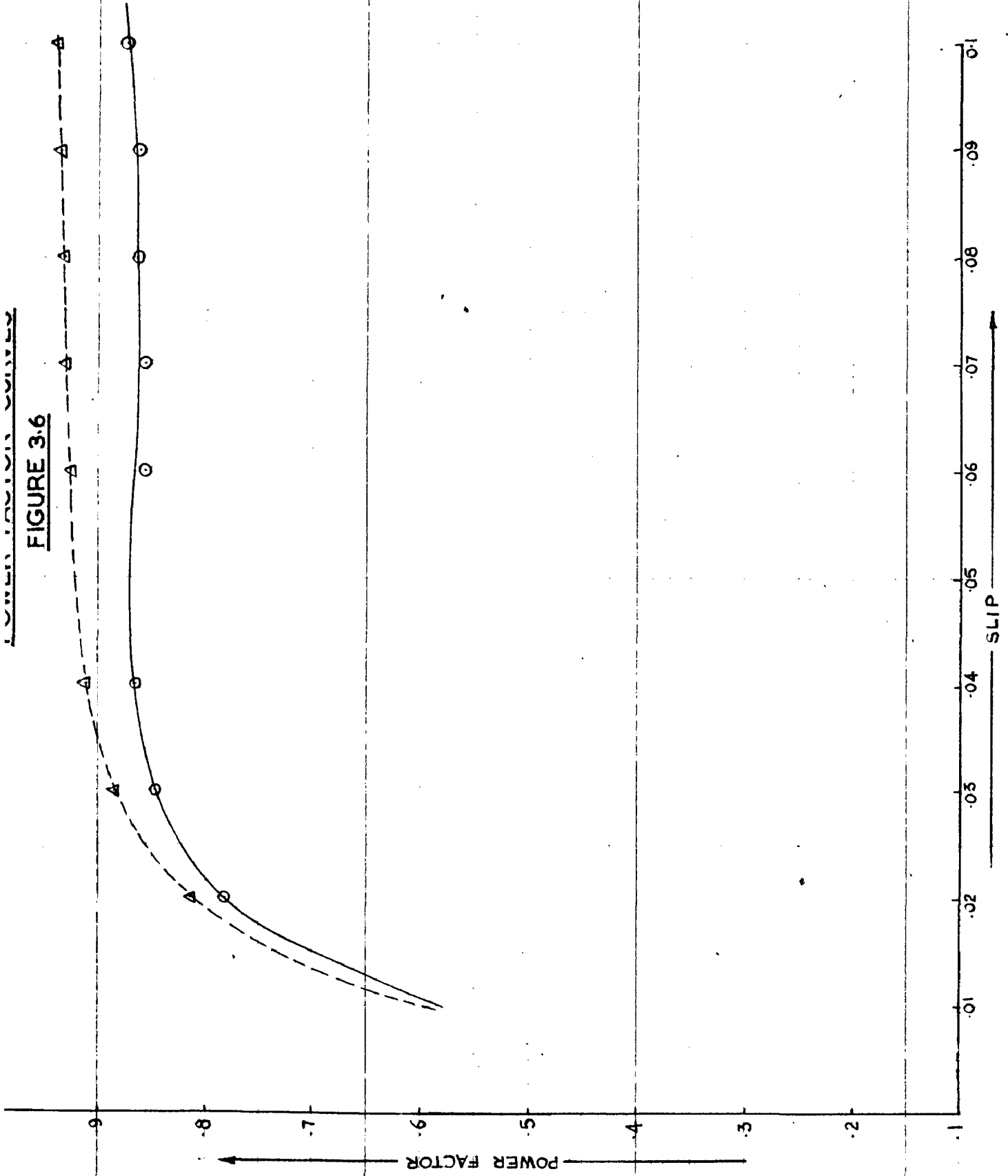


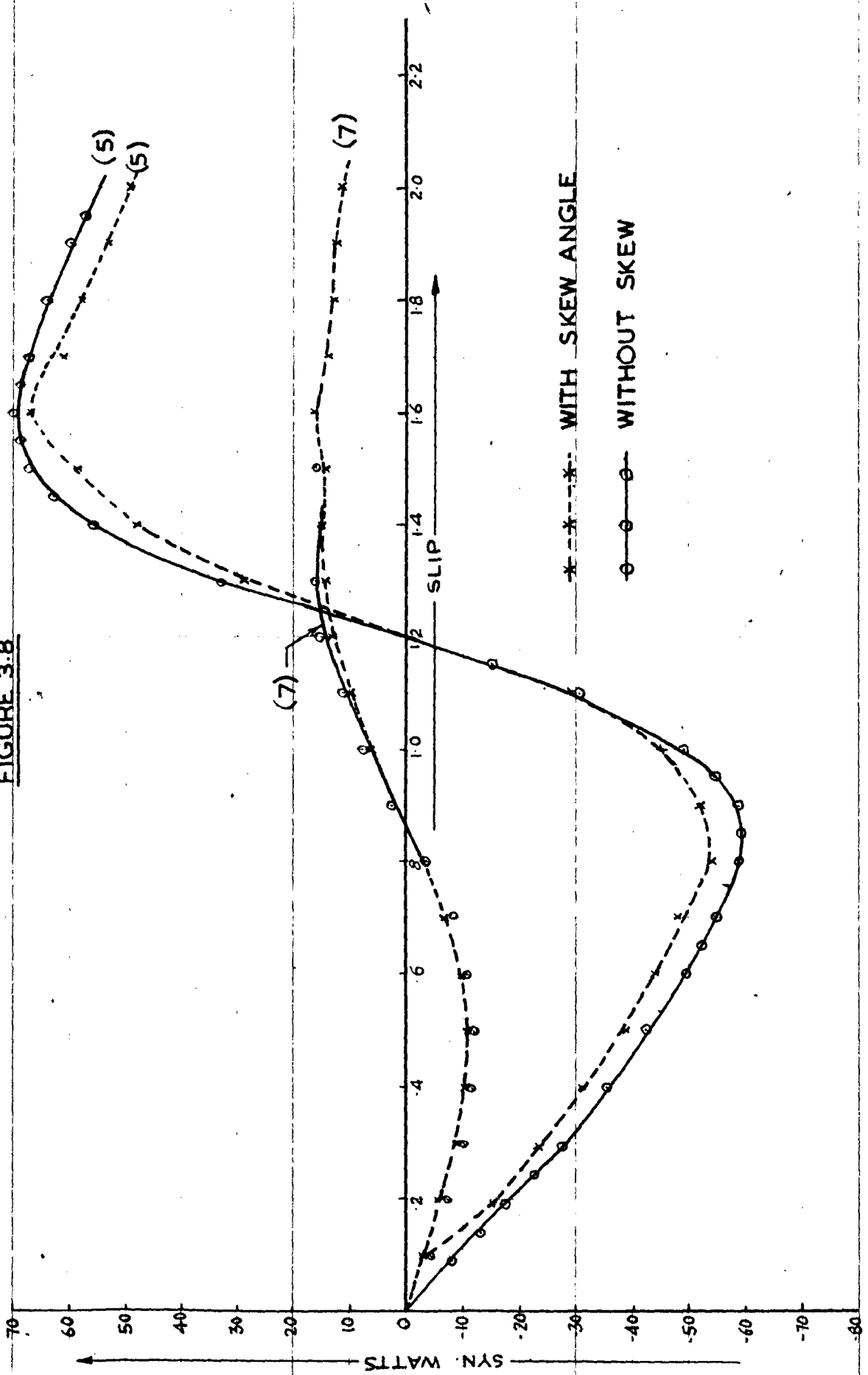
FIGURE 3.5

FIGURE 3.6



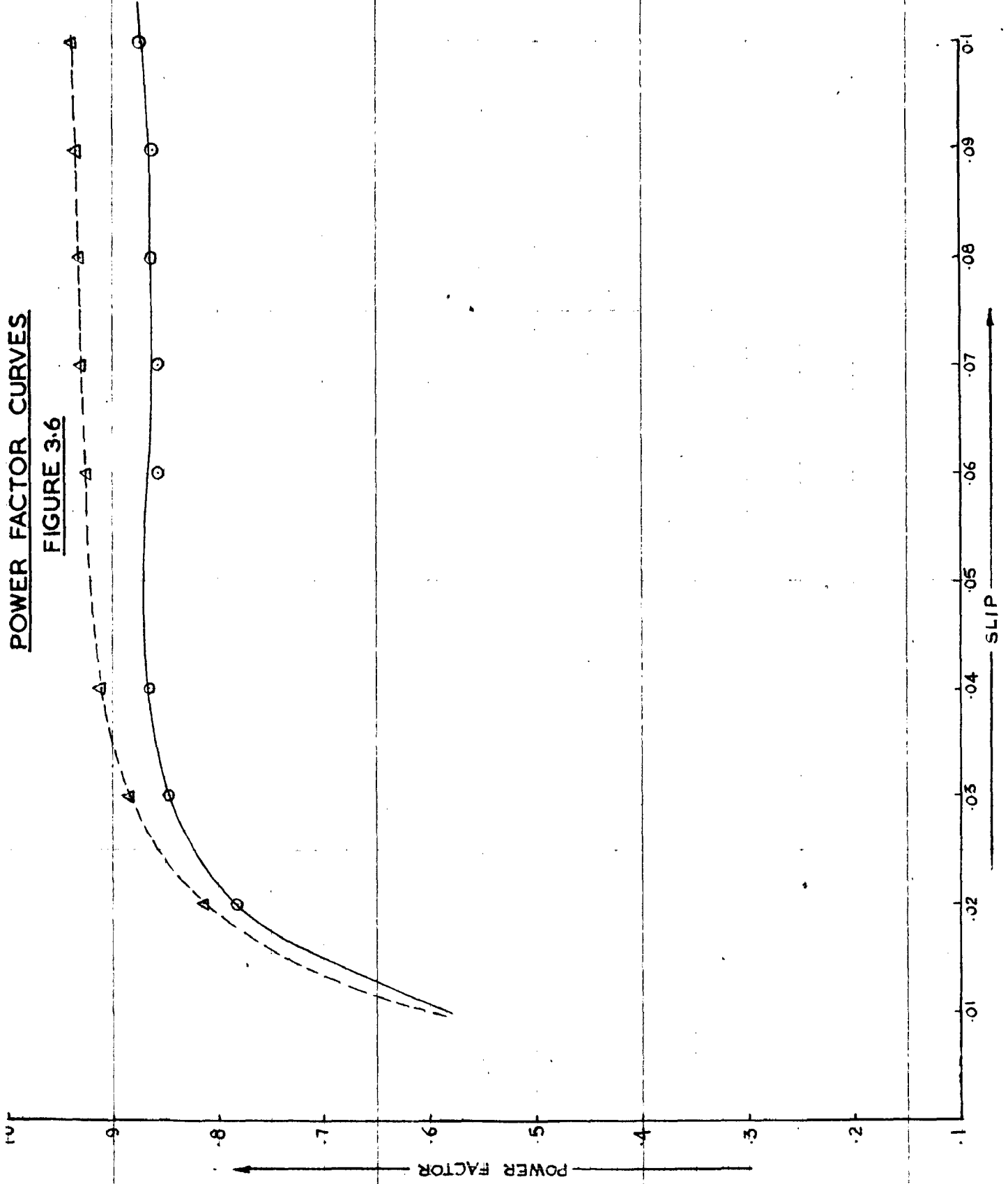
TORQUE SLIP CURVES OF 5TH AND 7TH HARMONICS

FIGURE 3.8



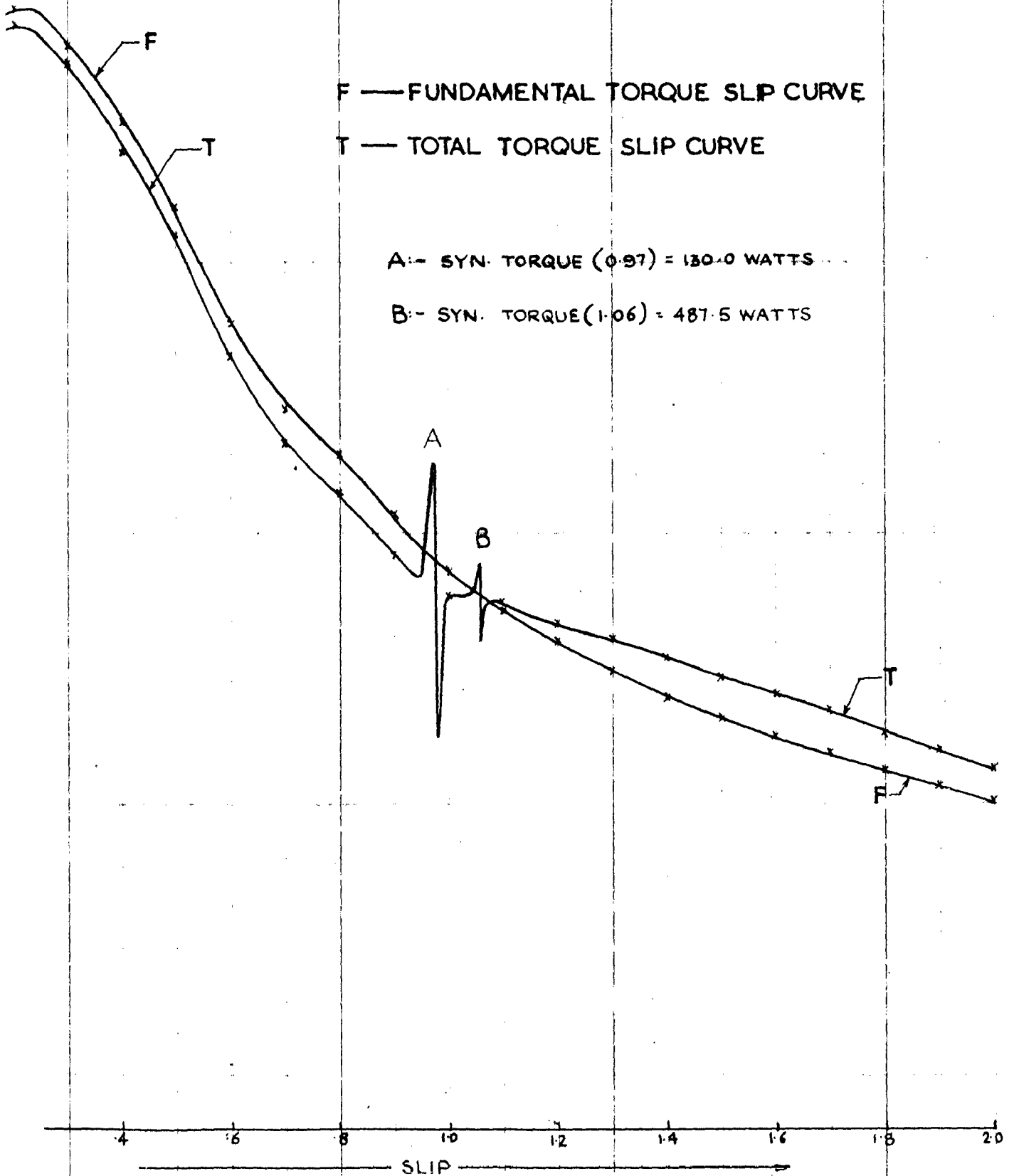
POWER FACTOR CURVES

FIGURE 3.6



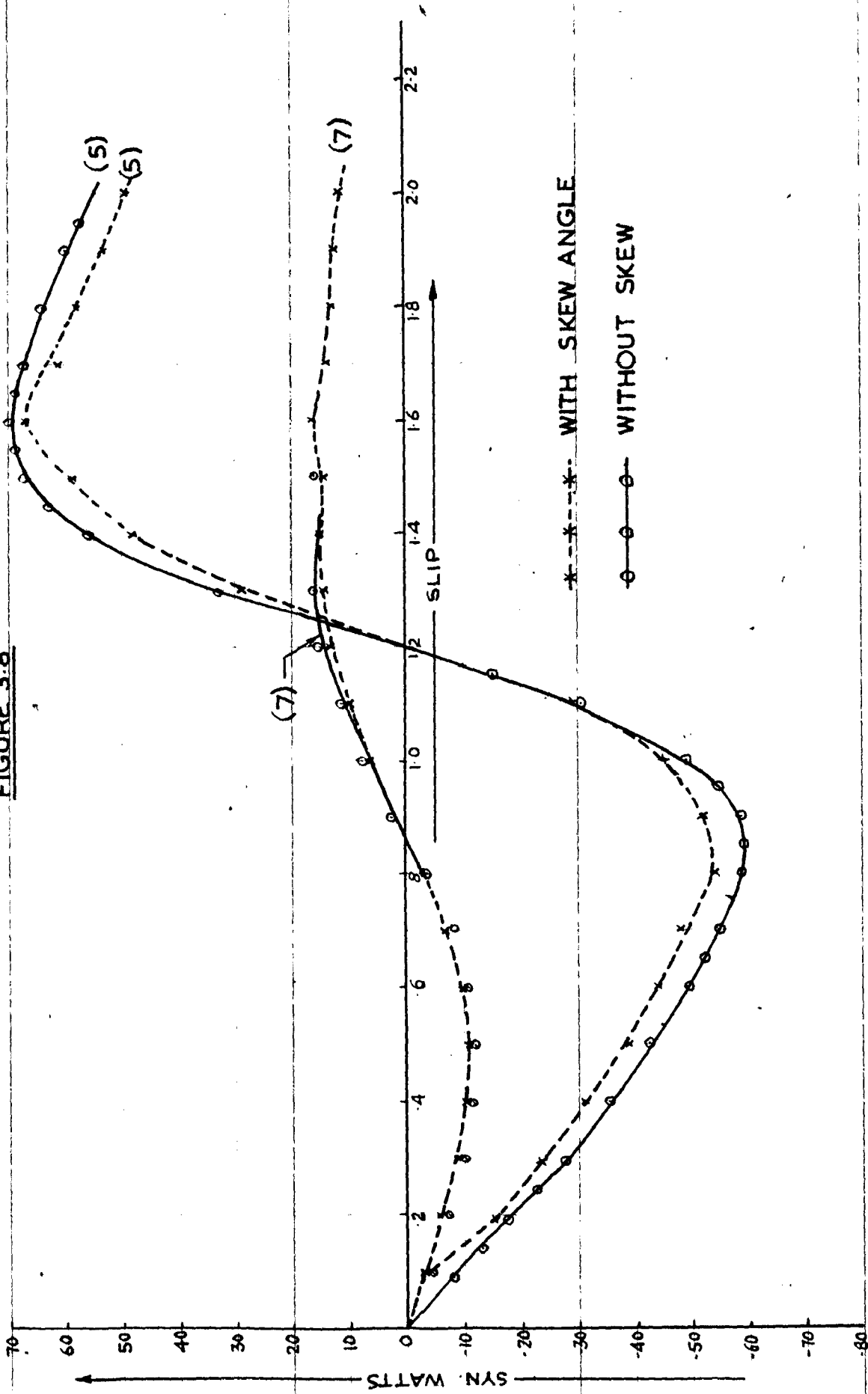
TORQUE SLIP CURVES WITH SKEW

FIGURE 3.7



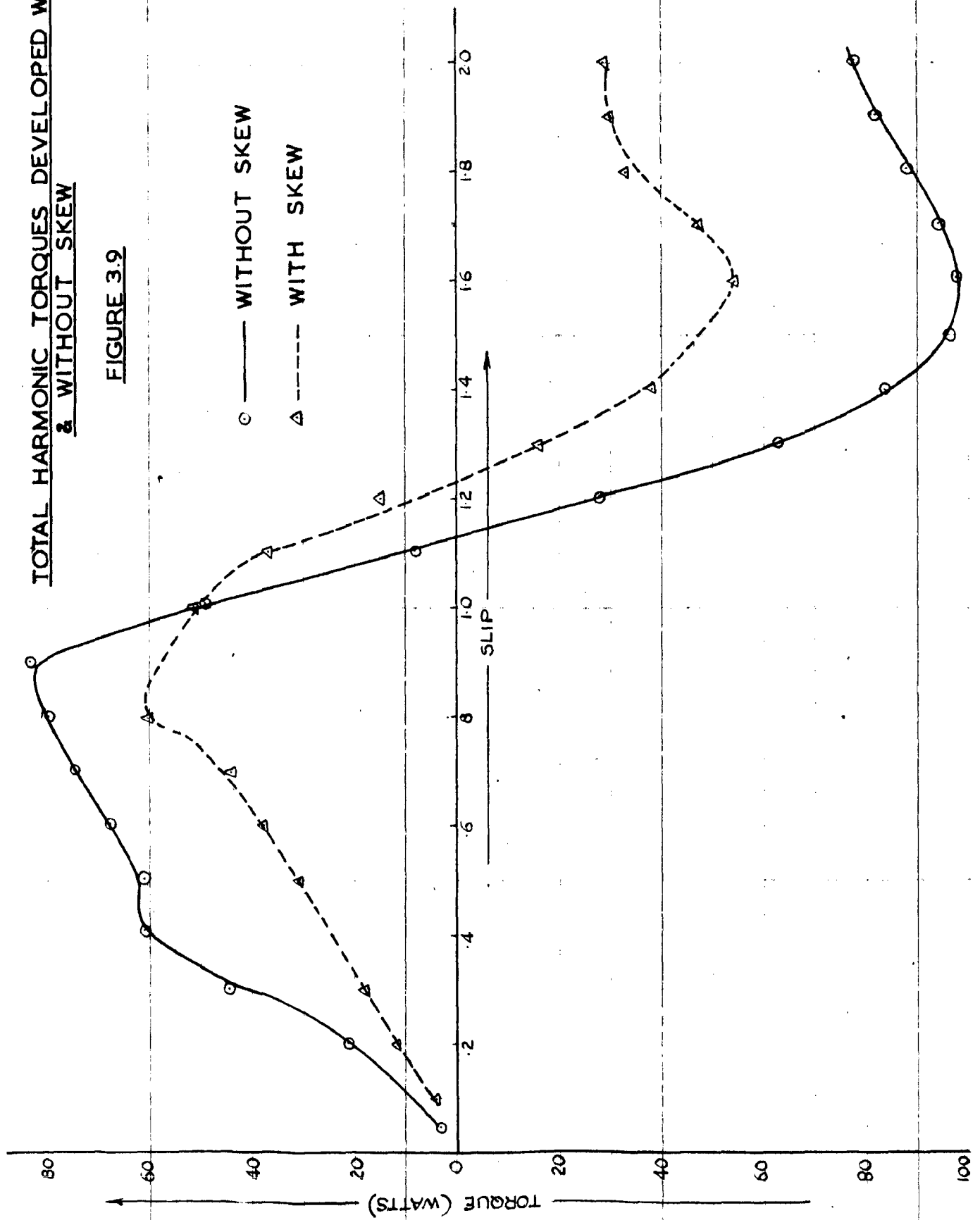
TORQUE SLIP CURVES OF 5TH AND 7TH HARMONICS

FIGURE 3.8



TOTAL HARMONIC TORQUES DEVELOPED WITH
& WITHOUT SKEW

FIGURE 3.9



TORQUE SLIP CURVES
WITHOUT SKEW

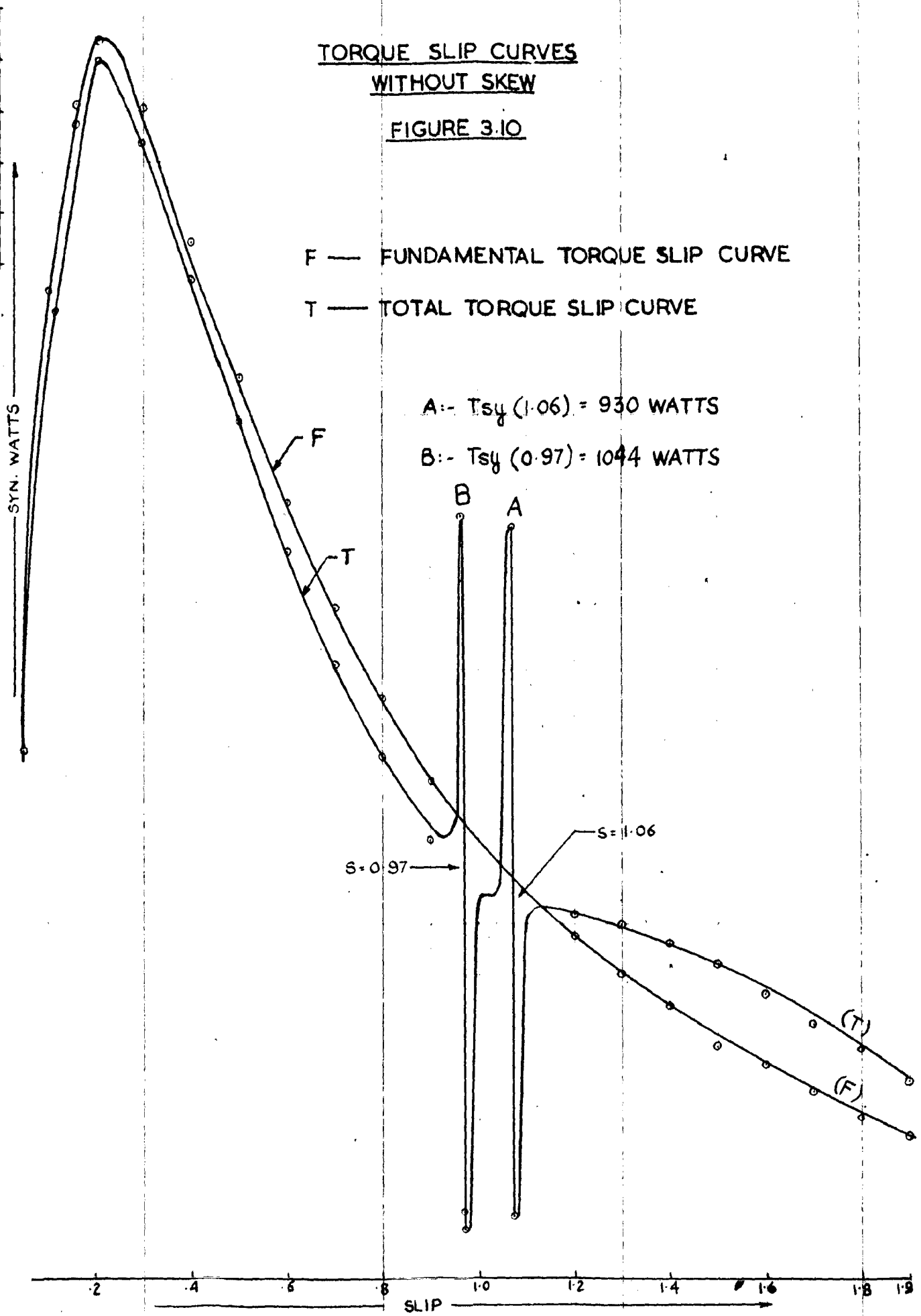
FIGURE 3.10

F — FUNDAMENTAL TORQUE SLIP CURVE

T — TOTAL TORQUE SLIP CURVE

A:- $T_{sy}(1.06) = 930$ WATTS

B:- $T_{sy}(0.97) = 1044$ WATTS



CHAPTER IV

SYNCHRONOUS PARASITIC TORQUES AND DEAD POINTS OF SQUIRREL CAGE INDUCTION MACHINE WITH AND WITHOUT ROTOR SKEWED

4.1. Synchronous Crawling Torques:

4.1.1. Speed of Synchronous Crawling Torques:

Certain squirrel cage motors are known to have a wide variation in starting torque and have a tendency to run at some speed way below that normally expected. This is sometimes called 'sub-synchronous' speed as the motor is said to be crawling. The one type of crawling called asynchronous crawling due to harmonic locking of stator and rotor has been already dealt under Chapter III. The other cause of crawling may be 'synchronous crawling'. Sometimes the motor fails to start and in extreme cases the torque may be actually negative at certain positions making the motor entirely useless. This phenomena of the motor failing to start is called by many names such as 'dead points' cogging and 'locking'. An analysis of the causes of such dead points behaviour will be presented in next article of this Chapter.

Concentrations for the present over synchronous torques⁽¹²⁾, as given by equation 3.5, both machine parts must have the same number of poles for a uniform useful torque to be produced by the machine. In the synchronous machine, the stator as well as the rotor are connected to sources of currents, therefore uniform torque is possible only at a single speed of the rotor. A torque produced in this manner is called a synchronous torque.

The harmonics produce asynchronous as well as synchronous torques in the induction motor. A synchronous torque will occur when stator harmonic ' m_a ' produces a rotor harmonic n_a which has the same order as another stator harmonic ' m_b ' linked by the equation (3.4)

$$n_a = \pm v_2 \left(\frac{R}{p} \right) + m_a$$

and $n_a = m_b$

and which at a single rotor speed is at stand still with respect to this second harmonic m_b , m_a is the source of excitation of the rotor, then only ' m_b ' torque can be produced

It can be seen from harmonic chart (Table 1.4) that the rotor harmonics which correspond to $v_2 = 0$ i.e., the first column of the rotor harmonics, have the same order as the stator harmonics producing them. As pointed out earlier the torque produced by these first order harmonic is asynchronous since the speed of the m th stator harmonic with respect to stator is

$$v_1 'm_a' = \frac{v_1}{n_a}$$

The speed of the ' m_a ' rotor harmonic with respect to the stator is equation 3.2.

$$v_1 'm_a' = \frac{1}{n_a} \left[1 + (n_a - m_a) (1-s) \right] v_1 \quad (4.1)$$

Where v_1 = fundamental speed.

In order that $v_1 m_a = v_{na}$ the condition is

$$(n_a - m_a) (1-s) = 0 \quad (4.2),$$

and since $n_a = m_a$ (first order harmonic), equation 4.2, is satisfied for all values of slips, thus asynchronous torque is

produced at all speeds.

In order that synchronous torque occur there must be

$$n_a = \pm n_b \quad \text{i.e.} \quad v_{na} = \pm v_{1nb} \quad (4.3)$$

$$\text{Since } v_{1nb} = v_1 / n_b \quad (4.4)$$

Equation 4.3 shows the two possibilities

Possibility one: When $n_a = + n_b$ the condition is $v_{na} = +v_{1nb}$

i.e. from equation (4.1)

$$1 = 1 + (n_a - n_b) (1-s) \quad (4.5)$$

$$\text{or } (n_a - n_b) (1-s) = 0 \quad (4.6)$$

Since $v_2 \neq 0 \therefore n_a \neq n_b$. Hence synchronous torques will occur only when $s = 1$.

This is a case of locking torque and we postpone the discussion over it for next section.

$$\text{Possibility two: When } n_a = - n_b \quad (4.7)$$

giving $v_{na} = v_{1nb}$

$$\text{equation 4.1 gives } -1 = 1 + (n_a - n_b) (1-s) \quad (4.8)$$

Since $n_a \neq n_b$ synchronous torque can occur only when

$$s = 1 + \frac{2}{(n_a - n_b)} \quad (4.9)$$

' n_a ' and ' n_b ' with proper sign.

$$\text{as } n_a = \pm v_2 (R/p) + n_b$$

$$n_a - n_b = \pm v_2 (R/p)$$

$$\text{Speed } n = - \left(\frac{120 f_1}{v_2 R} \right) \text{ for squirrel cage rotor} \quad (4.10)$$

(v_2 with proper sign)

Thus, if there exists equal number of poles fields in stator and rotor except those of first order, then synchronous torque at fixed speed given by equation (4.10) is produced. If the harmonic ' n_a ' corresponds to a negative v_2 , the synchronous cusp will occur at positive speed ($s < 1$), if the harmonic ' n_a ' corresponds to a positive v_2 , then synchronous cusp will occur at negative speed ($s > 1$).

4.1.2. Magnitude of cusp (Synchronous Parasitic Torques) in the Torque-slip Characteristic

From equation (3.6) (Chapter III) the torque is given by

$$P_d \text{ (Power developed)} \propto F_{na} F_{mb} \quad \text{(asynchronous torque)}$$

Since in this case, ' na ' is the exciter and produces flux distribution which reacts with maf of mb of stator, therefore

$$P_d \propto F_{na} F_{mb} \quad (4.11)$$

Biot - Savart's Law also gives the for one single conductor as

$$\begin{aligned} F_t &= 8.85 \times 10^{-8} B I L \sin \theta \quad \text{(lbs)} \\ &= 1 \times 10^{-1} B I L \sin \theta \quad \text{Kgm (m.k.s)} \end{aligned} \quad (4.12)$$

Considering the rotor skewed, distribution of A_{mb} is directly effected by rotor skewing (See equation)

$$\therefore P_d \propto B_{na} F_{mb} K_{amb} \quad (4.13)$$

Where A_{mb} = Ampere conductor distribution of harmonic ' mb '

Total Power developed is given by

$$T_{(mb) \text{ sy.}} \propto (PF) \int_0^{2\pi} b_{na} A_{mb} K_{amb} d\theta \quad (4.14)$$

where

$$b_{na} = B_{na} \cos \left[na\theta + \left\{ 1 + \left(\frac{v_2 R}{p} \right) (1-s) \right\} \omega t \right] \quad (4.15)$$

$$B_{na} = F_{(n)s} \times (\text{Air gap permeance})$$

$$B_{na} = F_{(n)s} \times \frac{0.4 W}{l_g'} \times (2.50) \text{ Lines / sq. in.} \quad (4.16)$$

$F_{(n)s}$ is given by equation (1-21) substituting it in (4.16)

$$B_{na} = 0.45 \frac{1}{(na) p} \frac{(3.19) m_1 R_1 \cdot k_{w1m} G_{(na)} I_1}{l_g' K_{ana}} \quad (4.17)$$

Where $G_{(na)}$ = Damping factor for rotor currents.

From Harmonic equivalent circuit (See fig. 3.3).

$$G_{(na)} = \frac{s_{(na)} X_{M(na)}}{\sqrt{R_{2(na)}^2 + s_{(na)}^2 (1 + T_{2na}^2 X_{M(na)}^2)}} \quad (4.18)$$

b_{na} given by (4.15) is not general enough for the computation of synchronous torque. The magnitude of the synchronous torque depends upon the relative position of the stator and rotor mmf's in addition to other factors. Equation 4.15 is derived on the assumption that at $t = 0$ the θ_1 of stator (θ_1) and rotor (θ_2) coincides i.e., $\theta_1 = \theta_2$

For present analysis, it should be dropped and equation 4.15 be generalised. By introducing new system of coordinates. Let at $t=0$

$$\theta_2 = \theta_1 = \theta_1' - v_2 t \text{ (at time } t) \quad (4.19)$$

Equation 4.15 in new coordinates defined by 4.19 becomes

$$b_{na} = B_{na} \cos \left[n_a \theta - (n_a - m_a) \theta_2' + \left\{ 1 + \frac{v_2 R}{p} (1-s) \right\} \omega t \right] \quad \dots(4.20)$$

Where α_{na} in the equation of b_{na} is necessary if B_{na} is expressed in terms of the primary current I_1 , since B_{na} is proportional to I_{2na} and I_{2na} lags I_1 by the angle

$$\alpha_{na} = \pi - \alpha_{na} \text{ where}$$

$$\tan \alpha_{na} = \frac{E_{2(na)}}{(1 + T_{2na}) S_{(na)} X_{M(na)}}$$

when current distribution super imposed over the winding groups is integrated it yields a_{na} curve. Therefore

$$f_{\theta} = \int_0^{\theta} a_{\theta} \cdot d\theta$$

Where a_{θ} = ampere conductor distribution and function of space angle θ .

$$\text{Conversely } a_{\theta} = \frac{d(f_{\theta})}{d\theta} \quad (4.21)$$

$$f(\theta, t) = 0.45 \cdot n_1 \frac{K_s(na) \cdot N_1}{m(p)} K_{w1(nb)} I_1 \cos (nb\theta \mp \omega t)$$

$$\therefore a(nb) = + A_{(nb)} \sin (nb\theta \mp \omega t) \quad (4.22)$$

$$A_{(nb)} = \frac{2 \cdot 2^{\frac{1}{2}}}{(PT)} n_1 N_1 K_{w1(nb)} K_s(na) I_1 \quad (4.23)$$

$P T$ = Total armature circumference.

Substituting -

$$\mp 2 + v_2 \left(\frac{R}{p}\right) (1-s) \omega t - (na-na) \theta'_2 + \alpha_{na} = \delta_1 \quad (4.24)$$

$$\mp v_2 \left(\frac{R}{p}\right) (1-s) \omega t - (na-na) \theta'_2 + \alpha_{na} = \delta_2 \quad (4.25)$$

$$C = \frac{0.369 \times 212.2 \times 10^{-8} (P T)^2 L_e B_{na} A_{mb}}{4 \pi^2} \quad (4.26)$$

Then equation (4.14) reduces to

$$\begin{aligned} T_{(mb)} S_y &= C \int_0^{2\pi} \cos \left[na\theta + \left\{ \frac{v_2 R}{p} (1-s) + 1 \right\} \omega t \right. \\ &\quad \left. - (na - na) \theta'_2 + \psi_{na} \right] \sin (mb\theta + \omega t) d\theta \\ T_{(mb)} S_y &= -C \int_0^{2\pi} \sin \left[(na + mb)\theta - \delta_1 \right] d\theta - C \int_0^{2\pi} \sin \left[(na - mb)\theta \right. \\ &\quad \left. - \delta_2 \right] d\theta \quad (4.27) \end{aligned}$$

For synchronous torque

$$na = -mb \quad (4.7)$$

$$T_{(mb)} S_y = 2\pi C \sin \delta_1 = 2\pi C \sin \left[v_2 \left(\frac{R}{p} \right) \theta'_2 - \psi_{na} \right] \quad (4.28)$$

Equation 4.28 indicates that synchronous torque varies with rotor position but independent of time.

$$T_{(mb)} S_y(\max) = 2\pi C \quad (4.29)$$

Therefore synchronous torque is of constant magnitude for particular order of harmonic 'mb' occurring at one slip given by

$$s = 1 + \frac{2}{na - mb}$$

Synchronous torque on torque/speed are represented by a straight line (see Fig. 4.1).

4.2. DEAD POINTS IN TORQUE SPEED CURVES

4.2.1. As already indicated under section 4.1 and 4.2, the dead points in torque speed curves are specifically the one type of synchronous torque when parasitic torque (cusp) occur at stand still or in other words in more clear terms, due to high locking torque motor does not start. As can be judged, it is more severe problem than any other. This phenomena was first named as 'Synchronous motor effect' in induction machines by Direese⁽²⁶⁾ and latter on Kron⁽⁴⁾, Alger⁽³⁾ also worked over it. Grahn⁽²²⁾ first tried to explain the causes of Dead points in induction machine. The classical theory does not explain this behaviour as it purely arises due to non-sinusoidal nature of the air gap field as discussed under section 4.1 of this Chapter.

4.2.2. Variation of Torque at Stand Still Over Slot Pitch

The phase relation between harmonics is shown in Fig. (4.1) Dead point torque explained by Grahn⁽²²⁾ with the help of harmonic phase relation is based on the assumption that nearly 180 degrees between stator and rotor currents when locked, . The actual angle depends upon power factor of the secondary air-circuit and ratio between magnetising current and load current.

Graham, performed tests over number of motors with different stator and rotor slot combinations. The variation of standard torque over a rotor slot pitch are shown here in Fig. 4.4 and 4.5 .

4.2.3. Magnitude of Dead Point Torque:

Equation 4.5 given that dead points occur if

$n_a = m_a$ and for the condition the torque is given

T_{AB} = MAGNITUDE OF SYN. TORQUE
 S = SLIP

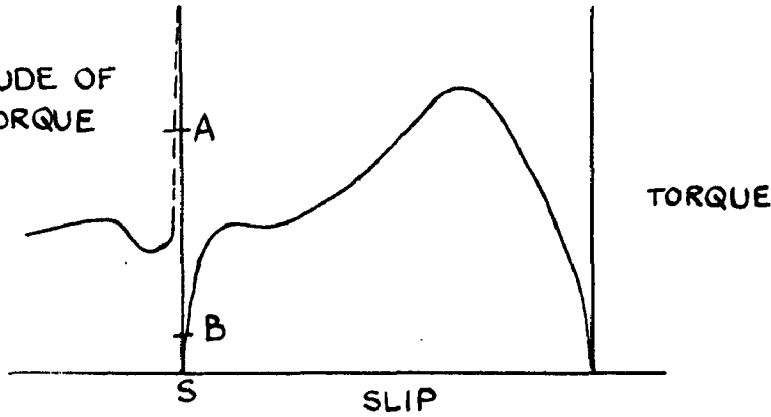
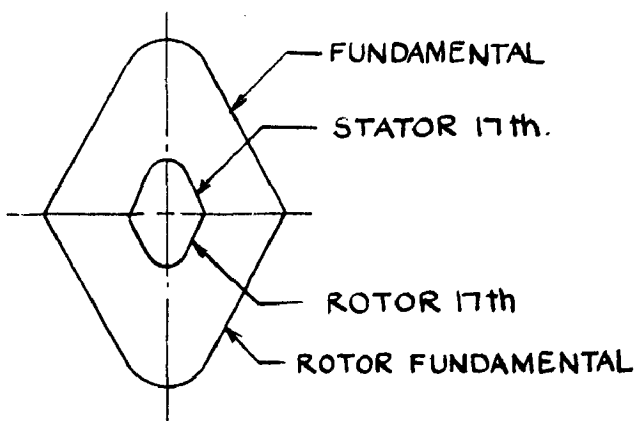
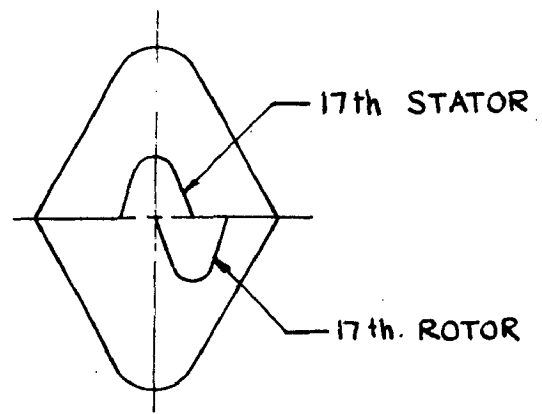


FIGURE 4.1



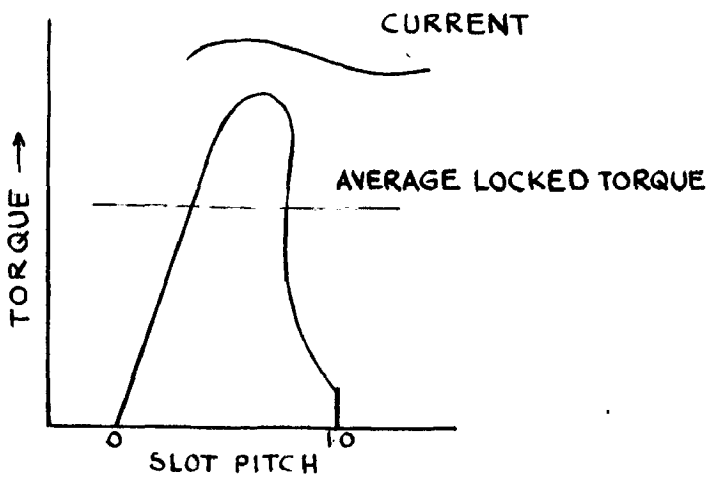
RELATION OF 17th HARMONIC WAVES OF STATOR & ROTOR WITH ROTOR ORIGINAL POSITION

FIGURE 4.2



RELATION OF 17th HARMONIC WHEN ROTOR HAS MOVED BY $\frac{1}{4}$ th OF SLOT PITCH

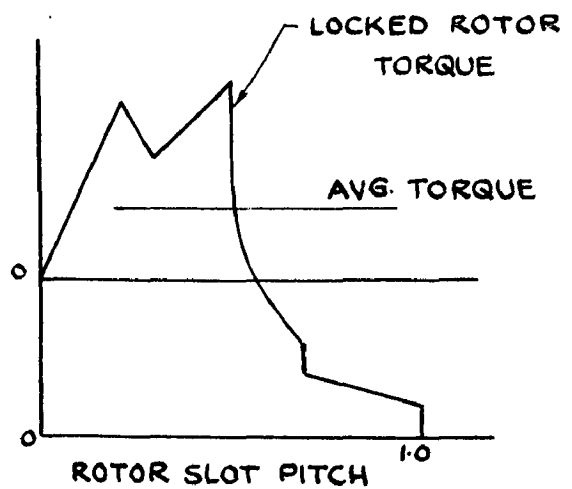
FIGURE 4.3



TYPICAL CURVE SHOWING VARIATION OF LOCKED ROTOR TORQUE WITH ROTOR POSITION.

(MACHINE ROTOR SKEWED)

FIGURE 4.4A



TYPICAL CURVE SHOWING VARIATION OF LOCKED TORQUE WITH ROTOR POSITION FOR MOTOR WITHOUT SKEWED SLOTS.

FIGURE 4.4B

by equation (4.27)

$$T_{(sy)d(max)} = 2 \pi C \sin \delta_1 \quad \text{and maximum torque is}$$

$$T_{ay d (max)} = 2 \pi C$$

When C is given by the equation (4.26).

4.3. RELATION OF PARASITIC TORQUES WITH SLOTS:

4.3.1. Asynchronous Parasitic Torques and Slots:

As such number of slots have no direct bearing over the asynchronous torque of Phase belt harmonics, which are the product of non-sinusoidal winding distribution. But as the equation 1-22, 1-14, 1-18, shows, slot harmonics and permeance waves are function of slot numbers.

$$ns = v_1(S/p) \pm 1, \quad np = v_1(S/p) \pm m, \quad ap = v_2(R/p) \pm m$$

But by properly selecting S and R , low order of slot and permeance waves which are more harmful can be avoided. By selecting (S/p) and (R/p) on higher side, distortion in Torque - speed in the working region can be avoided.

4.3.2. Elimination of Stand Still Locking (Dead Points)

Generalising the harmonics produced in combination with slot and rotor slots we get the following equations :

STATOR	ROTOR
1. m	1. n when $n = m$
2. $\pm v_1(S/p) \pm m$	2. $\pm v_2(R/p) \pm m$
	3. $\pm v_2(R/p) \pm v_1(S/p) \pm m$

m is substituted with proper sign.

For stand still locking - (from equation 4.5)

$$na = mb.$$

These are number of combinations all possible.

$$\text{Case (i)} \quad \pm v_2(R/p) + na = mb \quad (4.30)$$

This in no way provides any relation between R and S

$$\text{Case (ii)} \quad \pm v_2(R/p) + na = \pm v_1(S/p) + mb$$

$$\pm (v_2R - v_1S) = p(mb - na)$$

All are integer

$$\therefore \pm (v_2R - v_1S) = \text{EVEN or Zero} \quad (4.31)$$

If $v_1 = v_2 = 1$ or 2

Then (a) $\pm (R-S) = \text{even.}$

(b) $2(R-S) = \text{EVEN or Zero}$

$$\text{Case (iii)} \quad \pm v_2(R/p) \pm v_1(S/p) + na = mb$$

$$\therefore (v_2R + v_1S) = \text{even or Zero} \quad (4.32)$$

$$\text{Case (iv)} \quad \pm \left[\pm v_2(R/p) + v_1(S/p) + na \right] = \pm \left[\pm v_1(S/p) + mb \right]$$

(a) $v_2(R/p) = (mb - na)$ same as equation 4.30

(b) $\pm v_2(R/p) \mp v_1(S/p) + na = \mp v_1(S/p) \pm mb$

$$\pm v_2R \mp 2v_1S = p(mb - na)$$

$$\pm (v_2R \mp 2v_1S) = \text{Even or Zero} \quad (4.33)$$

Equations 4.30, 4.31, 4.32, 4.33 provides sufficient conditions for eliminating stand still locking.

$$m_a - m_b = 2 k \cdot q$$

where q = number of phase belts.

To sum up

$$(\nu_2 R \pm \nu_1 S) = 2 k q \quad \text{or} \quad (4.34)$$

$$(\nu_2 R \pm 2 \nu_1 S) = 2 k q \quad (4.35)$$

4.3.3. Elimination of Synchronous Torques:

For synchronous torques the necessary condition given by equation 4.7 is

$n_a = -m_b$ using this and all other relation from equation 4.33, the following new relations are established.

$$(\nu_2 R \pm \nu_1 S) = 2 (kq \pm 1) \quad (4.36)$$

$$(\nu_2 R + 2 \nu_1 S) = 2 (kq \pm 1) \quad (4.37)$$

where k = Integer including zero.

4.4. CALCULATION OF SYNCHRONOUS TORQUES:

Employing equations 4.29 and 4.26 Table T (1-4) T(2.1)A, Table (2.2), Table (2.3), Table (2.1B), the magnitude of synchronous torques in general for any pair of harmonics is given by

$$T_{(sy)} = 1.915 \times 10^5 \left[\frac{k_{w1ma}}{K_{ema}} G_{(ma)} k_{w(mb)} \frac{K_p(na)}{na} \right] \quad (4.38)$$

watts / phase.

The computed results are tabulated in Table (4-1) and Table (4-2) for skewed rotor and Table (4.3) for non skewed rotor induction machine. Values are indicated over the graphs in Fig. 3.8 and Fig. 3.10.

(i) At slip = 1.06

Total synchronous torque = 487.3 watts

(ii) At slip = 0.97

Total synchronous torque = 130.0 watts.

For skewed rotor
machines.

(iii) at slip = 1.06

Synchronous torque = 929.9 watts.

(iv) at slip = 0.97

Synchronous torque = 1043.5 watts.

For rotor not
skewed.

4.5. DETERMINATION OF DEAD POINTS:

Applying the relations of equation of 4.35 and 4.36,

with $R = 68$

$S = 48$

There is no dead point. So motor is free from starting locking tendency.

Table 4.1 CALCULATION OF SYNCHRONOUS TORQUES WITH ROTOR SKEWED

m_a	$m_a - m_b$	k_{wma}	k_{wmb}	G_{ma}	k_{wmb}	K_{sa}	Syn.-watts/ phase.
+1	+35	0.955	.998	0.98	.126	.53	340
-5	+29	.205	.987	.445	.205	.657	83.5
+7	+41	.157	.98	.043	.157	.391	1.97
-11	+23	.126	.946	.012	.95	.775	10.4
13	+47	.126	.925	.045	.955	.256	6.1
-17	+17	.157	.873	0	.157	.873	0
+19	+53	.205	.845	.0358	.205	.129	0.84
-23	+11	.955	.775	.0142	.126	.946	36.1
+25	+59	.955	.74	.038	.126	.0169	0.34
-29	+5	.205	.652	.0038	.205	.987	9.25
+31	+65	.157	.616	.0031	.157	.076	Negligible
-35	-1	.126	.127	2.0×10^{-5}	.955	.998	"
+37	+71	.126	.482	1.4×10^{-4}	.955	.147	"
-41	-7	.157	.391	.00036	.157	.98	"
-43	+77	.205	.346	.000298	.205	.193	"

Table 4.2. CALCULATION OF SYN. TORQUES (ROTOR SKEWED)

For $\nu = -2$

m_a	$n=-mb$	k_{wma}	G_{ma}	k_{wab}	$K_{\omega m}$	$K_{\omega ma}$	Syn.- watts/phase.
1	-67	.955	.95	.205	.102	.998	54
-5	-73	.205	.383	.955	.165	.987	38.0
7	-61	.157	.128	.126	.0164	.98	.13
-11	-79	.126	.0455	.157	.203	.946	Negligible
13	-55	.126	.015	.157	.09	.925	"
-17	-85	.157	.027	.126	.217	.873	"
19	-49	.205	1.007	.955	.212	.845	14.0
-23	-91	.955	.047	.205	.21	.775	Negligible
25	-43	.955	.0574	.205	.346	.74	23.5
-29	-97	.205	.003	.955	.184	.657	Negligible
31	-37	.151	.002	.126	.482	.616	"
-35	-103	.126	2.0×10^{-5}	.157	.144	.527	"
37	-31	.126	1.4×10^{-4}	.157	.616	.482	"
-41	-109	.157	.00036	.126	.096	.392	"
43	-25	.205	.000298	.955	.74	.346	"

Table 4.3 CALCULATED RESULTS OF SYNCHRONOUS TORQUES WITH ROTOR NOT SKewed

For ellip = 1.06						For ellip = 0.97					
ms	na -nb	k _{ms}	k _{w(mb)}	T _{sy}	na	na-nb	k _{ms}	k _{w(mb)}	T _{sy}		
1	35	.955	.126	675.0	1	-67	.955	.205	675.0		
-5	29	.205	.205	82.0	-5	-13	.205	.955	122.0		
7	41	.157	.157	27.0	7	-61	.157	.126	15.7		
-11	23	.126	.955	13.4	-11	-79	.126	.157	52.0		
13	47	.127	.955	24.6	13	-55	.126	.157	8.5		
-17	17	.197	.157	9.6	-17	-85	.157	.126	7.3		
19	53	.205	.205	6.4	19	-49	.205	.955	1.3		
-23	11	.955	.126	33.8	-23	-91	.955	.205	130.0		
25	59	.955	.126	38.0	25	-43	.955	.205	4.2		
-29	5	.205	.205	6.3	-29	.97	.205	.955	15.0		
31	65	.157	.157	.63	31	-37	.157	.126	0		
-35	-1	.126	.955	8.0	-35	-103	.126	.157	8.5		
37	71	.126	.955	2.7	37	-31	.126	.157	.09		
-41	-7	.157	.157	1.0	-41	-109	.157	.126	2.0		
43	77	.205	.205	1.1	43	-25	.205	.955	0.1		

CHAPTER V

ELECTROMAGNETIC NOISE AND MAGNETIC RADIAL FORCES OF SQUIRREL CAGE

POLYPHASE INDUCTION MOTOR

The term 'noise' is a very vague term defining nothing in particular of the source of noise. But to be more exact, it can be said that there is now a growing demand that motors should have good 'sonance design', i.e. they should give out just sufficient, steady pleasing hum, just loud enough to show that they are performing their duties properly, but not loud enough to be noticed.

5.1. QUALITATIVE ANALYSIS OF NOISE

5.1.1. Definition of Noise:

Before discussing noise measurement as noise phenomena a necessary preliminary is to define what we mean by noise. The old conception was that sounds which occupy the attention of a person could broadly be classified into music and noise. This classification was based solely on the characteristics of the stimulus i.e., on physical quantities such as the relations between the component frequencies. For our purpose we define noise as undesired or irksome sound. Sufficient work has been done by R.L. Wege, Church⁽³⁶⁾ in pulse science of Noise to which we are not much concerned at present.

In attempting, therefore to formulate a basis for noise measurement which would be acceptable for Engineering purposes, Church first considered the laws of response of the hearing system of the average individual to sounds to different characteristics, and then the choice of a practical method of noise measurement in accordance with those laws. The investigation of the laws in brief falls in three sections

vis., the determination of the threshold of hearing which provides a datum from which intensity levels may be reckoned, the determination of the relation between the magnitudes of stimuli of different frequencies which produce equal loudness sensations, and finally the relation between stimulus and sensation.

5.1.2. The Assessment of Total Noise:

While the problem of analysing a complex noise into its constituent tones and stating their magnitudes and frequencies presents some difficulties, yet the work involved is essentially in the realm of physics and the results are susceptible of incontrovertible statement in absolute units. Even when the intensity values are expressed in terms of the decibels above some generally accepted values of the threshold intensities at the respective frequencies, the results are still unassailable.

The methods of determining the total loudness of a noise can be roughly divided into two classes, subjective and objective, the former involving the judgement of the human ear and the latter the interpretation of instrumental measurements in the light of the available data relating to the properties of the ear. The two classes can be further subdivided in the following way.

5.1.3. Subjective Methods:

In the 'equality' or 'balance' method a reference tone which can be specified in frequency and intensity is adjusted so that it is judged by a representative person to sound as loud as the noise in question. The reference tone may be produced in free space but is more usually generated in either one or two telephone ear pieces spaced off the head, or in one telephone placed over one ear while the other

listens to the noise being measured.

5.1.4. Objective Methods:

Under the total noise is to be assessed by calculation from analysis, the several components of a noise are determined by analysis and their intensities weighed according to their frequencies and the sensitivity of the ear at those frequencies. The weighed components would then be summed mathematically in a way to correspond to the action of the ear. No method of summation of general validity has yet been put forward.

The methods briefly indicated above were considered in detail with a view to determining which is the most trustworthy for quantitative measurements under problems like ours of measuring noise produced by electrical machines. In the subjective and objective classes of assessment, while we have in the former a direct reference to the final judge, the human ear, we introduce the personnel factor into the observations, whereas in the latter the difficulty of stimulating instrumentally or mathematically the response of the ear is offset by the much greater consistency of instrumental readings. The relative importance of these points must be considered along with the other features, such as cost, convenience and speed of working.

Even supposing a method of summation by calculation were available the calculations would necessarily be extremely laborious owing to the complexity of the characteristic of the ear. Moreover, fairly elaborate analysing equipment is required to obtain the initial data. Calculation

from analysis is therefore never likely to become a method generally applicable to engineering problems. Specifically the mathematical analysis of noise generated by rotating electrical equipment is of very complex nature, but still the author has chosen objective analysis since they are of undoubtedly of value for research purposes.

5.2. UTILITY OF NOISE MEASUREMENT:

5.2.1. Typical Loudness Values:

One point of interest is the position assigned to common noise on the decibel and loudness scales. This is illustrated in Table 5.1 below. Columns (2) and (3) have the most practical interest but it is instructive to note how they are related to columns (4) and (5). The pressure values given in column (4) are those 800-cycle field pressure which would produce the same loudness sensations as the complex noise on an observer facing the source. Column (5) gives the sound energy flow per cm^2 in an equally loud 800-cycle field. The values in column (5) are derived from those in column (4) by the relation⁽³²⁾

$$W = \frac{p^2}{\bar{d}v} \times 10^{-7}$$

Where W = rate of flow of energy in watts per cm^2

p = r.m.s. pressure in dynes / cm^2

\bar{d} = Intensity of air

v = velocity of sound in air cms/sec.

Decibels above threshold are given in terms of the pressure by the expression $20 \log_{10} (p/p_0)$ when p_0 is the threshold field pressure viz. $0.000215 \text{ dynes/cm}^2$.

63893

Table 5.1 THE MAGNITUDES OF COMMON NOISE ON VARIOUS SCALES.

1.	Loudness -dB 2	Equivalent 800-cycle magnitudes		
		D_b dB 3	Field pressure 4	Energy flow 5
1. Two circular saws	160	110	75	13×10^{-6}
2. Loud motor horn at 100 ft.	100	100	25	13×10^{-7}
3. In suburban steam	50	84	3.6	3×10^{-9}
4. Conversation (3 ft)	20	69	0.65	1×10^{-9}
5. Quiet Elect. motor (2 ft)	5	49	0.065	1×10^{-11}

5.2.2. Effect of Number of Sources:

The total effect of a number of sources operating simultaneously has often to be considered in practice. It has been suggested that since two similar sources emit twice as much sound energy as one and since the number of decibels difference is given by $10 \log_{10} (w/w_0)$ where w and w_0 are the energy levels in the two cases, an increase of 3 db is caused whatever the initial level. This simple rule cannot apply to the equivalent 800-cycle tone outside that frequency range; The issue is further complicated in the case of a noise containing a harmonic range of frequencies e.g., as electrical rotating equipment.

5.2.3. Effect of Distance:

In considering the effect of distance from the source on the sensation of loudness experienced, it should be borne in mind that the effect is simple only in the case of a point source emitting a pure tone

of a frequency between 800 to 4000 cycles per sec. in free space with zero background noise. Under point source free space conditions the acoustical pressure varies inversely as the distance from the source. With complex sounds the conditions will be again modified.

5.2.4. Effect of Enclosures:

It is not necessary to emphasize the fact that, in the case of a source placed in a building, the noise audible to a person outside may be totally different, both in composition and in amplitudes, from that heard inside. The attenuation of sound through the walls of a building depends upon the mass per unit area of the walls. A discussion of the design of enclosures is beyond the scope of this volume.

5.2.5. Effect of Noise Background:

A subject which is of vital importance in making noise measurement on machinery and in considering how much noise it is permissible for a machine to make in a given situation, is the background of noise present. The sound sensations from a given source perceived by a listener may be greatly modified if, another source is introduced. One sound can 'drown' other. Almost any motor would be unobjectionable, if not inaudible, in surroundings of loudness 85 db.

5.2.6. Problem of Windage Noise:

The problem of windage noise is of great importance particularly only in large - high speed machines. It becomes the one and only noise, but in medium sized machine, magnetic noise is the biggest problem, so windage noise can easily be overlooked in this context. It

is sufficient from the designer's point of view to know the causes, in terms of dimensions and other Physical constants of the generation of magnetic noise. This would enable him to avoid certain constructions which might magnify as radiate electromagnetic noise.

5.3. Sources of Noise in Motors:

The physical factors that make an induction motor a machine for converting electric energy into mechanical energy also make it a machine for converting this energy into accoustical energy. The problem of resonance design⁽³²⁾ is to reduce the accoustical efficiency of these machines so that they will produce less noise. Induction motors noise may be classified in three main groups:

1. Magnetic Noise.
2. Mechanical noise.
3. Aerodynamic noise.

Any one or more may be predominant in any motor, but here we will devote our studies to first type only to see the 'effects of Harmonics on Noise' and then subsequently demonstrate, the effect of rotor skewing.

The noise producing parts can vibrate in several ways. A torsional vibration of the stator and rotor as a whole results from periodic torque pulsations, such a vibration may be particularly objectionable as it is transmitted directly through the motor feet to the supporting structure. Most of the vibrations are forced vibration i.e., their frequency is not near to critical frequency. The method of determining the noise tendency of a motor is to tabulate quantitatively all the possible harmonic fields and examine for each two fields differing in number of poles.

5.3.1. Electromagnetic Noise in Electrical Rotating Machines:

Three main types of noise occur in electrical rotating machines. These are (1) Magnetic noise originating in the air gap flux density distribution on no load. This distribution remains substantially unchanged on load (2) load noise originating in the mmf wave of the stator winding. (3) Windage noise due to the rotation. Of these types of noise, the first is the one requiring most thought, since not only is it difficult to predict, but even more difficult to suppress or reduce when the machine is completed. The cause and cure of noise in electrical rotating machines is of perennial interest to both manufacturers and users.

Walker and Leschitzg⁽²⁸⁾ recently gave a solution to the problem of determining the noise in synchronous as well as induction machines. The author has also attempted to find the noise level of the machine under test by exhaustive calculation carried over IBM 1620 computer. In order to predict the noise level of a electrical machines the author describes the magnetic forces that cause the magnetic noise of Polyphase induction machine, and the corresponding modes of motion of the motor cores and frames. Approximate equations are used for the decibel sound levels that motors of normal design may be expected to produce, and variations due to core and frame resonance are discussed. The principal types of magnetic noise, due to the radial forces of the fundamental harmonic air gap fields are considered.

5.3.2. Natural Behaviour of Motor:

Early research in the magnetic noise of induction motors was closely linked with investigations of other effects of higher

harmonics magnetic flux density⁽³⁴⁾ waves in the air gap. Even until recently the recommendation for low magnetic noise level induction motors was intimately related to slot combinations. Heondl, Hildebrand and Moruil have discussed in great detail the question of slot combinations and the calculations of the mode, frequency and the magnitude of the radial force waves, responsible for the vibration and noise of induction motors.

Alger⁽³⁵⁾, who was the first to provide a simplified, comprehensive treatment embracing all phases of the problem, was also the originator of the concept of 'sonance design'. According to him, the induction motor as regards its mechanical vibrations can be represented as a simple in extensional ring, and he analysed the motor's natural behaviour on this basis. To analyse its acoustic behaviour Alger chose to represent the motor by infinitely long vibrating cylinder. He provide the designer with formulas and curves of sound intensities of the noise radiated from the induction motor simultaneously, Jordon in Germany provided a simplified solution. His assumptions regarding the vibrational aspect of the motor is approximated by a radiating sphere, and Gauss's theorem is used to determine the sound power level at a distance from 'stiffening effect', which is quite, justified from medium sized motors.

The magnetic field in the air gap of an induction motor creates rotating force waves with frequencies of 2 to 40 or more times the line frequency. These frequencies cause elliptical or nodal deformations of the motor laminations and frame, (See Fig. 5-1) thereby producing high frequency vibrations and noise. This analysis provides an illustration of the work that sonance designers are being called on to

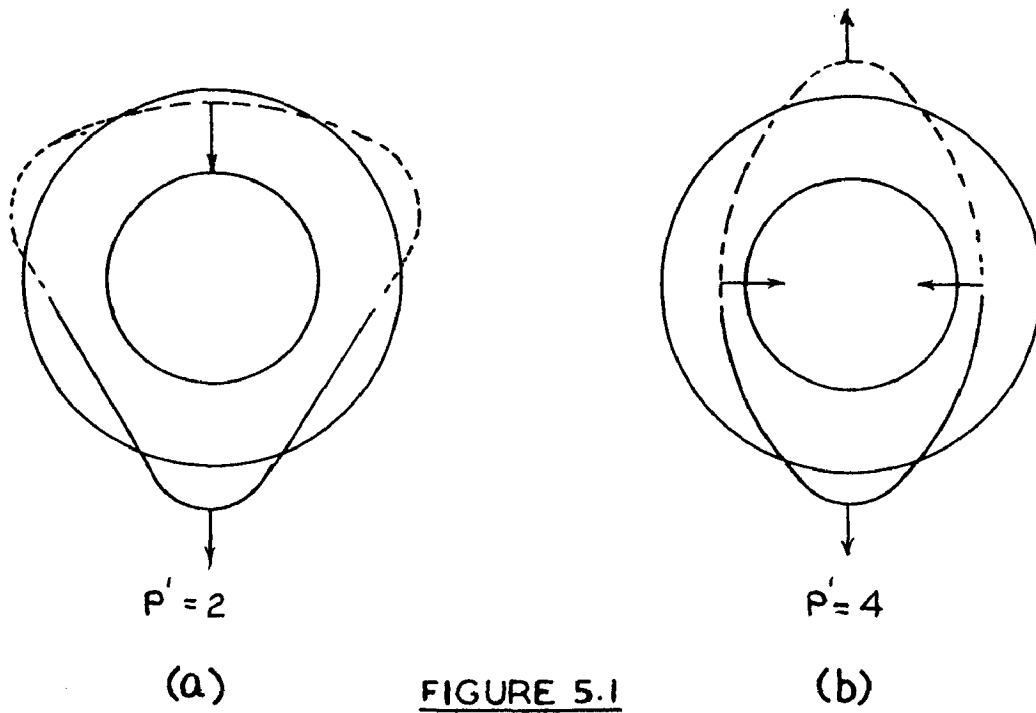
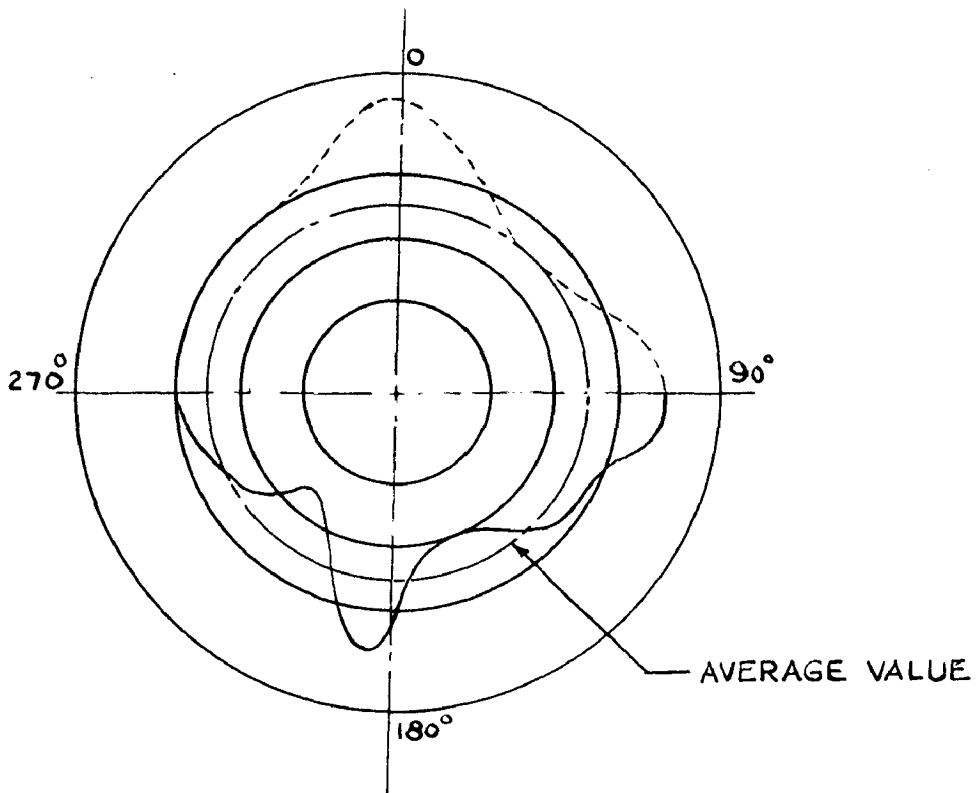


FIGURE 5.1



ELECTRO MAGNETIC DISSYMETRY OF THE ROTOR

FIGURE 5-2

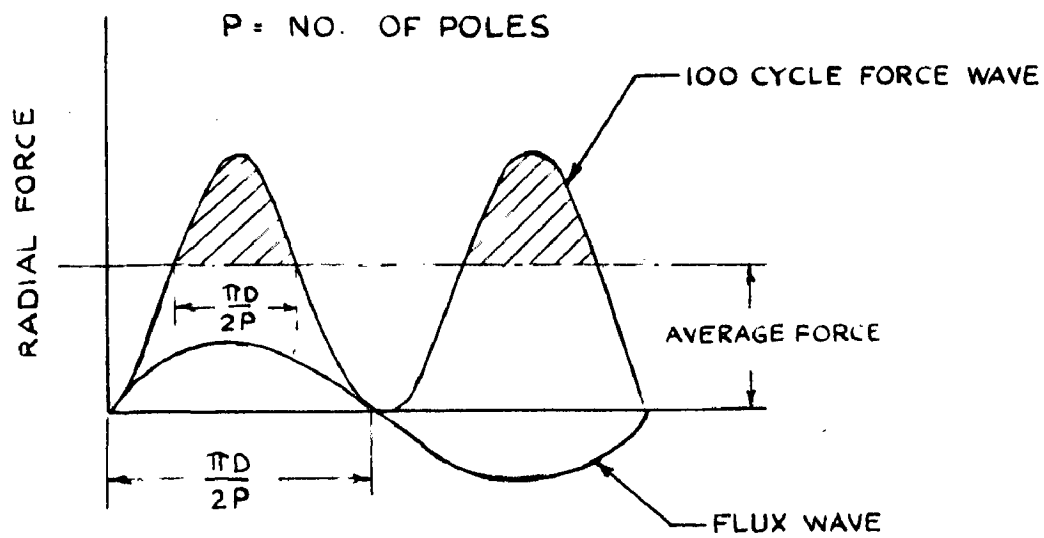
do in the broad programme for the reduction of the industrial noise that is presently under way. There are three distinct types of motor magnetic noise. First, there is the double line frequency noise (transformer Hum) caused by the rotating force wave of the fundamental magnetic field. Second there is a slot frequency noise caused by the slot ripples superposed on the fundamental air gap field. Third, there is the torque noise, caused by pulsations in the motor torque that occur as investigated due to presence of harmonic field. The mathematical analysis for all these is presented here.

The conductors themselves can usually be neglected as a noise source as the forces on them, being situated in the relatively weak leakage field, are small likewise we can neglect whatever internal stress may exist in the magnetic parts as the rigid parts are not deformed appreciably.

$$\begin{aligned} \text{Amplitude of force wave (31)} &= \frac{1}{2} \frac{10^7}{4^n} B'_r B'_p \text{ Newtons/m}^2 \\ &= \frac{1}{2} (55.6) B'_p B'_r \text{ lbs/in}^2 \end{aligned} \quad (5.1)$$

5.3.5. Influence of Skewing

Skewing has two different effects on the flux distribution and consequently on the force waves. The force waves created by the interaction of flux distribution waves caused by fundamental currents are not reduced by skewing. The force wave itself appears twisted to the left and to the right along the rotor axes, as shown in Fig. 5.3 i.e., the force distribution which has been uniform along a generatrix of the rotor will vary for skewed bar rotors. The effect of skewing can be analysed by resolving the force waves into two



RADIAL MAGNETIC FLUX AND FORCE WAVE

FIGURE 5.3

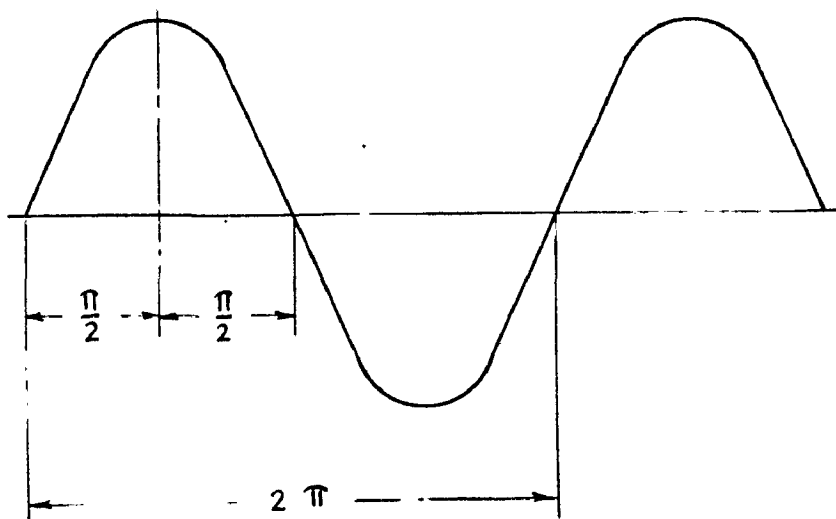


FIGURE 5.4

component waves . The force waves caused by higher harmonic rotor currents may be considerably reduced by skewing, because of the increased differential leakage reactance of the squirrel cage Induction machine.

5.5.4. Double Line Frequency Hum (100 cycle Hum)

In normal operation, with 50 cycle power supply, the 4 pole magnetic field rotates at 1500 rpm, so that the flux density at each point in the air gap varies sinusoidally. But when steel is magnetised, it expands slightly the axis of magnetisation. Hence the core are increases and decreases with flux density, causing tiny variations in peripheral and radial axis. Since the flux distribution system revolves, so total peripheral length remains unchanged.

As shown in Fig. (5.4) the developed air gap of an induction motor, with two poles of the revolving flux wave. The magnetic flux exerts a radial pull across the air gap, proportional at each point to the square of the flux density. The force wave being square of flux wave is fully displaced sine wave of double frequency as shown in Fig. 5.4. The average force intensity is half the peak value, and is uniform around the periphery. The radial pull exerted in a 2 Pole motor by one of its 4 pole force wave (cross hatched area in 5.4) is equal to

$$W = \frac{1}{2} (\text{peak force intensity}) \times \frac{2}{\pi} \times (\text{area of the force Pole}).$$

The full treatment of this is given under Mathematical analysis section of this Chapter.

5.4. MATHEMATICAL ANALYSIS OF MAGNETIC NOISE IN POLYPHASE INDUCTION MOTOR (30)

5.4.1. General Approach:

The parasitic radial force is given by equation (5.1)

$$f_r = 1.39 b^2 \times 10^{-8} \text{ lb - in}^2$$

where b = flux density in the air gap b lines / sq. in.

also $f_r = \frac{10^7}{8 \pi} b^2$ Newton / m² (b in weber/m²) writing

flux density in terms of stator and rotor harmonics.

$$b(\theta, t) = A_s(m) \sum_{m=1}^{\infty} \cos(m\theta' \mp \omega_{mt}) + A_s(n) \sum_{n=1}^{\infty} \cos(n\theta' \mp \omega_{nt})$$

$$\therefore f_r = 1.39 \times 10^{-8} \left[A_s(m) \sum \cos(m\theta' \mp \omega_{mt}) + A_s(n) \sum \cos(n\theta' \mp \omega_{nt}) \right]^2 \quad \dots(5.2)$$

$$f_r = 0 \left[\sum^m \left\{ A_s(m) \cos(m\theta' \mp \omega_{mt}) \right\}^2 + \sum^n \left\{ A_r(n) \cos(n\theta' \mp \omega_{nt}) \right\}^2 + 2 A_s(m) A_r(n) \sum^{h_1} \cos(m\theta' \mp \omega_{mt}) \cos(n\theta' \mp \omega_{nt}) + 2 A_s^2(m) \sum^{h_2} \cos^2(m\theta' \mp \omega_{mt}) + 2 A_r^2(n) \sum^{h_3} \cos^2(n\theta' \mp \omega_{nt}) \right]^2$$

Where

$$h_1 = m \times n \quad (5.4)$$

$$h_2 = \frac{|m|}{|m-2|} \quad (5.5)$$

$$h_3 = \frac{m}{\sqrt{n-2} \sqrt{2}} \quad (5.6)$$

The equation 5.3 can best be studied in five groups as marked the range of each group is indicated over the summation sign

$$h_1 + h_2 + h_3 = \frac{m+n}{c_2} = h \quad (\text{Total multiple terms})$$

Each group can further be bifurcated into simpler terms.

$$\cos \left\{ (m+n) \theta' - (w_n - w_m) t \right\} + \cos \left\{ (n-m) \theta' - (w_n + w_m) t \right\} \quad (5.7)$$

Equation 5.7 shows that the radial force produced by any two harmonic fluxes consists of two travelling force waves, with the following velocities and pair of poles (Hence forth to be called 'Force wave poles').

$$p_1 = p (n-m) \quad \text{with velocity } (w_n - w_m) \quad (5.8)$$

$$p_2 = p (n+m) \quad \text{with velocity } (w_n + w_m) \quad (5.9)$$

5.4.2. Self Stator harmonic Force Waves:

A single travelling flux wave of the stator produces a force wave, this is obtained from equation 5.3 (Group I)

no. of force pole pairs = p_2

$$p_2 = 2m, \quad \text{frequency} = 2f \quad (5.10)$$

Equation 5.10 show that stator flux harmonic alone produce force waves of double line frequency. These force waves are seldom disturbing with respect to magnetic noise.

5.4.3. Self Rotor Harmonic Force Waves:

Equation (5.3) (Group II) also gives the similar results for rotor harmonics also, producing double line frequency force waves

$$p_2 = 2n, \text{ frequency} = 2f.$$

5.4.4. Rotor-Stator Harmonic Force waves:

The major disturbing magnetic noise in induction motors is produced by combinations of stator and rotor harmonics. From another equation 5.3, we get the following.

$$\begin{aligned} p_1 &= n - m & f_1 &= (n - m) (1-s)f \\ p_2 &= n + m & f_2 &= (2 + (n-m) (1-s)) f \end{aligned}$$

Since

$$v_n = \left[1 + (n-m) (1-s) \right] 2\pi f.$$

and $n = \frac{1}{2} v_2 (R/p) + m$

$$\therefore p_1 = n - m \quad f_1 = v_{2a} (R/p) (1-s) f \quad (5.11)$$

$$p_2 = n + m \quad f_2 = \left[2 + v_{2a} (R/p) (1-s) \right] f \quad (5.12)$$

It is seen from the equations 5.11 and 5.12 that the frequency of the vibration produced by a stator flux harmonic in combination with rotor flux harmonic does not depend upon the order of the stator harmonic. It depends upon slip and v_{2a} (Rotor permeance factor)

for $v_{2a} = 0$ we get the same equation as (5.10)

5.4.5. Force Waves of Stator Harmonics only :

Group IV of equation 5.3 deals with stator harmonics only giving

$$w_n = w_m = 0 = 2 \pi f$$

$$\text{and } p_1 = n - m \quad f_1 = 0 \quad (5.13)$$

$$p_2 = n + m \quad f_2 = 2 f \quad (5.14)$$

Equation (5.13) indicates that standing force waves are also produced.

5.4.6. Force Waves of Rotor Harmonics only:

Group V of equation 5.3 deals with rotor harmonics only giving:

$$n = n_a \quad \text{and} \quad n = n_b$$

when $n_a = \pm v_{2a}(R/p) + m_a$ and $n_b = \pm v_{2b}(R/p) + m_b$

$$p_1 = n_a - n_b \quad \text{Velocity } w_{na} - w_{nb} \quad (5.15)$$

$$p_2 = n_a + n_b \quad \text{Velocity } w_{na} + w_{nb} \quad (5.16)$$

Where

$$w_{na} - w_{nb} = \left[(n_a - m_a) - (n_b - m_b) \right] (1-s) f \times 2 \pi$$

$$w_{na} + w_{nb} = \left[2 + \left\{ (n_a - m_a) + (n_b - m_b) \right\} (1-s) \right] 2 \pi f$$

Simplifying

$$f_1 = (v_{2a} - v_{2b}) R/p (1-s) f \quad (5.17)$$

$$f_2 = \left[2 + (v_{2a} + v_{2b}) R/p (1-s) \right] f \quad (5.18)$$

5.47 Slot Frequency Force Waves

(a) For the squirrel cage rotor; $v_2 = \pm 1$ yields the largest amplitude for the rotor flux harmonic. For this rotor, from equation 5.17 and 5.18 with $v_{2a} = \pm 1$ and $v_{2b} = \pm 1$

(i) When $v_{2a} \neq 0$ $v_{2b} = -1$ or $+1$ (both)

$$f_1 = 0 \quad (5.19)$$

$$f_2 = \left[1 \pm (R/p) (1-s) \right] 2f \quad (5.20)$$

(ii) When v_{2a} and v_{2b} are of different signs.

$$f_1 = (R/p) (1-s) 2f \quad (5.21)$$

$$f_2 = 2f$$

Equation 5.19 through 5.22 gives slot frequencies variable with slip (speed of the motor).

(b) Slot Relations:

From figure (5.1) , it is clear that force wave poles should be as large as possible to avoid its effect or $p = 1$, (one pair of pole) should be avoided. Here conditions under 5.4.4. will be discussed , as this is produced in combination of stator and rotor slot harmonics. Only 2- Pole force wave conditions are discussed ^(5B)

For $p_1 = p_2 = \pm 1$, the following equations must be satisfied.

$$p_1 = n - m \quad \text{and} \quad p_2 = n + m$$

If $n_a = \pm v_{2b} (R/p) + 1$

and $m_b = \pm v_{2a} (S/p) + 1$ (slot harmonic)

then $p_1 = \pm v_{2b} (R/p) \mp v_{2a} (S/p) = 1$

$$p_2 = 2p \pm v_{2a} (S/p) \pm v_{2b} (R/p) = 1$$

or $\pm v_{2b} (R) \mp v_{2a} S = p 1 \quad (5.23)$

$$2p \pm v_{2a}(s) \pm v_{2(b)} R = 1 \tag{5.24}$$

for $v_{2b} = v_{2a} = \pm 1$

$$\left. \begin{aligned} R \pm S &= \pm 1 \\ P \pm R \pm S &= \pm 1 \end{aligned} \right\} \text{should be avoided} \tag{5.25}$$

5.5. Magnitudes of Force waves:

From equation 5.1

$$F_r = 1.39 \times 10^{-8} \times 2L \int_{-\pi/2}^{+\pi/2} b_{na} b_{mb} d\theta \tag{5.26}$$

Fig. 5.5. shows the resultant distribution as sinusoidal, the integrand is

$$\begin{aligned} F_r &= \frac{1.39 \times 10^{-8}}{p'} DL B_{mb} B_{na} \\ &= 4.23 \times 10^4 DL B_{mb} B_{na} Kga \text{ (mks)} \end{aligned} \tag{5.27}$$

Where p' = order of force wave poles.

Flux densities can be found from equation (4.17).

5.6. DEFLECTION OF FRAME AND SOUND INTENSITIES

5.6.1. Deflection of Frame:

If we develop the stator lamination ring into a straight line, and consider it as a beam, we can use well known equations to calculate the deflection produced. This continuous beam will bend into a shape similar to the sinusoidal wave of applied force, with node at each zero point of the force wave. Each of the nodes may be treated as free support. The deflection of such a freely supported beam under a sinusoidally distributed load is :

$$d = \frac{3 W D_s^3 \times 10^6}{4 E n^3 h^3 L} \quad (\text{micro inch}) \quad (5.28)$$

where d = deflection.

W = load in lbs.

D_s = mean diameter of the stator core inches.

= $D_g + 2$ (slot depth) + h

h = radial depth of the stator core behind the slot in inches.

n = one half the number of nodes of core flexure.

E = modulus of Elasticity.

= the number of Poles of the force wave.

Taking equation in C.G.S. syste,, the equation 5.28 gives deflection in Cms.

Equation is a approximate equation derived from beam theory.

The true equations for the deflection of a thin ring under a sinusoidal radially applied force are

$$\text{for } n = 2 \quad d = \frac{W D S^3 10^6}{6 E h^3 L} \quad (5.29)$$

$$\text{for } n = 3 \quad d = \frac{9 W D S^3 10^6}{256 E h^3 L} \quad (5.30)$$

$$\text{for } n = 4 \quad d = \frac{W D S^3 10^6}{75 E h^3 L} \quad (5.31)$$

The natural frequency of a thin steel ring, vibrating in $2n$ nodes, is :

$$f = \frac{36,700 n (n^2 - 1) h}{D S^2 \sqrt{n^2 + 1}} \quad \text{C PS} \quad (5.32)$$

5.6.2. Sound Intensity of Plane Wave:

The sound intensity is defined by the equation

$$I_d = 10 \log \left(\frac{I}{I_0} \right) \text{ db} \quad (5.33)$$

where I = actual sound intensity in watts / cm^2 in the direction of propagation.

$$I_0 = \text{Reference sound intensity} = 10^{-16} \text{ watts / cm}^2$$

This reference sound intensity corresponds to a sinusoidal double amplitude displacement of the air at normal pressure and temperature equal to $2.20 / f \times 10^{-6}$ cms.

This gives for the sound intensity of plane wave

$$I = 1.3 \times 10^{-16} (2 \pi f)^2 \text{ watts / cm}^2$$

thus from 5.33

$$I_d = 7 + 20 \log_{10} (2 \pi f) \text{ db} \quad (5.34)$$

5.6.3. Correction factor:

To find the plane wave of sound that is equivalent to the wave produced by the motor frame, we can make use of the work of Morse and others as shown in Fig. 5.6., and Fig. 5.7 . The curves of Fig. 5.6 give the number of decibels that must be added to the sound intensity computed from equation 5.34, to obtain the intensity of sound produced by an indefinitely long cylinder vibrating with the same surface amplitude. The cross-section depends upon the number of nodes ($2m$) and the value of k_{ro} , which is the ratio of the cylinders periphery to the wave length of sound in air at the frequency considered.

$$\begin{aligned} k_{ro} &= \frac{(2\pi m r_o)}{c/f} \\ &= 0.00559 f r_o \end{aligned} \quad (5.35)$$

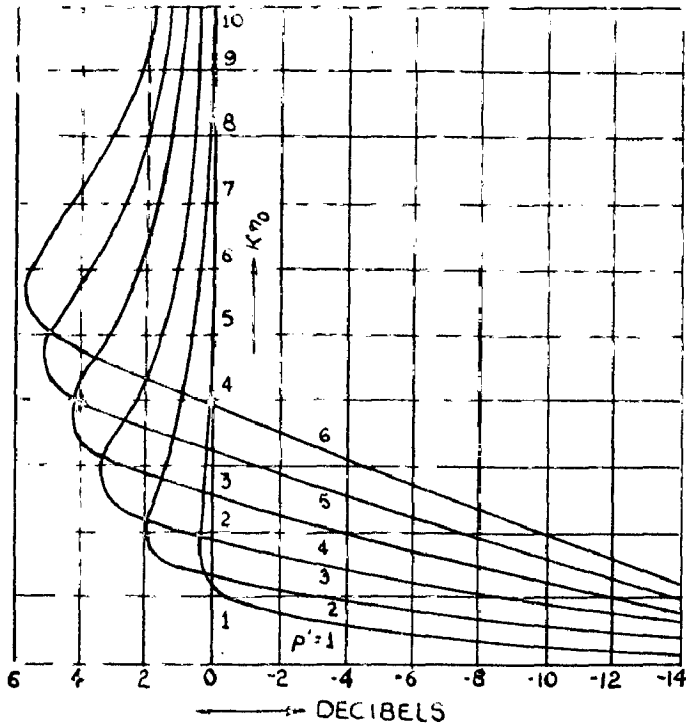


FIGURE 5.6

CORRECTION FOR AN INDEFINITELY LONG CYLINDER

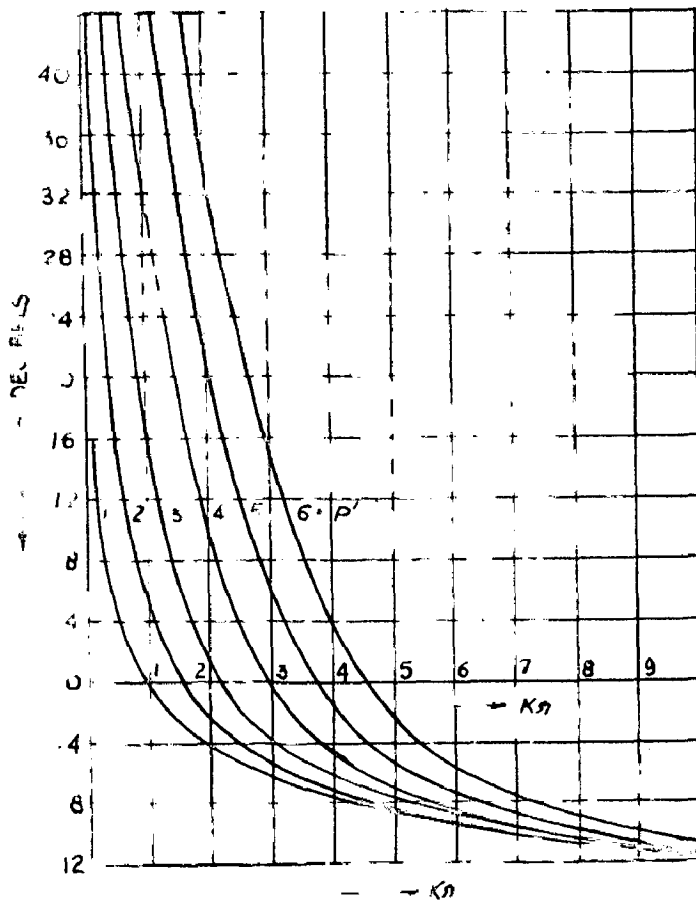


FIGURE 5.5

CORRECTION FOR DISTANCE FROM THE MOTOR SURFACE

Where C = velocity of sound in air.

r_0 = Cylinder radius in feet.

(b) Distance Correction:

The rate at which the sound intensity falls off with distance also depends upon on the ratio kr_0 (equation 5.35) as shown in Fig. 5.7. When the cylinder is small, as the frequency is low, the intensity falls off very rapidly as the distance from the cylinder or high frequency it falls off in accordance with the usual inverse square law.

CHAPTER VI

RESONANCE CALCULATIONS OF SQUIRREL CAGE INDUCTION MACHINE WITH AND WITHOUT SKEW

6.1. PROCEDURE:

Magnetic noise is produced by mechanical vibration of the motor frame or components, where the vibromotive force is supplied by the magnetic fields of the motor. The noise produced by the slot harmonics is generally the most objectionable magnetic noise, since this has a relative high frequency. It is caused by radial motions of the stator in nodal patterns of four, six, or more nodes (See Fig .e). By knowing the frequencies and number of poles of these forces and the vibratory characteristics of the stator and frame, it is generally possible to avoid the coincidence of a forcing frequency and an objectionable resonance. The frequencies and pole structures of the most bothersome force waves in large motors can be calculated from the following equations:

Frequency of force waves.

Number of nodes in force waves.

$$\left[\frac{R(1-s)}{P} - 2 \right] f$$

$$(2R - 2S - 4P)$$

$$\left[\frac{R(1-s)}{P} \right] f$$

$$2(R-s)$$

$$\left[\frac{R(1-s)}{P} + 2 \right] f$$

$$(2R - 2S + 4P)$$

The author gives a general procedure for calculating in decibels the slot frequency and other harmonic frequency sound pressure level produced the machine under test operating at any arbitrary speed and load. To do this, it is necessary, first, to calculate the frequencies, pole numbers and magnitudes of the important air gap magnetic fields; second, to

calculate from these the frequencies and magnitudes of those air gap force waves with relatively few nodes those are most likely to produce noise; third, to calculate the stiffness and resonant frequencies of the frame structure for vibrations of low numbers of nodes; fourth, from all these, to calculate the radial deflections of the stator core and frame that are due to the significant slot frequency force waves; and fifth, to calculate the decibel level of sound pressure at any point in space that is caused by the calculated deflection of the frame. Under this Chapter the author presents the numerical results of carried over on IBM 1620 Computer. The author passes with him the other results but only significant results are presented here.

6.2. CALCULATIONS

All the possible combinations as detailed under Section 5.4 of Chapter V are considered for calculation noise intensity, and the computed results are tabulated from Table 6.1 to 6.7.

For this purposes:

Diameter of motor at air gap (10 = 17.0 cms.

Length of armature = 7.5 cms.

E = 3×10^7 (for steel)

h = 3.5 cms.

Slot depth = 2.1 cms.

D_m = 24.7 cms.

B = 256 turns The results are plotted in Fig. 6.1 to

6.6.

$$F_r = \frac{255.0}{p'} \frac{k_{w1ma} D_{mb} G_{ma} k_{w1mb} I_1^2}{n_a k_{ama} mb} \quad (6.1)$$

Where,

$$D_{mb} = \frac{(1 - G_{mb} \cos \phi)^2 + (C_{mb} \sin \phi)^2}{\sqrt{\left[S_{mb} X_{M(mb)} (1 + T_{2mb}) \right]^2 + \left[S_{mb} X_{M(mb)} R_{2(mb)} \right]^2}}$$

$$C_{mb} = \frac{R_{2mb}^2 + \left[S_{mb} X_{M(mb)} (1 + T_{2mb}) \right]^2}{2}$$

$$\tan \phi = \frac{R_{2(mb)}}{S_{mb} X_{M(mb)} (1 + T_{2mb})}$$

$$D_{mb} \approx 1 - \frac{1}{1 + T_{2mb}} \quad (\text{Neglecting } R_{2(mb)})$$

Since in for higher harmonics, only differential leakage reactance predominates.

$$\therefore D_{mb} \approx 1 - \frac{1}{T_{2hmb}}$$

$$D_{mb} \approx 1 - H^2 K_{sub}^2 \dots \dots (6.2)$$

$$\text{Where } H = \frac{\sin \left(\frac{p}{R} \right)}{R}$$

$$\therefore G_{sub} \approx H^2 K_{sub}^2 \quad (\text{from Chapter II})$$

$$\therefore F_r \propto \frac{(1 - H^2 K_{sub}^2) H^2 K_{sub}^2}{(K_{sub})}$$

$$F_r \propto (1 - H^2 K_{sub}^2) H^2 (K_{sub}) \dots \dots (6.3)$$

Equation 6.3. directly gives the effect of skewing of rotor bars.
 skewing reduces the radial forces and subsequently the sound emitted
 by magnetic fields

$$\text{As deflection} = d = 0.75 \frac{F}{L_0} \frac{D^3}{p'^3} \frac{\pi \times 10^6}{E h_0^3} \text{ Micro inch.}$$

$$\text{and Sound Intensity } (I_d) = 7 + 20 \log (d \times f_s) \text{ dbm}$$

6.3. NATURAL FREQUENCY

The natural frequency of the frame, considering it as simple ring

$$f_n = \frac{36,700 p' (p'^2 - 1) h_0}{D_m^2 \sqrt{p'^2 + 1}} \text{ CPS}$$

The minimum $p' = 4$ (without cage)

$$\therefore f_n = 7560 \text{ CPS}$$

The natural frequency being very high, there is no possibility of mechanical resonance.

Table 6.1. NOISE PREDICTED BY 17th & 19th HARMONICS (HIGH FOR R SKIN)

For $\text{slap}(s) = 0.1$ to 2.0

β	$\sigma = 0.01$					$\sigma = 0.1$					$\sigma = 0.2$					
	\mathcal{E}	P	d	I_d	\mathcal{E}	P	d	I_d	\mathcal{E}	P	d	I_d	\mathcal{E}	P	d	I_d
	For 17th Harmonic.															
4	100	0	0	0	100	1.1	0.05	21.0	100	2.7	0.125	29	100	2.7	0.125	29
4	1600	0	0	0	1630	.2	.009	30.6	1630	.4	.013	36.6	1630	.4	.013	36.6
8	100	0	0	0	100	.4	.002	-	100	1.0	.005	-	100	1.0	.005	-
16	100	0	0	0	100	1.1	-	-	100	1.4	.007	-	100	1.4	.007	-
16	1600	0	0	0	1630	.2	$.12 \times 10^{-3}$	-	1630	.4	-	-	1630	.4	-	-
	For 19th Harmonic															
4	100	0	0	0	100	1.3	5.8×10^{-2}	21.3	100	2.7	.12	20.6	100	2.7	.12	20.6
8	100	.2	-	-	100	2.0	.0157	11.0	100	6.2	.055	17.8	100	6.2	.055	17.8
8	1900	0	0	0	1430	.1	.055	-	1200	.2	1.1×10^{-3}	11.0	1200	.2	1.1×10^{-3}	11.0

Table 6.1 Contd..

p'	s = 0.5					s = 1.0					s = 2.0					
	f	P	d	I _d	f	P	d	I _d	f	P	d	I _d	f	P	d	I _d
For 19th harmonic																
4	100	5.6	.25	35.0	100	6.4	.285	36.0	100	10.7	.475	40.5	100	10.7	.475	40.5
4	875	1.0	.04	37.8	100	1.2	.053	21.4	1700	1.3	.05	45.4	1700	1.3	.05	45.4
8	100	2.4	.126	9.0	100	2.6	.015	10.2	100	2.9	.016	11.0	100	2.9	.016	11.0
16	100	5.0	.03	7.9	100	5.5	.03	8.0	100	6.9	.04	8.2	100	6.9	.04	8.2
16	875	.8	.03	-	100	.1	-	-	1700	1.1	.67x10 ⁻³	8.2	1700	1.1	.67x10 ⁻³	8.2
For 19th harmonics.																
4	100	5.1	.23	34.2	100	6.4	.28	36.1	100	7.9	.35	38.0	100	7.9	.35	38.0
8	100	12.9	.07	24.2	100	14.6	.082	25.2	100	19.1	.1	27.0	100	19.1	.1	27.0
8	775	.5	2.8x10 ⁻³	13.7	100	.7	-	-	1800	.8	3.9x10 ⁻³	24.0	1800	.8	3.9x10 ⁻³	24.0

Table 6.2 NOISE INTENSITY OF 5th HARMONICS (WITH ROTOR SKEWED)

s = .01		s = 0.1		s = 0.2								
p'	f	d	I _d	f	P	d	I _d	f	P	d	I _d	
<u>FOR 5th Harmonics</u>												
8	100	16.5	.09	25.0	100	226.5	1.26	49	100	522.0	2.9	56.2
8	1680	0	-	-	1630	1.8	$.53 \times 10^{-2}$	22.0	1360	8.1	1.84×10^{-2}	36.0
20	100	.6	-	-	100	4.1	-	-	100	9.0	-	-
4	100	.9	.04	5.0	100	10.3	.45	15.0	100	8.7	.39	38.0
<u>For 23rd Harmonic</u>												
4	100	1.0	.04	19	100	20	.89	46.0	100	44.0	1.97	52.8
8	100	.2	$-.11 \times 10^{-2}$	-	100	2.8	1.59×10^{-2}	9.8	100	6.2	3.48×10^{-2}	17.8
16	1680	0	0	-	1630	.2	$.14 \times 10^{-3}$	9.9	1360	6.8	$.35 \times 10^{-3}$	-
20	100	0	-	-	100	.8	-	-	100	1.9	-	-
I _d = 19.0												
<u>For 25th Harmonic</u>												
4	100	1.0	.22	19	100	20.0	.021	46.0	100	43.9	.023	52.8
8	100	.1	-	-	100	1.7	-	-	100	3.8	.02	13.5
I _d = 19.0												
I _d = 70.6												
I _d = 46.0												
I _d = 66.3												

Table 6.2 (Contd..)

p'	θ = 0.5				θ = 1.0				θ = 2.0			
	f	F	d	I _d	f	F	d	I _d	f	F	d	I _d
4	100	51.4	2.3	54.0	100	67.9	3.0	56.5	100	61.3	2.74	55.0
8	875	.9	.2	18.4	100	8.6	1.8x10 ⁻²	22.0	1700	8.5	1.84x10 ⁻²	36.5
8	100	1083	6.0	64.6	100	1222	6.8	65.0	100	1495	8.3	66.4
20	100	19.4	-	-	100	21.3	-	-	100	201	7.2x10 ⁻³	-
For 23rd Harmonic												
4	100	904	4.02	59.0	100	104	4.5	60.0	100	125.4	5.6	62.0
8	100	13.0	7.3x10 ⁻²	24.2	100	14.6	8.1x10 ⁻²	25.0	100	17.0	9.5x10 ⁻²	26.5
16	875	1.1	.91x10 ⁻²	-	100	1.03	.91x10 ⁻³	-	1700	1.3	.91x10 ⁻³	13.0
20	100	42	-	-	100	5.9	-	-	100	5.3	1.9x10 ⁻³	-
For 25th Harmonic												
4	100	9.06	.46	59	100	100.4	.5	60.0	100	125.5	.72	62.0
8	100	7.71	4.3x10 ⁻²	-	100	8.9	4.96x10 ⁻²	21.0	100	10.8	6.0x10 ⁻²	22.5

TABLE 6.3 TOTAL 4 POLE SOUND INTENSITY LEVEL
OF TEST MACHINE.

Slip	f	P	B	I _d
<u>ROTOR NOT SKEWED</u>				
.01	100	3.5	.157	31
.1	100	47.7	2.13	57
.2	100	104.7	4.67	64.0
.5	100	239.7	10.7	70.0
1.0	100	236.3	10.6	70.0
2.0	100	323.9	14.5	78.0
<u>ROTOR SKEWED</u>				
.01	100	2.0	.09	23
.1	100	31.4	1.41	29
.2	100	71.5	3.22	50
.5	100	138.2	6.2	63
1.0	100	178.0	8.0	65
2.0	100	205.0	9.2	68

Table 6.4. TOTAL RADIAL HARMONIC FORCE WAVE WITHOUT SCREW

p^i	$s = 0.01$	$s = 0.1$	$s = 0.2$	$s = 0.5$	$s = 1.0$	$s = 2.0$
2	3.5	47.7	104.7	238.7	236.3	323.9
4	11.6	165.3	363.7	756.2	863.4	1031.6
6	17.0	140.8	342.2	792.7	1775.9	993.1
8	0	2.8	5.0	14.3	21.7	17.7
10	0	5.7	10.8	28.2	32.9	32.1
12	0.0	4.1	10.3	23.4	29.1	27.2
14	0.0	2.9	8.1	13.4	15.0	14.1
16	1.5	15.8	46.6	73.6	80.1	83.8
18	1.9	30.5	118.0	221.7	249.5	271.9
20	1.0	16.6	39.2	75.9	89.8	99.3

Table 6.5 TOTAL RADIAL HARMONIC FORCE WAVES
WITH SKEW

p'	$s = 0.01$	$s = 0.1$	$s = 0.2$	$s = 0.5$	$s = 1.0$	$s = 2.0$
4	2.0	31.4	71.5	138.2	178.0	205.0
8	13.7	205.1	390.1	915.1	1015	1170.0
12	13.0	90.1	291.1	675	1053	850
16	0.0	1.7	3.1	9.3	11.6	13.7
20	0.0	3.0	7.2	21.1	29.0	27.6
24	0.0	3.2	7.3	19.1	21.1	23.2

Figures indicate lbs.

Table 6.6 HIGH FREQUENCY SOUND GENERATED BY MAGNETIC FIELDS

(ROTOR SKEWED)

Frequency	Harmonic Sound Intensity (db)					Dist Harmonics
	5th	17th	19th	23rd	25th	
750	-	-	13.7	-	-	7.0
850	-	10.4	37.4	-	-	-
950	-	-	-	-	-	52.0
1250	0	-	-	-	-	16.0
1350	0	36.5	36.6	-	-	-
1450	0	-	-	7.0	-	-
1450	-	-	-	-	44.0	44.0
1550	22.0	30.6	-	-	-	-
1600	0	-	-	-	-	60.0
1700	0	37.0	53.2	-	13.0	-
1800	0	-	7.0	24.0	-	-

Table 6.7 HIGH FREQUENCY SOUND GENERATED BY MAGNETIC FIELDS

(ROTOR UNSKEWED)

750	0	-	-	11.7	-	7.0
850	0	40.0	37.0	-	-	77.0
950	-	-	-	-	-	52.0
1250	0	16	21.4	-	-	16.0
1350	0	40.0	38.6	-	-	-
1450	0	-	-	7.0	-	11.0
1450	-	-	-	-	-	44.0
1550	0	33.0	30.8	-	-	-
1600	0	-	-	-	-	60.0
1650	-	-	-	-	-	32.0
1700	0	49.5	62.5	-	-	-
1800	0	-	-	27.0	14.6	30.0

6.4. REDUCTION OF PARASITIC TORQUES AND NOISE OF INDUCTION MACHINE WITH ROTOR SKEWING

Simplifying the expressions for parasitic torques and noise, we can arrive at simpler function in terms of skew factor and certain other constants of the machine. The functions thus obtained, can give the range of variations in magnitudes of the parasitic torques and noise for a corresponding change in skewing of rotor bars.

Defining Unit values:

$$\text{Unit value of (mth harmonic)} = \frac{\text{value of mth harmonic quantity with skew}}{\text{value of mth harmonic quantity without skew.}}$$

6.4.1. MAXIMUM PARASITIC TORQUES

As, our previous study reveals, for the test machine 5th, 19th and 25th harmonics are more predominant. So, effect of skewing for these harmonics will be considered primarily. From equation (3.16)

$$S_{mP.O} = \frac{R_2(m)}{X_M(m) + X_2(m)}$$

$$\therefore S_{mP.O} = \frac{A_1}{1 + T_2(m)}$$

$$\text{and } \tau_m(\text{max}) = 0.369 \frac{R}{w} \frac{X_M(m) I_1^2}{1 + T_2(m)}$$

Assuming I_1 constant)

$$\tau_m(\text{max}) \propto \frac{1}{1 + T_2(m)} \tag{6.4}$$

$$\text{Unit Max. Torque} = \frac{1 + T_2(m)_0}{1 + T_2(m)} \tag{6.5}$$

Results are tabulated and plotted in Fig. 6.9A.

6.4.2. Synchronous Torque:

From equation (4.29)

$$T_{sy(max)} = 2 \pi C B_{na} A_{nb}$$

$$= \left[\frac{B_m A_2}{\left(\frac{R_{2(m)}}{X_M(m)} \right)^2 + \omega^2 (1 + T_{2(m)})^2} \right] \frac{K_{ana}}{K_{ama}}$$

substituting for B_m equation (4.9)

$$T_{sy(max)} = \frac{1}{(1 + T_{2(m)})} \left(\frac{A_2}{H(m)^2 + 1} \right) \frac{K_{ana}}{K_{ama}}$$

when $H(m) = \frac{R_{2(m)}}{X_M(m)}$

$$\therefore T_{sy(max)} = \left(\frac{K_{ana}}{K_{ama}} \right) \frac{1}{1 + T_{2(m)}}$$

and Unit synchronous torque = $\frac{K_{ana}}{K_{ama}} \left(\frac{1 + T_{2(m)0}}{1 + T_{2(m)}} \right)$

Where $T_{2(m)0}$ = Ratio of secondary leakage reactance to Magnetising reactance, with rotor unskewed.

The results are tabulated and plotted in Fig. 6.9 B.

6.4.3. Noise:

From equation (5.27) and (6.2)

$$\text{Radial force } F_r = \frac{\left[1 - \frac{2}{\xi(m)} K_s(m) \right] K_s(m)^2}{\left[1 - \frac{2}{\xi(m)} \right] K_{ana}} \dots 6.7$$

But since sound intensity is defined as

$$I_d = 7 + \log (d \times f)$$

$$\text{Where } \xi(m) = \frac{8 \sin m p^w / 12}{(m p^w / 12)^2} \quad 6.8$$

Considering only 100 cycle hum and radial force wave of 4 poles.

$$I_d \approx \log (d \times f)$$

$$\text{As } d \propto F_r$$

$$\therefore I_d \propto \log (F_r \times f)$$

$$\therefore \text{Unit Noise} = \frac{\log (F_r \times f)}{\log (F_{ro} \times f)} = \log \left(\frac{F_r}{F_{ro}} \right) \quad 6.9$$

Substituting 6.7 in 6.8

$$\text{Unit Noise} = \log \left(\frac{1 - \xi(m)^2 K_{sm}^2}{1 - \xi(m)^2} \right) = \frac{K_{sm}^2}{K_{am}^2} \quad 6.10$$

$$\text{where } m = \pm v (R/p) + m$$

equation 6.9 gives the following conclusions.

- (i) For decreasing effect in noise, unit values are negative.
- (ii) Increasing and decreasing effect not only depends upon skewing but the magnitude of (m) also which is again function of Rotor slots and order of curves are plotted in Fig. 6.8. For following pairs of harmonic giving 4 pole, 100 cycle noise.

1. 5th and 7th
2. 19th and 17th
3. 25th and 23rd.

Table 6.8. HARMONIC SKEW FACTORS.

Angle Elec.	1	5	7	17	19	23	25	29	53	35	59
5	.999	.995	.993	.91	.895	.84	.815	.75	.32	.65	.214
10	.996	.97	.95	.674	.6	.45	.378	.227	.215	.029	.176
15	.995	.93	.875	.356	.246	.043	.04	.186	.088	.224	.128
20	.994	.88	.775	.06	.05	.19	.215	.186	.018	.028	.074
30	.99	.74	.53	.218	.195	.043	.076	.127	.07	.028	.017
40	.98	.56	.266	.06	.05	.123	.073	.06	.018	.028	.047
50	.97	.416	.029	.123	.11	.057	.091	.005	.039	.028	.022
60	.955	.19	.137	.056	.05	.04	.038	.033	.018	.027	.016
70	.94	.085	.24	.08	.07	.07	.027	.05	.025	.027	.027
80	.90	.18	.13	.043	.047	.039	.036	-	.034	.026	.015

Table 6.9 CALCULATION OF $\frac{q}{2(m)}$ FOR DIFFERENT SKEW ANGLE

Angle	1	5	19	25
0	0	0.16	33.8	101.0
5	.002	.17	42.5	154.0
10	.01	.23	95.5	715.0
15	.015	.34	574.0	6.4×10^4
20	.015	.50	1.26×10^4	22.20
30	.02	1.10	916.0	1.74×10^4
40	.04	2.63	1.32×10^4	1.89×10^4
50	.065	5.70	2880	1.22×10^4
60	.1	30.8	1.39×10^4	7.1×10^4
70	.15	159	$.71 \times 10^4$	35.2×10^4
90	.23	35.8	1.53×10^4	7.9×10^4

Table 6.10 VARIATION OF MAXIMUM ASYM. TORQUES OF HARMONICS WITH SKEW

$$T_{n(\max)} \frac{1 + T_{2(n)0}}{1 + T_{2(n)}}$$

1	5	19	25
1.0	1.0	1.0	1.0
.995	.995	.0	.66
.99	.945	.35	.14
.935	.869	.05	.0016
.925	.77	2.76×10^{-3}	.046
.93	.55	3.8×10^{-2}	.005
.95	.52	2.63×10^{-3}	.0034
.94	.17	1.21×10^{-2}	.003
.91	.035	2.5×10^{-3}	.0014
.87	.007	4.9×10^{-3}	.0003
.815	.03	2.3×10^{-3}	.0013

Table 6.11 HARMONIC SYM. TORQUES WITH DIPP. SKEW ANGLE

$$T) \frac{[1 + T_{2(n)0}] K_{\text{sym}}}{[1 + T_{2(n)}] K_{\text{dip}}}$$

1	5	19	25
1.0	1.0	1.0	1.0
.65	.755	.225	.174
.028	.225	.13	.057
.22	.17	very low	v.l.
.028	.16	v.l.	v.l.
.027	.033	v.l.	v.l.
.026	.036	v.l.	v.l.
.026	.037	v.l.	v.l.
.026	.06	v.l.	v.l.
.025	.002	v.l.	v.l.
.024	-	v.l.	v.l.

**Table 6.12. VARIATION OF HARMONIC SOUND INTENSITY
WITH SKEW**

Angle	5th Harmonic (5) =0.965 na =7	19th harmonic (19)=0.55 na=17	25th Harmonic (25) =.32 na = 25
0	0.0	0.0	0.0
5	.06	-.02	-.23
10	.25	-.17	-.46
20	+ .44	-.62	+1.34
20	+ .66	-1.22	-.49
30	.85	-.61	-.83
40	1.3	-1.22	-1.3
50	1.86	-.85	-.78
60	.55	-1.3	-1.42
70	.31	-1.15	-1.92
90	.53	-1.4	-1.49

$$\text{db} \log_{10} \frac{\left[1 - \xi_{(na)}^2 \right] K_{na}^2}{\left[1 - \xi_{(na)}^2 \right] K_{na}^2}$$

Considering only 4 pole, 100 c/s hum.

- | | | | |
|----|----|------|----|
| | na | | na |
| 1. | -5 | with | +7 |
| 2. | 19 | with | 17 |
| 3. | 25 | with | 25 |
- ‡

HARMONIC SOUND INTENSITY CURVES

FIGURE 6.2

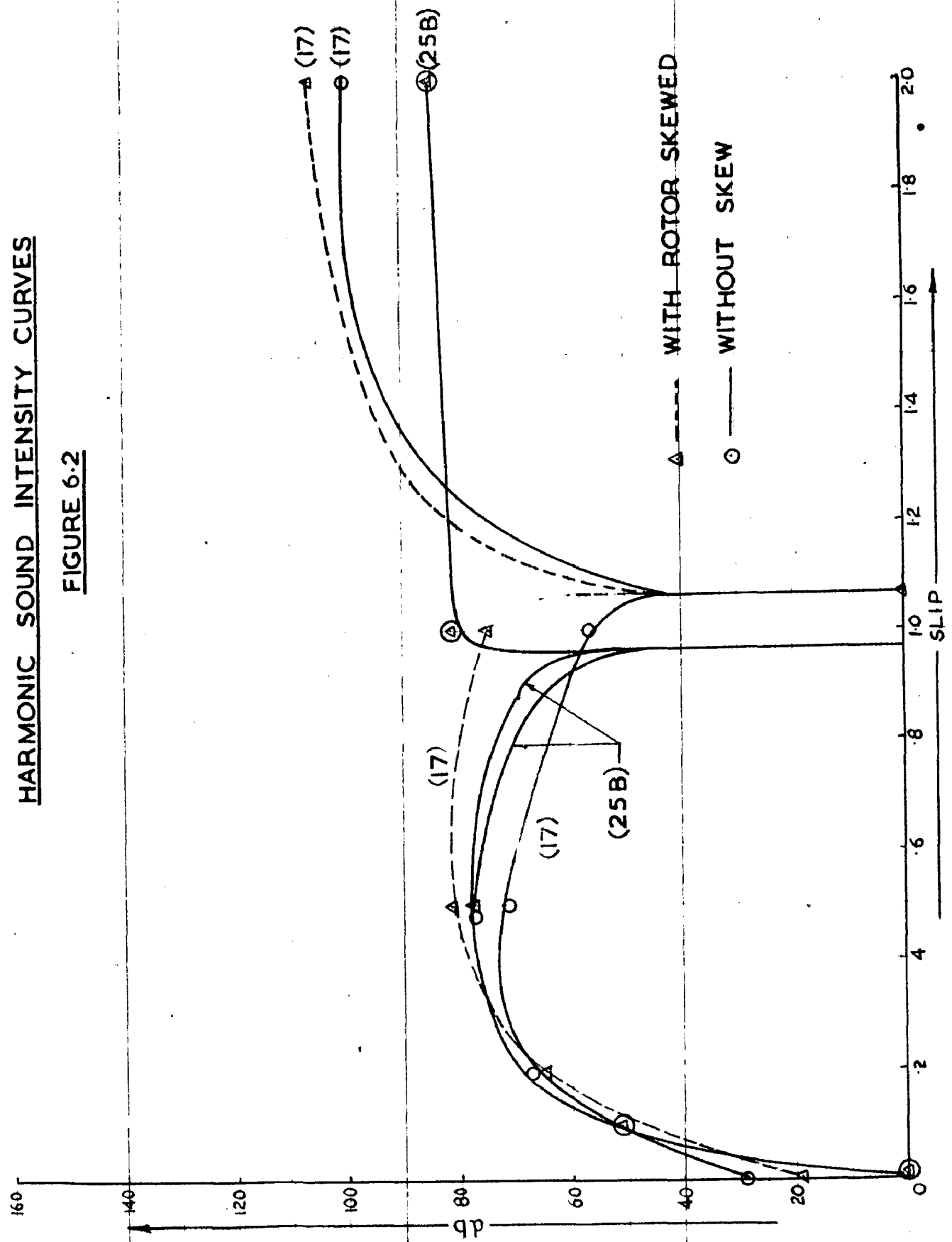
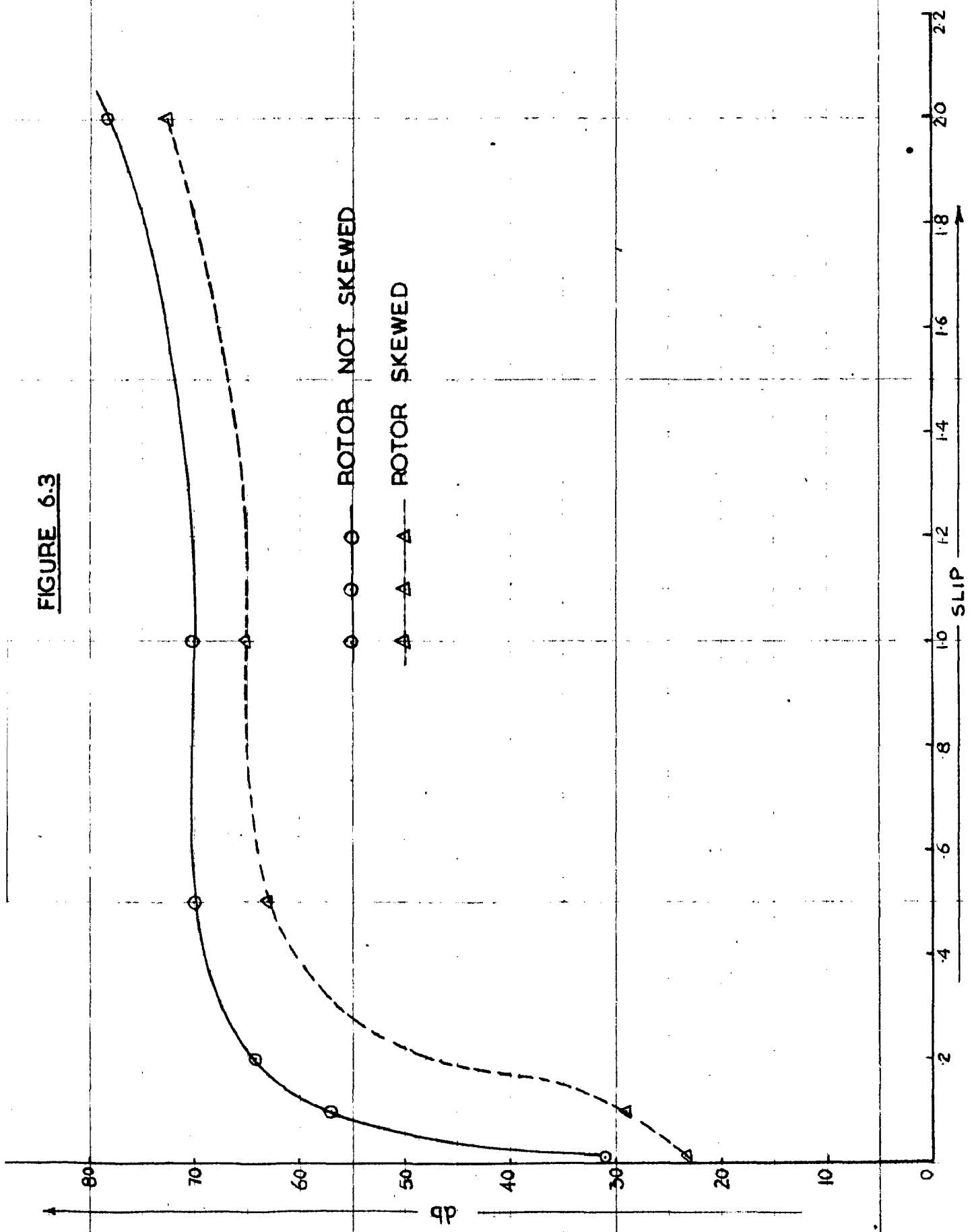
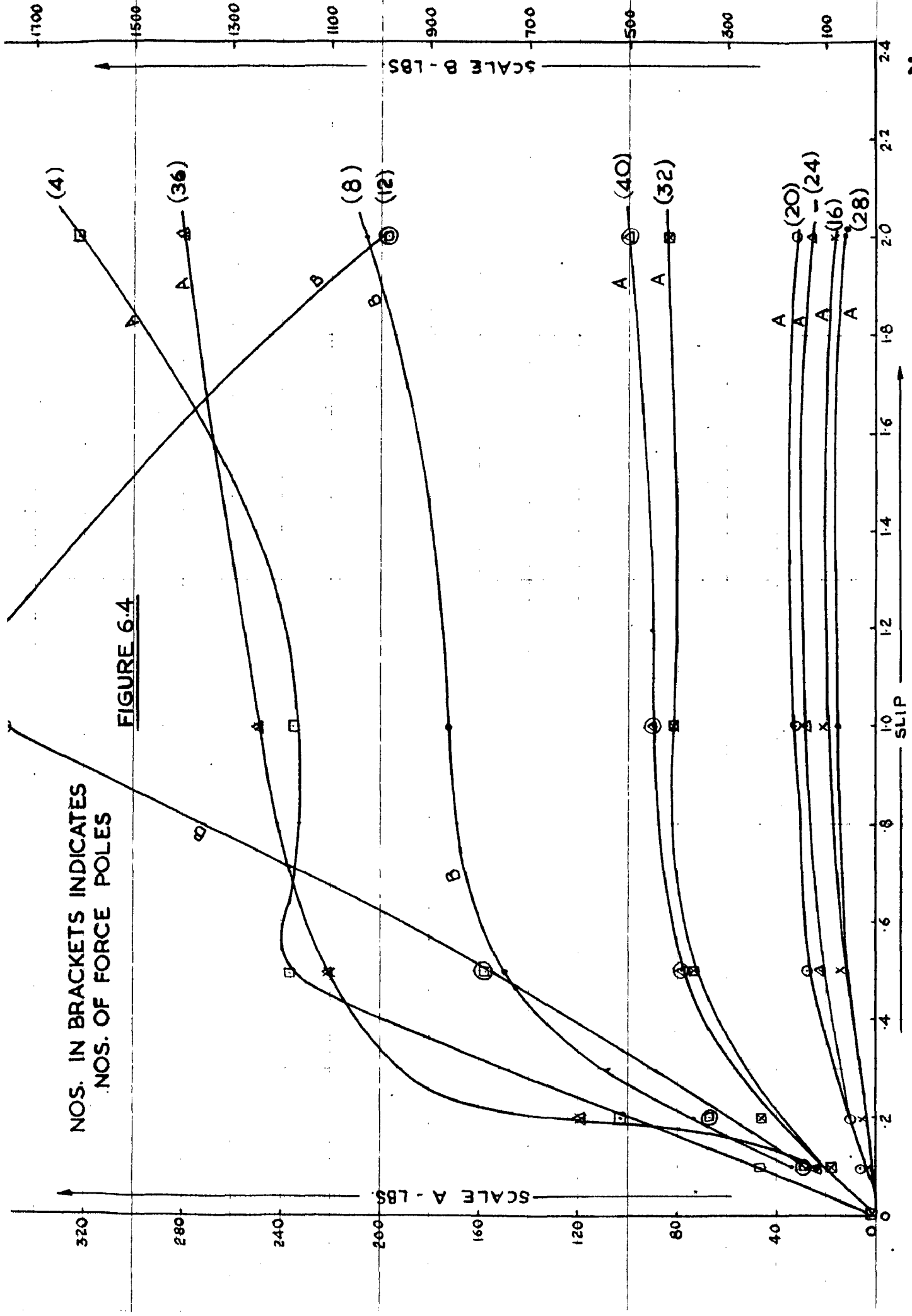


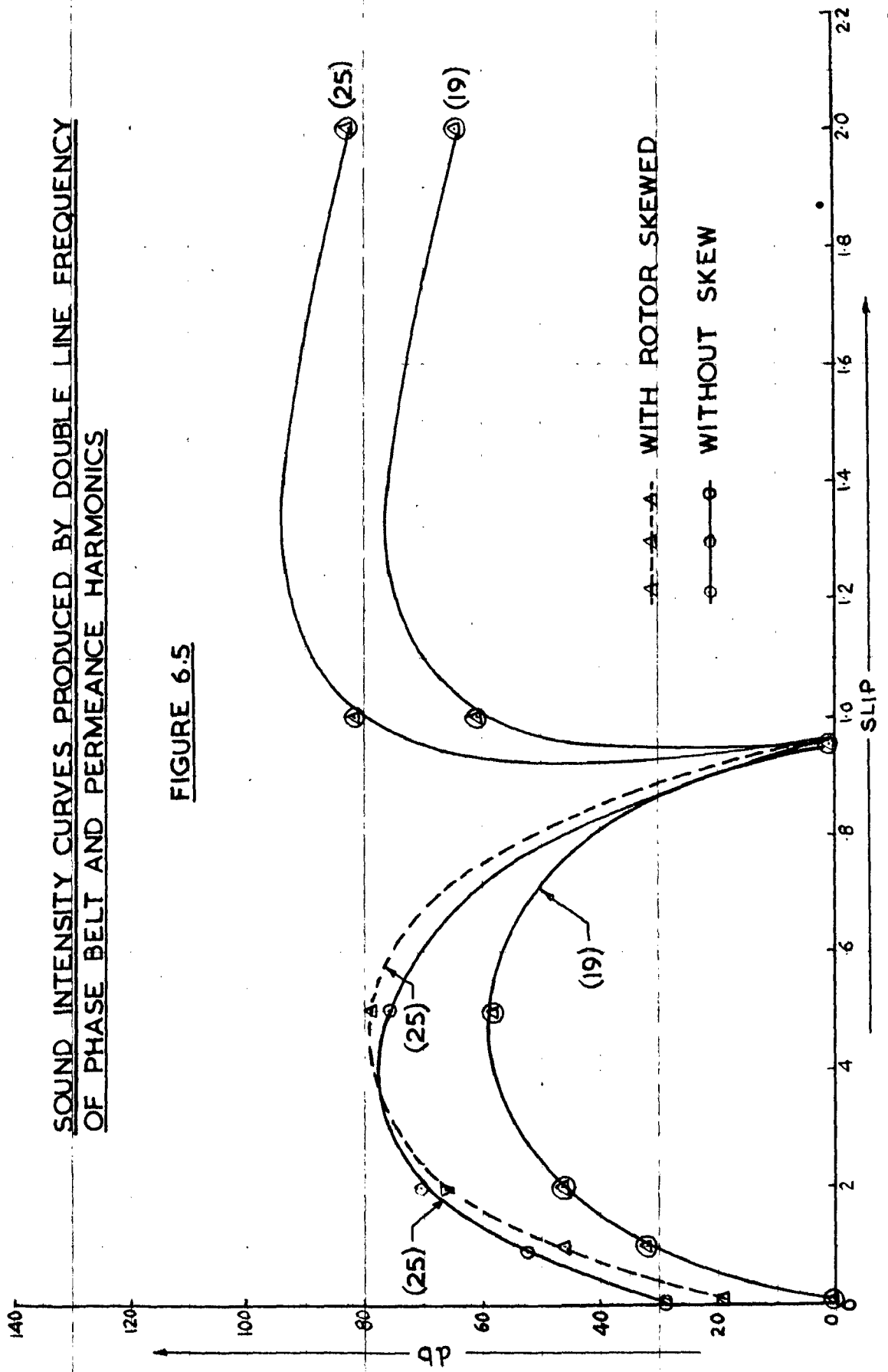
FIGURE 6.3





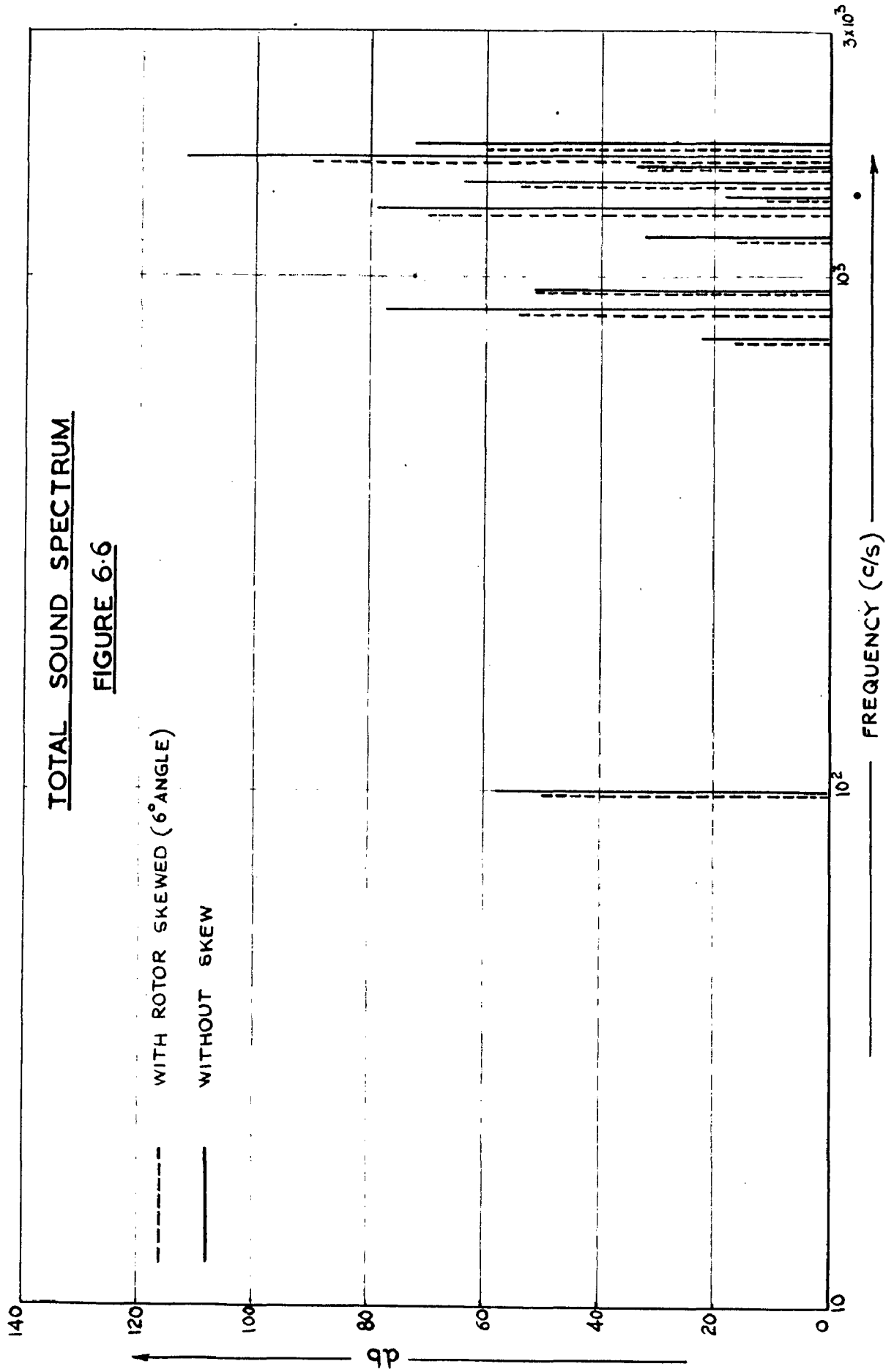
SOUND INTENSITY CURVES PRODUCED BY DOUBLE LINE FREQUENCY
OF PHASE BELT AND PERMEANCE HARMONICS

FIGURE 6.5



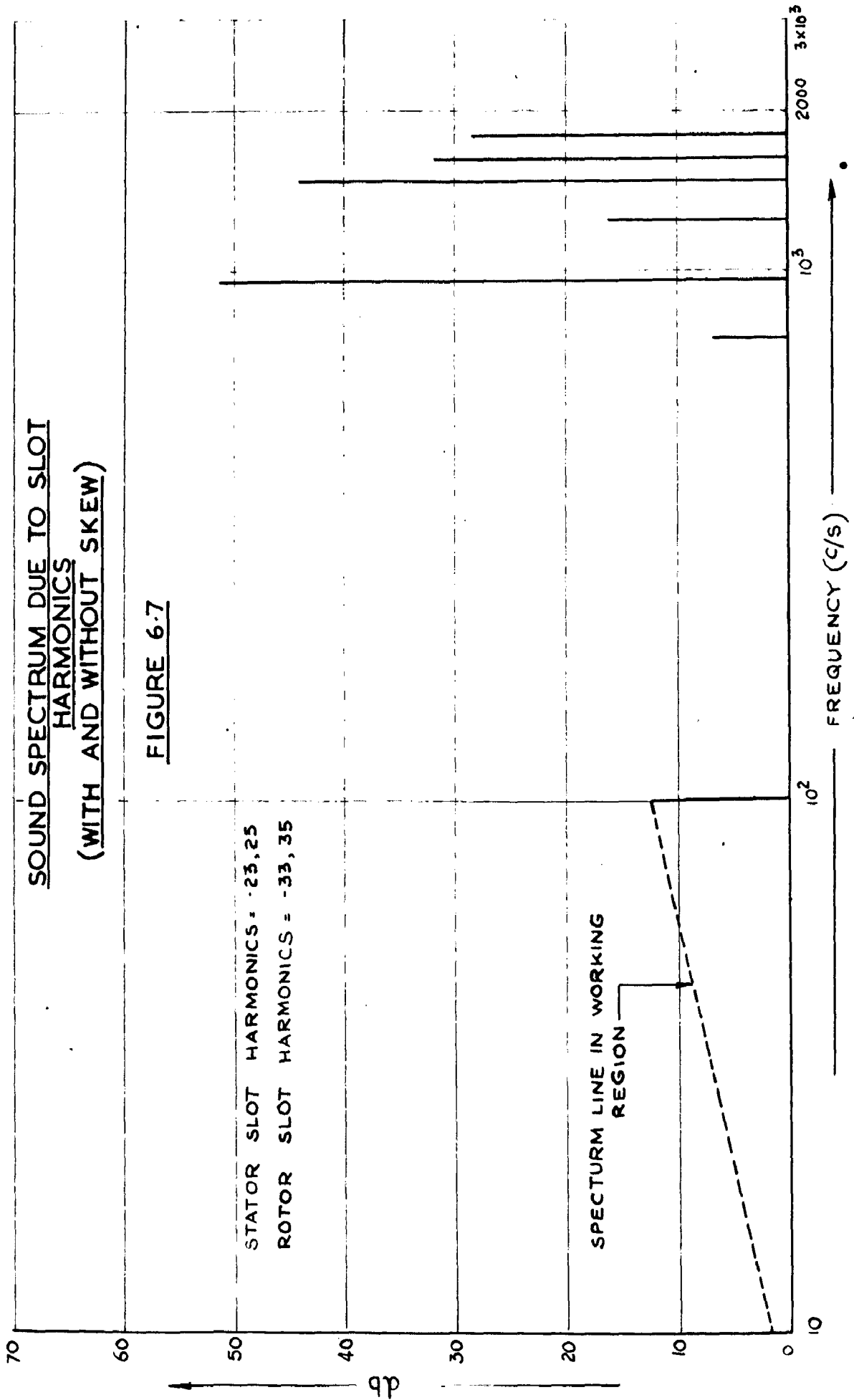
TOTAL SOUND SPECTRUM

FIGURE 6.6



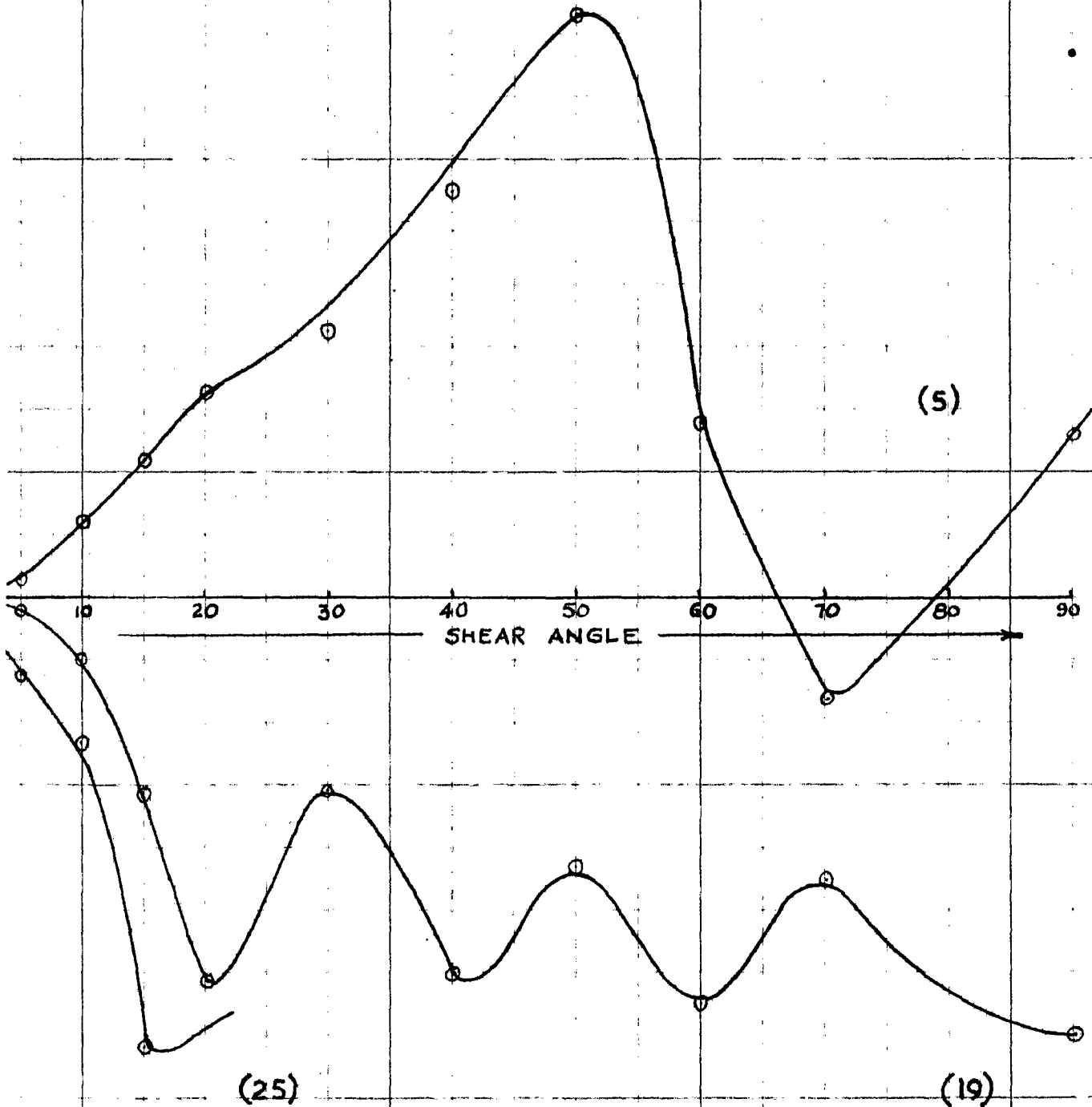
SOUND SPECTRUM DUE TO SLOT HARMONICS
(WITH AND WITHOUT SKEW)

FIGURE 6.7



HARMONIC SOUND INTENSITY WITH VARIED SKEW
ANGLE

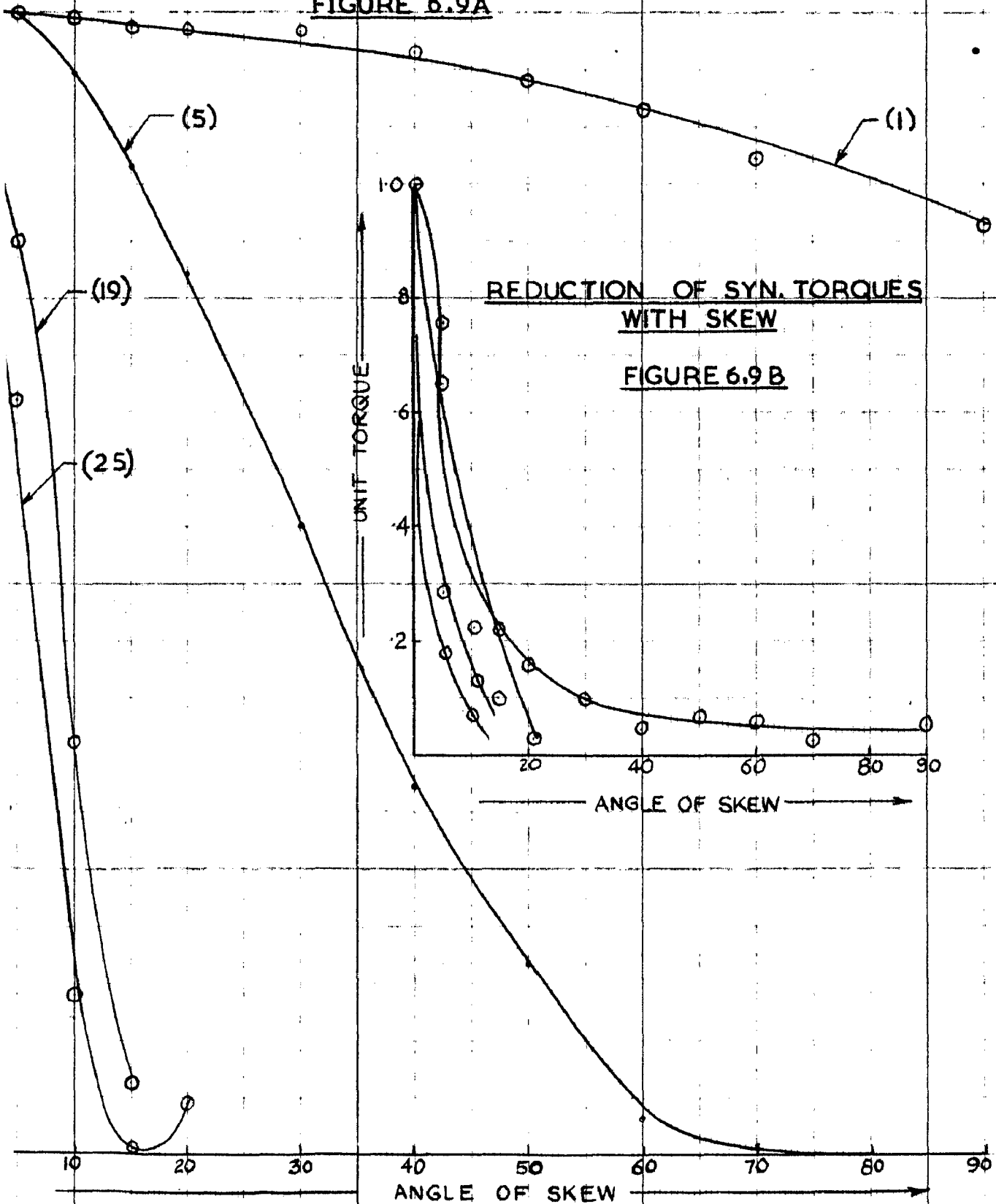
FIGURE 6.8



NOS IN BRACKETS INDICATE ORDER OF
HARMONIC

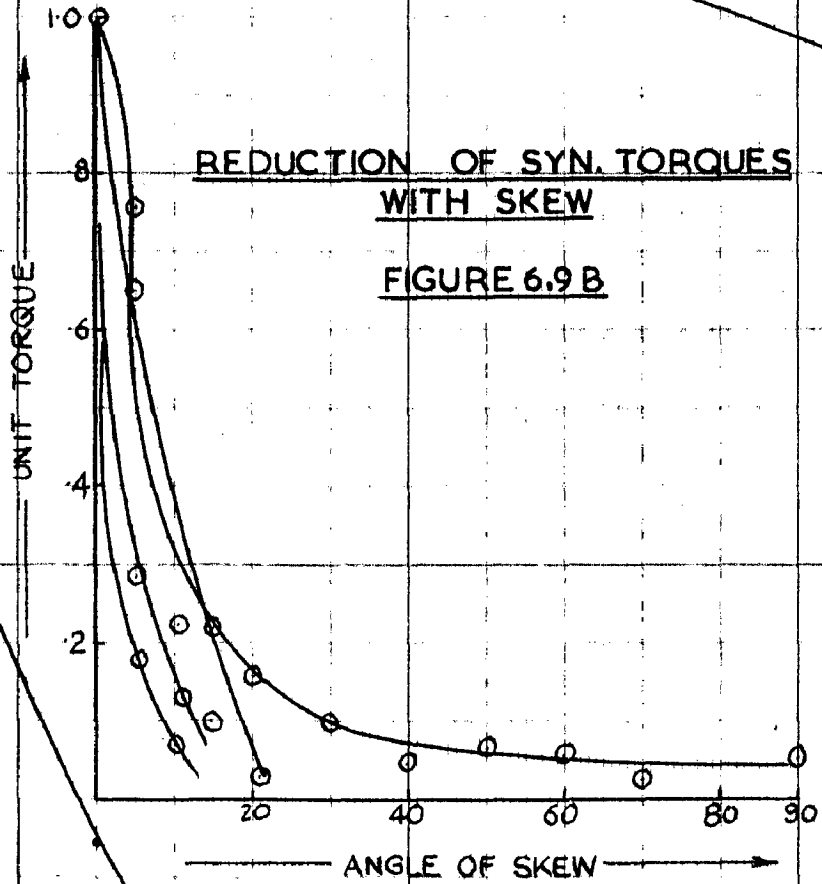
EFFECT OF SKEW OVER ASYN. MAX. TORQUES

FIGURE 6.9A



REDUCTION OF SYN. TORQUES WITH SKEW

FIGURE 6.9B



CHAPTER VII

EXPERIMENTAL RESULTS

In addition to the tests as already specified under section 2.9, some tests over the test machine, with rotor bar skewed (6° Elect) are conducted to check the validity of the calculated performance curves equations and equivalent circuit obtained in previous Chapter.

The specification of the motor is:

440 V, 5 Amps, 1440 r.p.m., 3 H.P., 50 c/s.

3 Phase, skewed bar induction motor.

Though calculations for unskewed rotor, induction motor are also done but due to practical difficulties, unskewed motor could not be made available so observations for skewed motor only are presented.

7.1. Measurement of Resistances:

7.1.1. Measurement of Primary Resistances:

The primary resistance is measured using Kelvin's Double bridge. Since resistance is function of temperature, the measurements are carried out while the machine is hot and these hot values are used in calculation of machine characteristics.

$$R_1 = 5.1 \text{ Ohm.}$$

7.1.2. Secondary Resistance:

The effective (referred to primary) rotor resistance is found by usual short-circuit test and using the value computed of R_1 .

$$R_2 \text{ (referred to primary) } = 1.95 \text{ Ohm.}$$

7.2. TORQUE - SPEED CURVE:

By simple loading, the full range speed-torque curve can not be determined, since motor cannot develop more than the maximum torque and after that motor enters the unstable region. For this Ward Leonard speed control is adopted. In this the test machine is run by separately excited d.c. machine, the speed of which is controlled by another separately excited d.c. machine coupled to constant speed (synchronous motor) motor - This way speed from zero to synchronous is obtained. For accuracy sake, speed is recorded by sabbatroscope.

Since machine draws very high current at low speed and inverse rotation and cannot withstand it for longer time so proper arrangement for extra cooling are made.

7.3. RECORDING OF CURRENT CHARACTERISTIC

The current slip characteristic is recorded over the G.R.O. using the circuit shown in Fig. 7.4. For speed signal, a tachogenerator generating voltage proportional to speed is used and current being alternating is fed through a rectifier bridge to the y - Plate of the oscilloscope beam. The inductance in speed signal and current signal circuits are meant for filtering any undesirable alterations caused due to vibration etc. For the change in speed corresponding change in current is recorded. (See Photograph Fig. 7.5).

DISCUSSION OF THE RESULTS:

The evidence of fairly good agreement between experimental and theoretical results of current, power factors torque of skewed rotor induction machine justifies the belief that not only is the theory of harmonics and skew within its inherent limitations basically sound

but also that the methods, used for measurement of machine parameters are fairly accurate.

The discrepancy between the calculated and experimental curves may be due to the following reasons.

1. In calculating, it has been assumed that all the parameters are constant, but actually some parameters are dependent on the operating conditions (e.g., leakage reactance on current etc)
2. The Iron loss occurring in the motor could not be properly accounted.
3. Throughout, the frictional losses of d.c. machine has been neglected and that of induction machine assumed constant irrespective of speed.
4. Instrument errors and errors in recording might have introduced some deviation in the calculated and observed results.

Table 7.1. PERFORMANCE TEST OBSERVATIONS

Slip	speed	Current	Watts.	Voltage	P.f.	Stator Copper loss	(per phase) Power developed	M.L.
.03	1470	5.1	1276.0	440	0.95	81.5	1000	195
.05	1420	6.4	1502	440	0.93	127.0	1180	195
.08	1330	8.9	2035	430	0.92	294.0	1590	195
.12	1320	10.4	2391	430	0.92	410.0	1800	181
.17	1240	13.5	3035	423	0.89	835.0	1970	181
.20	1200	14.6	3190	426	0.87	1060	1930	180
.27	1100	16.8	3450	425	0.82	1430	1830	180
.30	1020	18.0	3600	425	0.82	1620	1830	180
.34	990	19.0	3930	420	0.83	1850	1800	180
.39	975	19.0	3930	440	0.75	1850	1600	180
.38	930	20.0	3635	440	0.715	2040	1400	195
.53	790	22.0	3665	440	0.69	2460	1210	195
.55	675	22.0	3745	440	0.67	2460	1090	195
.8	300	24.0	4125	440	.675	2940	990	195
1.0	0	24.0	-	440	-	2940	-	195
1.1	1350	24.0	4135	440	.675	2940	1000	195
1.2	1200	24.0	4095	440	.67	2940	960	195
1.3	1030	24.4	4050	430	.60	2940	935	195
1.4	900	24.9	4255	435	.67	3160	900	195
1.5	750	25.3	4075	435	.64	3020	860	195
1.6	600	26.0	4105	435	.63	2920	990	195
1.7	375	27.0	3900	430	.58	3000	705	195

TEST CURVES

FIGURE 7.1

- 1. — TEST TORQUE SLIP CURVE
- 2. — TEST CURRENT SLIP CURVE
- 3. — TEST POWER FACTOR SLIP CURVE

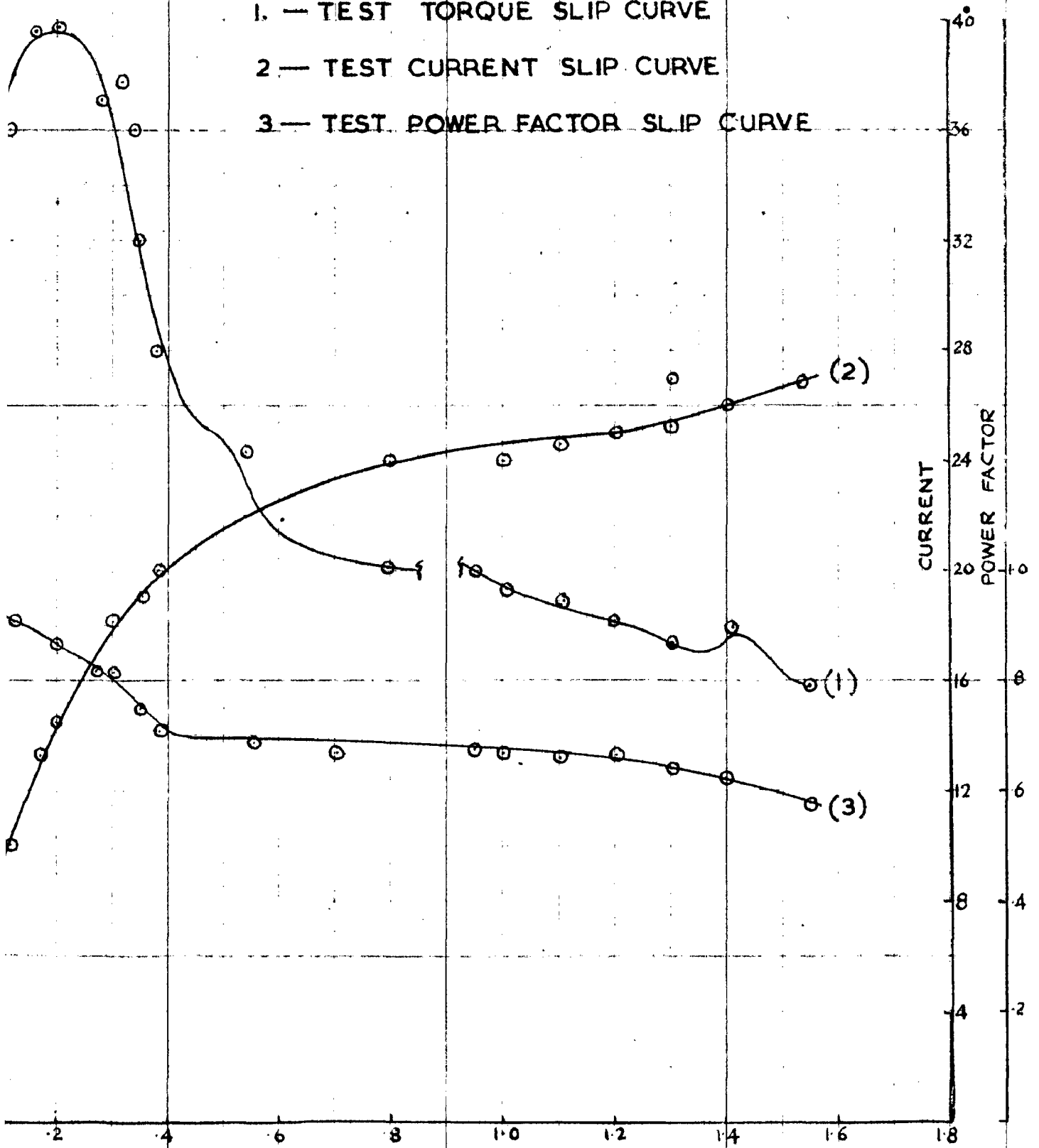
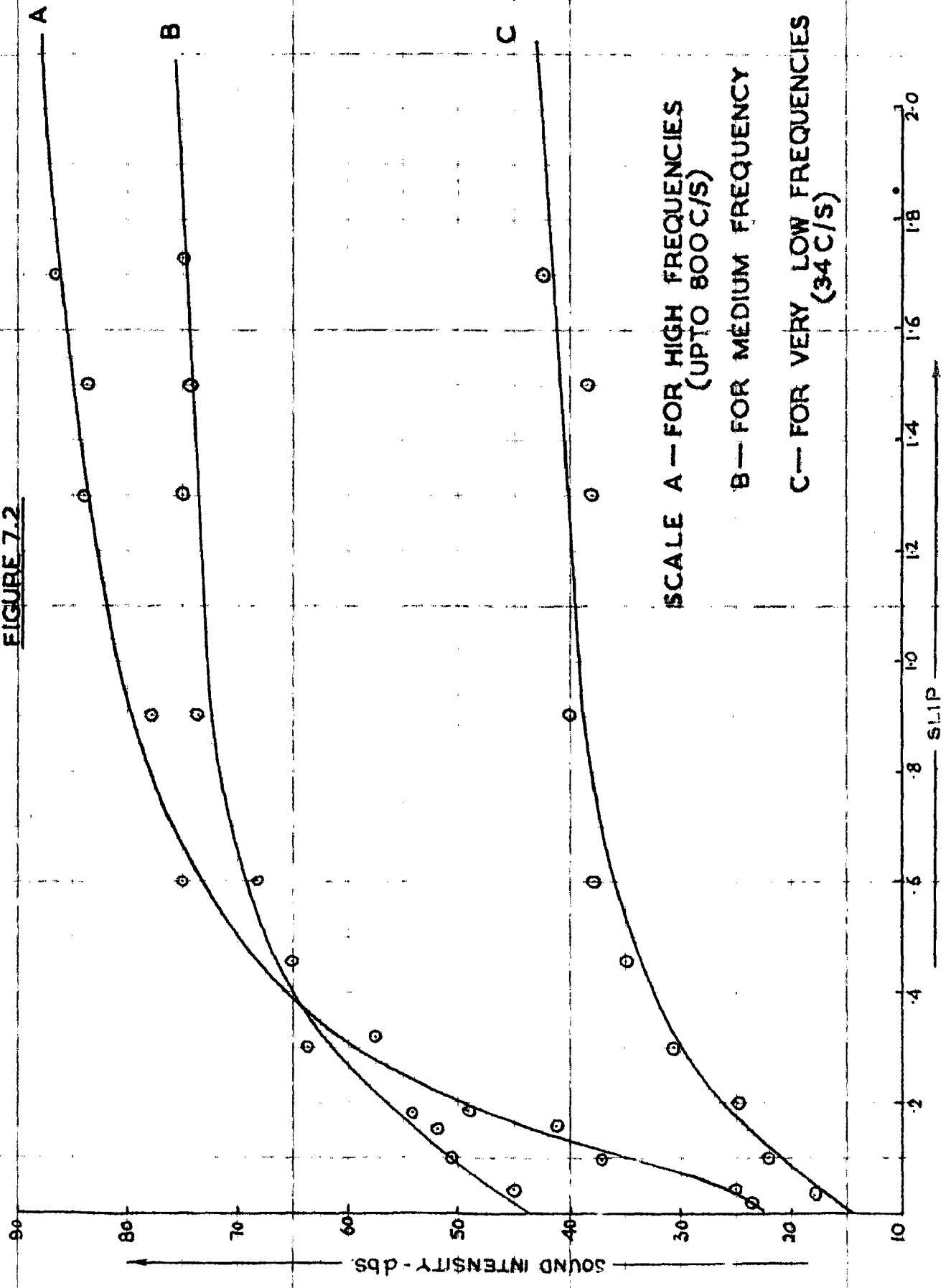


FIGURE 7.2



SCALE A — FOR HIGH FREQUENCIES
(UPTO 800 C/S)
B — FOR MEDIUM FREQUENCY
C — FOR VERY LOW FREQUENCIES
(34 C/S)

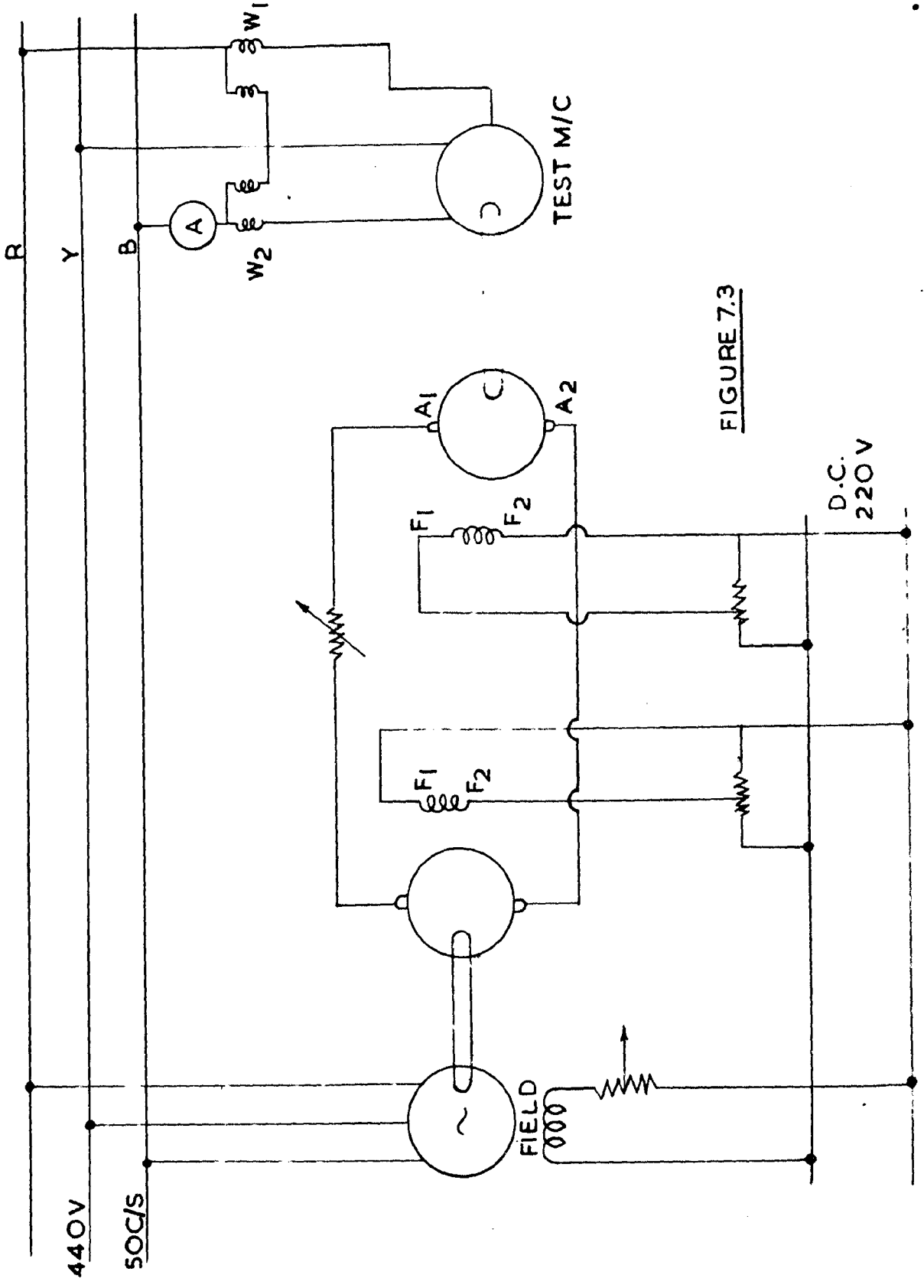


FIGURE 7.3

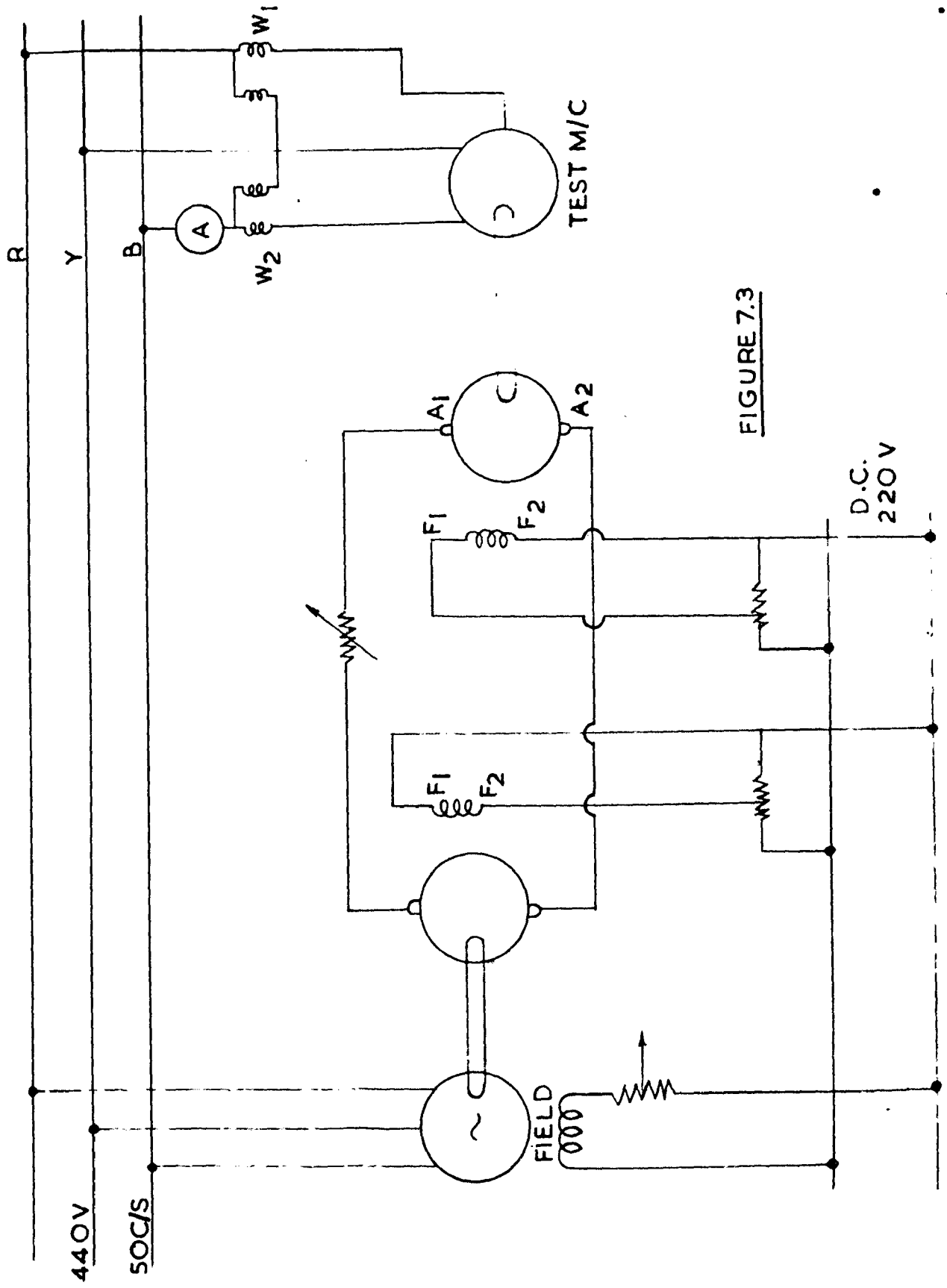
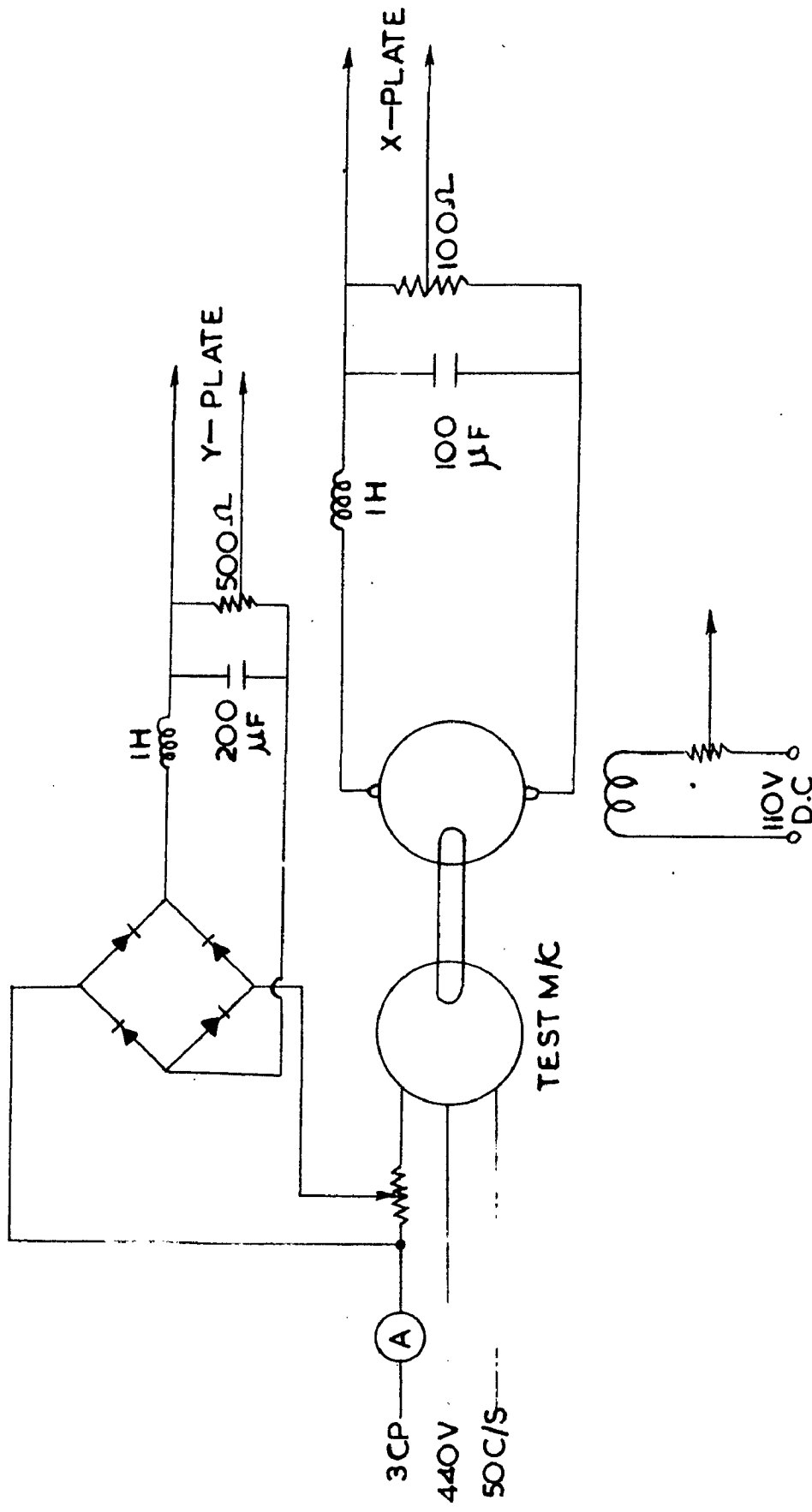
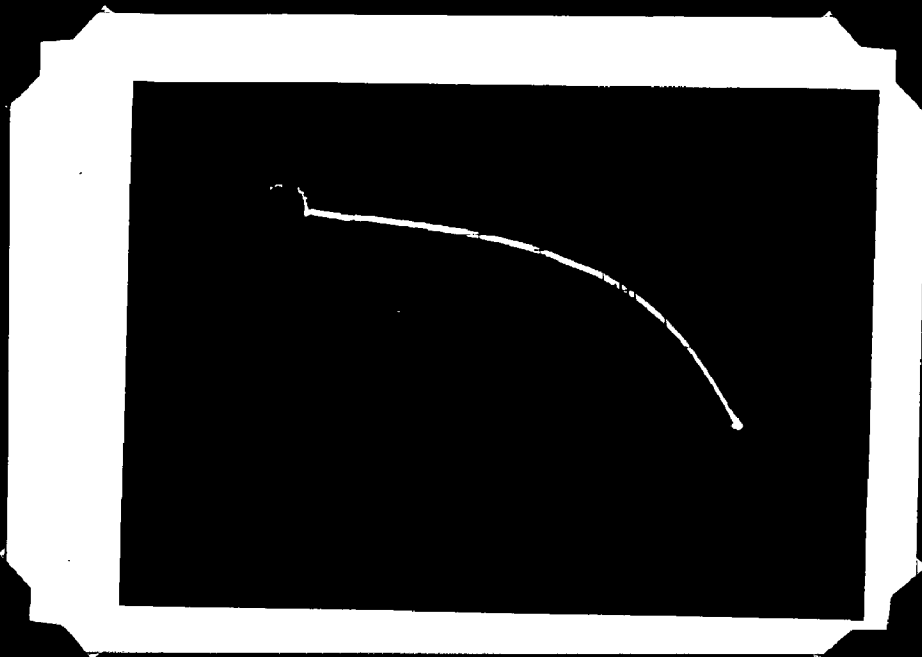


FIGURE 7.3



CIRCUIT FOR CURRENT RECORDING

FIGURE 7.4



Speed/current curve
(speed Zero to Syn)



CONCLUSION

The performance of a induction machine is considerably affected by the skewing of rotor bars. The fact is revealed by the comparison of the figures 3.4 to 3.10.

The skewing effects on the constants of the machine are very important as detailed out in theoretical consideration of Chapter II. Except for certain portion of leakage (slot leakage) all the other (harmonic differential leakage) rotor circuit constants are inversely proportional to the square of skew factor.

The equivalent circuit of Fig. 2.14, 2.15 provides an accurate picture of the harmonic fields phenomena and of skewing effect in a squirrel cage motor. Comparison of calculated and test results confirm the usefulness of this circuit in theoretical prediction.

The two sets of calculations carried out with and without skew angle of the rotor bar shows, that spiralling or skewing, of rotor bar of an induction motor increases the reactance and affects the performance e.g. reduction in starting current; reduction in dips, peaks of torque - speed curve; reduction in cusps, improvement in power factor; reduction in maximum torque; increase in starting torque, decrease in efficiency and increase in stray load losses; besides reducing the magnetic noise and vibrations. Methods for clearly visualising and calculating its effects have been provided which should be immediately useful in machine design.

It is shown that some motors, with good relation of number of slots can as well be adopted without skew as in case of test machine or any harmful harmonic can be skewed out by providing a proper skew (Fig. 6.8 A, B).

As discussed in Chapter VI, the parasitic torques and noise can be further reduced by skewing more the rotor bars. After a certain limit the performance ceases to make any substantial progress but, increases the cost of production quite comparatively.

The test machine is found to be 'Quiet' in working zone (high speed) and 'Noisy' at low speeds, producing high frequency noise. The noise being the complex function of magnetic fields and circuit constants, the exact behaviour of particular harmonic for variable skew cannot be predicted. However when noise level of 19th and 25th harmonic decreases with skew, the noise level of 5th harmonic increases considerably. So a compromise value of skew is to be selected in such cases.

It is shown (Fig. 6.8, & 6.9) that skewing of 5° to 20° (Elect.) is most proper range.

APPENDIX I

I-1 AIR GAP PERMEANCE EQUATIONS FROM CONFORMAL TRANSFORMATION THEORY

Equations derived from conformal-transformation theory have been used by E.M. Freeman⁽⁹⁾ to calculate the shape and hence the harmonic content of tooth ripple flux-density wave from large values for any value of s/g and $0 < s/\lambda < 0.8$ with the help of electronic computer.

The conformal - transformation holds good under the following assumptions:

- a. Curvatures of the surfaces of air gap is neglected.
- b. Depth of the slot has so little influence on the results that it can be considered infinite, this assumption is reasonable if $d > 1.65$
See Fig. (I-3).

Fig. (I-2) indicates values of Z - plane. The value 'a' is arbitrarily fixed but 'b' is not independent of a.

After going through the conformal transformation from one plane to another the flux density distribution in a plane is given by the following equation (See Gibb's book)

$$B = \frac{(1-w) B_{\max}}{\sqrt{(a-w)(b-w)}}$$

where w is the independent variable $a = 1/b$ and b is determined by the equation

$$\frac{b-1}{b^2} = \frac{1}{g}$$

The distance along the pole face is given in the form

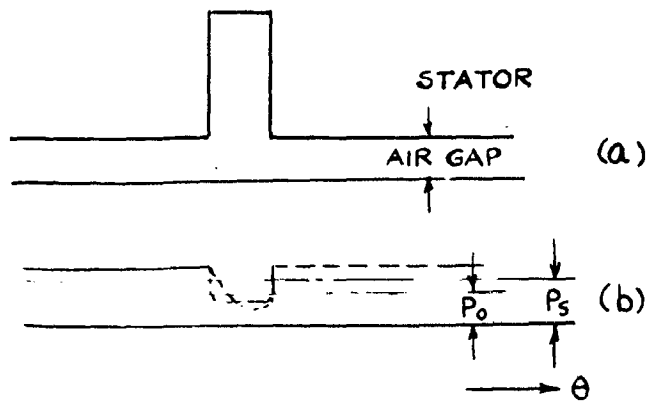


FIGURE I-1

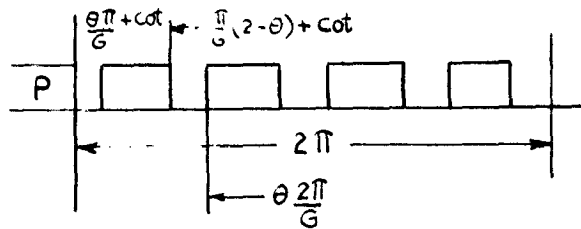


FIGURE I-2

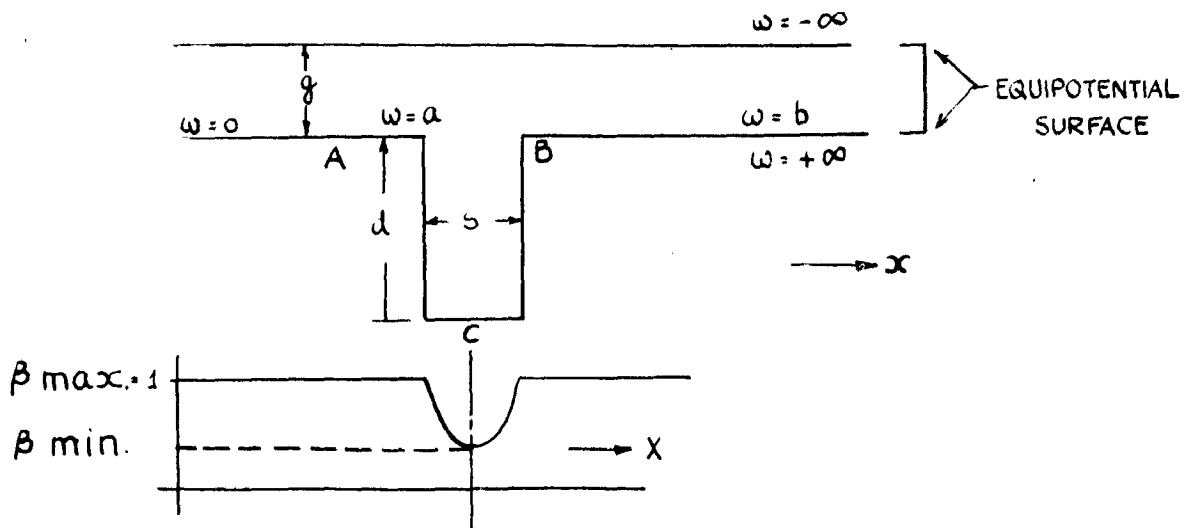


FIGURE I-3

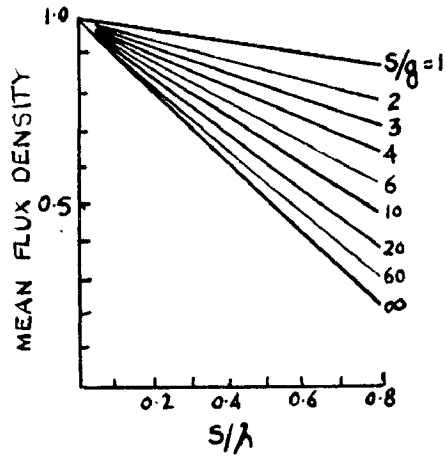


FIGURE I-4

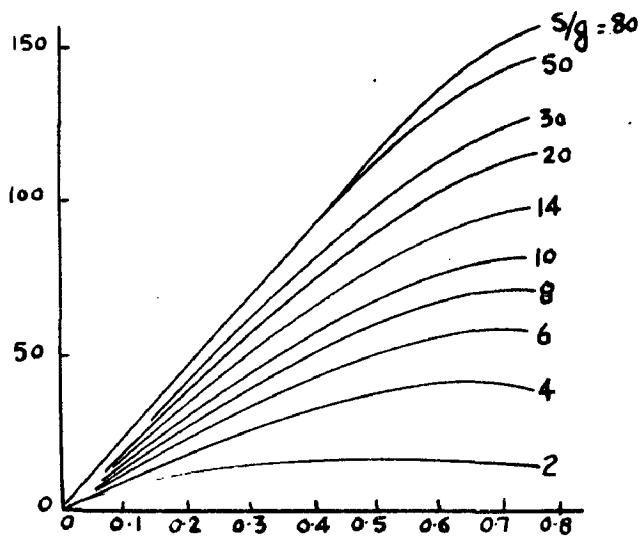


FIGURE I-5

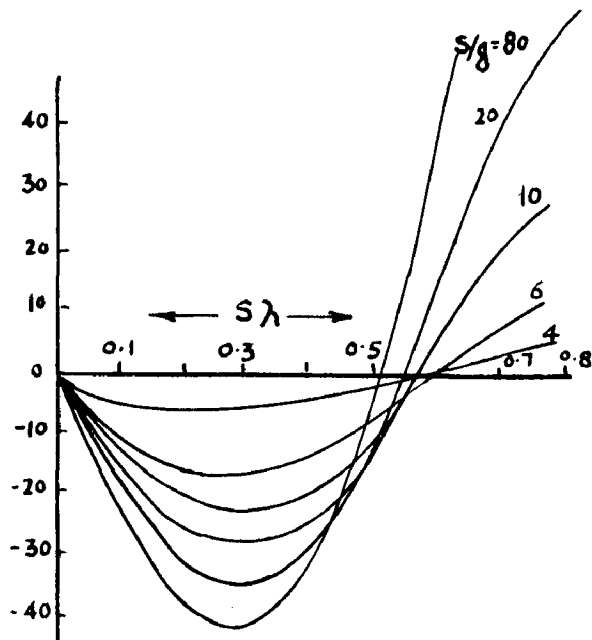


FIGURE I-6

$$x = \frac{K}{\pi} \left[+ \log_e \left| \frac{1+p}{1-p} \right| - \log \left| \frac{b+p}{b-p} \right| - \frac{2a}{\pi} \tan^{-1} \frac{p}{b+p} \right]$$

which is modified to

$$x = \frac{K}{\pi} \left[- \log_e \left| \frac{1+p}{1-p} \right| + \log \left| \frac{b+p}{b-p} \right| + \frac{2a}{\pi} \tan^{-1} \left(\frac{p}{b+p} \right) \right] - 0.55$$

$$\text{where } p^2 = \frac{b-w}{a-w}$$

The flux density curves taking B_{\max} unity have been calculated for different value of w beginning from -1 to smaller values. The values of B and x thus computed are then used in a harmonic analysis sub-routine to calculate the mean value of the flux density and the amplitudes of harmonics. The equation of flux density wave form may be written from section I-1 and I-2 as

$$B = \bar{B} \left(1 + \sum_{r=1}^{\infty} v_r \cos vR (x - wt) \right)$$

where \bar{B} = average mean flux density.

The extensive results obtained by Freeman are reproduced here.

APPENDIX II

(TO CHAPTER III)

II-1 HARMONIC LEAKAGE REACTANCE OF SQUIRREL CAGE WINDING WITH RESPECT TO

THE HARMONIC

From equation (1-19) the amplitude of m th mmf wave is

$$F(m) = 0.9 \frac{k}{m} \left(TP \frac{k_{wm}}{P} \right) I_1$$

If $m' = m \times p$ and $B(m') = .45 m_1 N_1 \left(\frac{k_{w1m}}{m'} \right) \frac{3.19}{1.8} I_1$

The corresponding flux is

$$\phi(m) = \frac{2}{\pi} \frac{T}{m'} L_g B_{m'}$$

It links with $N_1 k_{w1m}$ turns so flux linkage is

$$\mathcal{L}_{m'} = \phi(m) N_1 k_{w1m}$$

But harmonic leakage reactance is

$$X_{sl}(m') = 2 \pi f \frac{\mathcal{L}_{m'}}{2^{1/2} I_1}$$

$$\therefore X_{sl}(m') = 2 \pi f \frac{1}{2^{1/2} I_1} \sum \mathcal{L}_{m'} \times 10^{-8} \text{ Ohm / Phase.}$$

After simplifying it

$$X_{sl}(m') = \frac{5.2 m_1 f_1 N_1^2 T L_g \times 2.54 \times 10^{-8}}{P 1.8} \sum \left(\frac{k_{w1m}}{m'} \right)$$

Ohms / phase.

Similarly for Rotor winding $m_2 = Q_2$; $N_2 = \frac{1}{2}$ $k_{w2m} = 1$

$$X'_{m2(m')} = \frac{0.8R \ell_1 T^{L_0}}{P l'_g} K_{sm}^2 \times 2.54 \times 10^{-8} \sum_{v_2 \neq 0} \frac{1}{\left(\frac{v_2 R}{p} + 1\right)^2}$$

Ohm per bar.

Again the consideration of the magnetic energy in the gap yields a simple expression for the sum, as found by Lischits - Garik

if $\frac{2}{3} \leq (w/T) \leq 1$

and

$$\left(\frac{k_{w1m}}{m}\right)^2 = \frac{\pi^2}{18} \frac{(5q^2+1) - \left\{ 3q(e-q) + \frac{2}{3} \left[(e-q)/q \right] + (e-q)^2 - \frac{2}{3} \left[(e-q)^2/q \right] \right\}}{4q^2} - k_{w1}^2$$

Where e = chording angle of coil w = coil span = Pole pitch

q = Number of slots per pole per phase.

and also $\sum \left[\frac{1}{\left(\frac{v_2 R}{p} + m\right)} \right]^2 = \frac{1}{m^2} \left[\frac{1}{\left\{ \frac{e^2}{m} K_{sm}^2 \right\}} - 1 \right]$

$$E_m = \frac{\sin \frac{mp^\pi}{R}}{\frac{m \pi p}{R}}$$

$$\therefore X'_{m2(m)} = 0.80R \ell_1 \frac{L_0 T}{P l'_g} K_{sm}^2 \times 2.54 \times 10^{-8} \left[\frac{(mp^\pi)^2}{(R K_{sm})^2} \cos^2 \frac{mp^\pi}{R} - 1 \right] \frac{1}{m^2}$$

Referring it to primary side

$$X_{s2}(m) = \left\{ \left[\frac{m p^2}{R K_{Sm}} \csc \frac{m p^2}{R} - 1 \right]^2 \right\} \frac{X_{M(m)}}{\quad} \quad (\text{II-1})$$

Considering the harmonic chart (T (1-3)), the m th stator harmonic for example $m = 5$ produces row of rotor harmonics $n = 5, 29, 39, 63, 73$ ——— for $v_2 = 0, + 1, + 2$ etc. It will be shown in Chapter IV that any harmonic m produces with corresponding harmonic n , when $v_2 = 0$ a torque characteristic of the same shape as main wave., With respect to it, all harmonic pairs all produced for different value of v_2 constitute the harmonic leakage. Therefore directly the harmonic leakage reactance for permeance wave can be written as

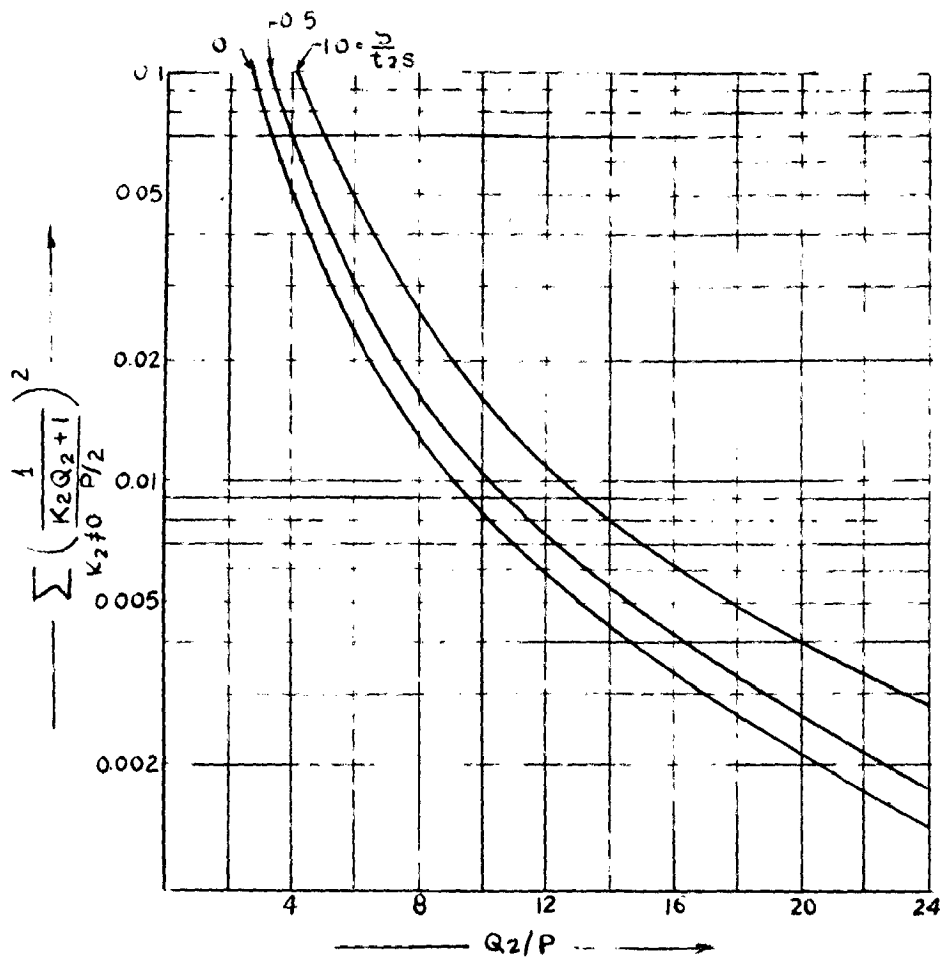
$$X_{s2}(mp) = \left\{ \left[\frac{(mp)p^2}{s K_{Sm}} \csc \frac{(mp)p^2}{s} - 1 \right]^2 \right\} \frac{X_{M(mp)}}{mp^2} \quad (\text{II-2})$$

II-2 SKIN EFFECT IN BARS OF SQUIRREL CAGE ROTORS:

The aim is to give an analytical solution for the skin-effect in the most used squirrel cage bars. This interests more to us, as our problem is directly linked with calculation of Parasitic torques. For this purpose the author is reproducing some of the recent work done by Licoschitz⁽¹⁵⁾ over straight simple bars of squirrel cage machine. For resistance:

$$\frac{\text{a.c. resistance}}{\text{d.c. resistance}} = \frac{R_{ac}}{R_{dc}} = \beta \quad (\Delta)$$

$$\text{Where } \beta \Delta = \frac{\Delta \sinh 2\Delta + \sin 2\Delta}{\cosh 2\Delta - \cos 2\Delta} \quad (\text{II-4})$$



HARMONIC DIFFERENTIAL LEAKAGE CURVE OF A SQUIRREL
CAGE WINDING

FIGURE II-1

FIGURE II-2

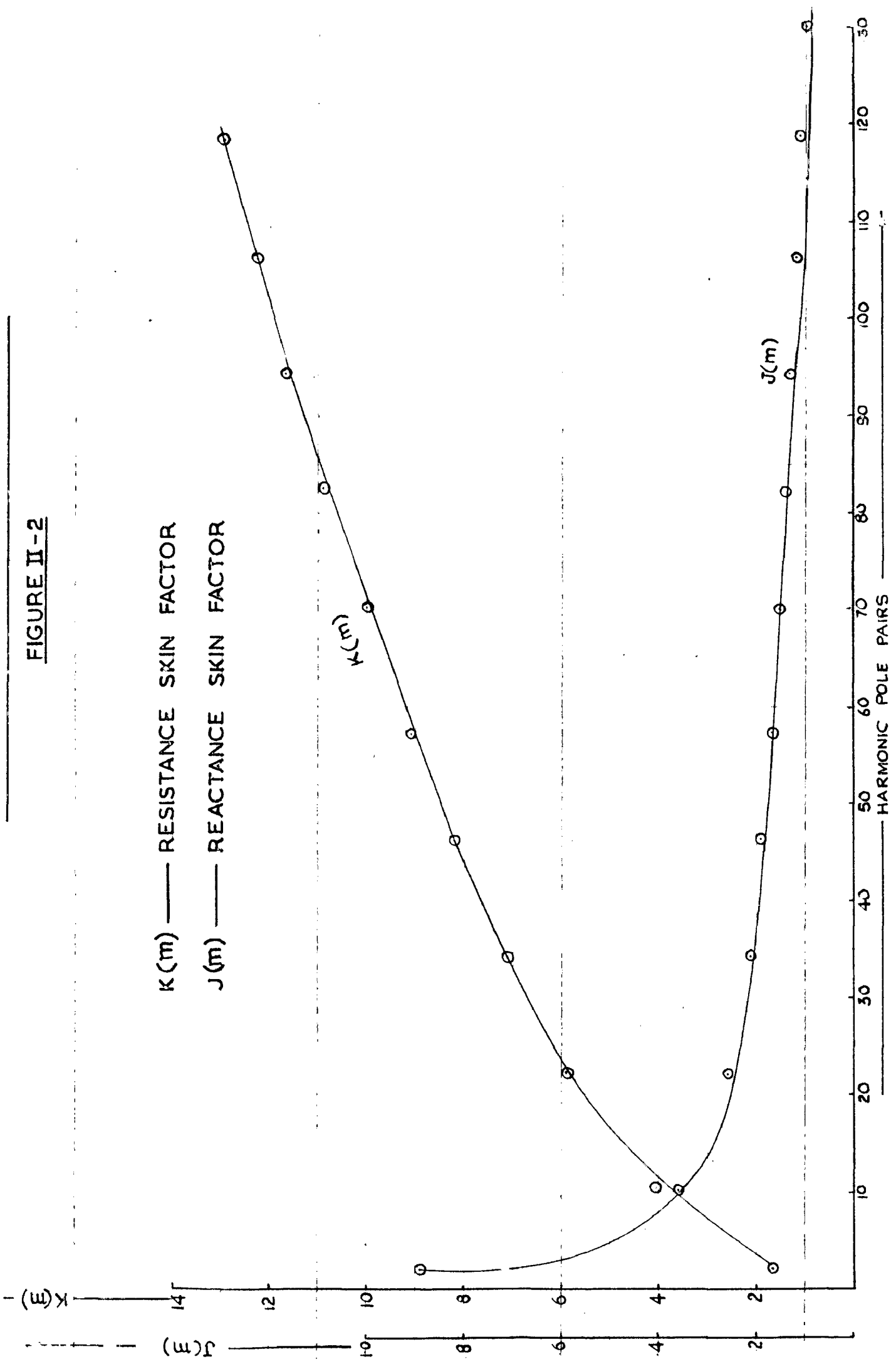
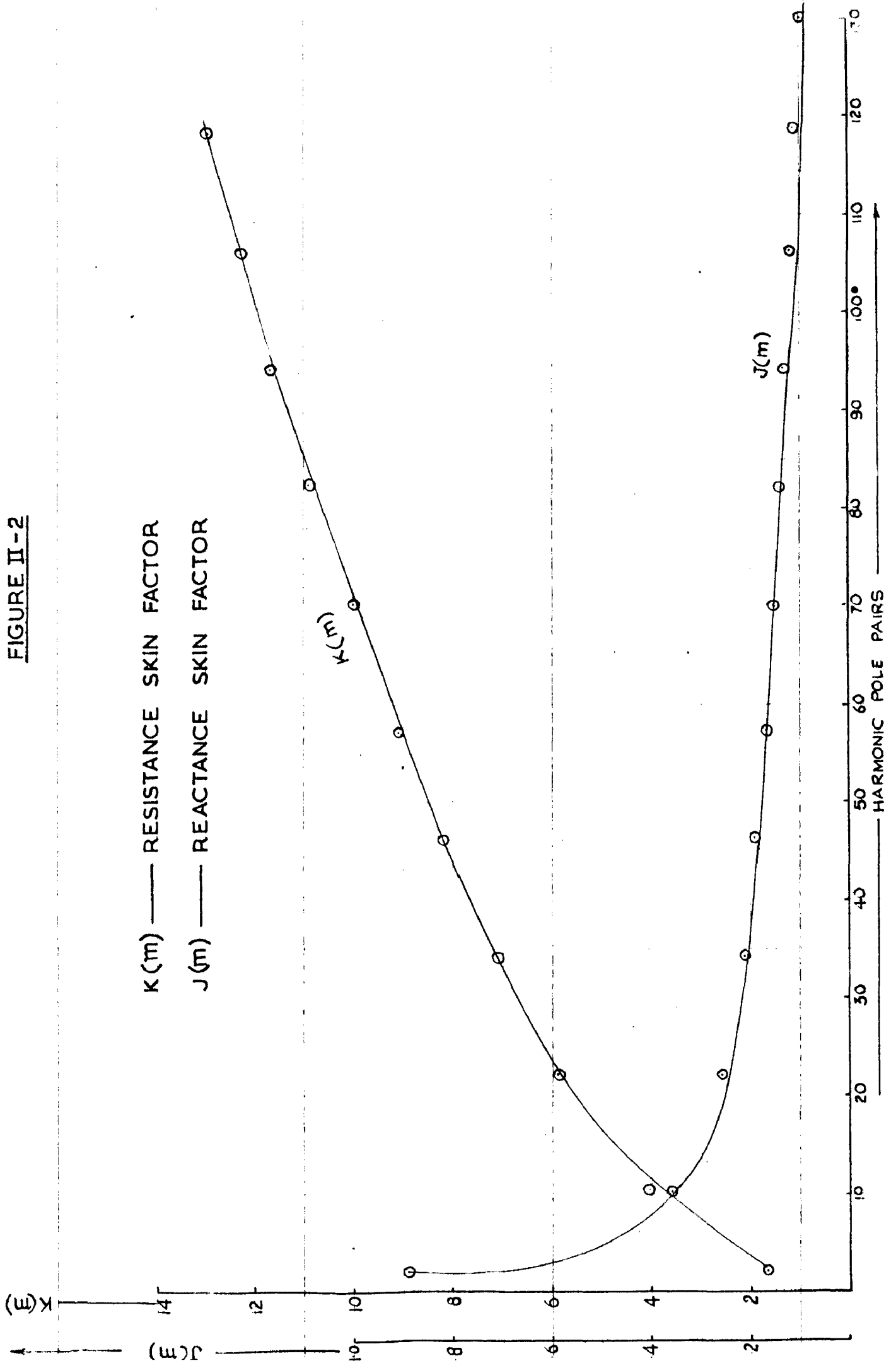


FIGURE II-2



and

$$\frac{l_{ac}}{l_{dc}} = (A) = \frac{\text{a.c. inductance}}{\text{d.c. inductance}} \quad \text{of bar.}$$

$$\text{When } (A) = \frac{3 \sin h 2A - \sin 2A}{2 A \cos h 2A - \cos 2A} \quad (\text{II-5})$$

$$\text{When } A = 0.316 h \sqrt{\frac{bb}{bs} \frac{f_1}{P} \frac{1}{S_m}} \quad (\text{II-6})$$

where

bb = width of bar

bs = width of slot

f_1 = line frequency

h = Height of bar

S_m = Slip of the rotor of mth wave.

P = Bar resistivity micro ohms per inch. putting the following values.

bb = 0.2 cms.

bs = 0.2 cms (approx.)

f_1 = 50 cFS

h = 2.0 cms.

S = Unity (for fundamental)

Values are tabulated in Table (II-1)

Table II-1 HARMFUL SKIN FACTORS FOR IONON RESISTANCE AND REACTANCE

α	1	5	7	11	15	17	19	23	25	29	31
$k(m)$	1.69	4.1	4.1	5.8	5.8	7.1	7.1	8.2	8.2	9.2	9.2
(m)	.895	.360	.36	.258	.258	.21	.21	.19	.19	.16	.16
α	35	37	41	43	47	49	53	55	59	61	65
$k(m)$	10.0	10.0	10.9	10.9	11.7	11.7	12.3	12.3	13.0	13.0	13.5
(m)	.15	.15	.15	.130	.138	.13	.13	.122	.122	.115	.105

APPENDIX III

SAMPLE COMPUTER PROGRAMMES ARE PRESENTED HERE

III - 1 SOLUTION OF CIRCUIT

```
C C   OPQ
      DIMENSION R(30), G(30), H(30), T(30)

      DO 37 J = 1,5    § J2 = 3 * J    § J1 = J2 - 2
37    READ 38, (R(K),G(K),H(K)) K = J1,J2 )
38    FORMAT ( 3 (F 7.5, F7.5, F7.5))

      READ 39, V
39    FORMAT (F 7.3)

      S = 0.05 §

200   T(1) = S § T(2) = 6.-5T § T(3) = 7.*S - 6.
      T(4) = 12. - 11.*S § T(5) = 13.*S - 12 § T(6) = 18.-17.*S
      T(7) = 19.*S = 18. § T(8) = 24.-23.*S § T(9) = 25.*S -24.
      T(10) = 24.-23.*S § T(11) = 25.*S -24. § T(12) = 48.-47.*S
      T(13) = 49.*S - 48.

      X1 = 5.0
      Y1 = 3.9

      DO 41 I = 1, 13 § A = R(I) /T(I) § B = G(I) + H(I)
      C = A * A + B * B § X = A * GI * GI/C
      Y = (A*A*G(I)) +G(I)*H(I)*B/C

      X1 = X1+X § Y1 = Y1 + y §

41    D = SQRT(X1 *X1*Y1*Y1)
      E = V/D § F = X1/D

      PUNCH 60, S, X1 , Y1 , E , F.
```

Appendix III

```

60      FORMAT (F4.2, 4 F 10.4)
        S = S + 0.05  $ IF (S-2.0) 200,200,201
201     STOP
        END

```

DATAS

1.930	141.250	2.830	.600	0.260	0.054	0.460	0.077	0.038
0.520	0.020	0.020	0.520	0.014	0.020	0.0750	0.013	0.035
1.0	0.018	0.070	0.0	0.261	1.880	6.0	0.221	2.480
1.930	0.261	01.380	1.930	0.221	1.980	1.930	0.062	1.360
1.930	0.058	1.160						

V = 254

III -2 SYN. TORQUES WITHOUT SKEW

```

CC      O.P.GARG - SYN. TORQUES. W.O. SKEW
        DIMENSION R(20), G(20), H(20), Z(25), P(25) L(20), T(20), E(20)
        DO 37 J = 1,5 $ J2 = 3 * J $ J1 = J2-2
37      READ 38, (R(K),G(K),H(K),K = J1, J2)
38      FORMAT (3 (3F 7.0))
39      READ 36, (L(I) I = 1,.15)
36      FORMAT (15I 5)
        DO 49 J = 1,2 $ J2 = 11 * J $ J1 = J2 - 10
49      READ 48, (Z(I), I = J1, J2)
48      FORMAT ( 7 (2F 4.0) )
        S = 1.06

```


REFERENCES

BOOKS

1. Langsdorf, A.S. Theory of Alternating Current Machinery Wiley, 1955.
2. Puchstein, A.F.; Uoyd, T.C.; Conard, A.G., Alternating current Machine, 3rd ed, Wiley 1954.
3. Alger, P.L. Nature of Polyphase Induction Machines Wiley, 1951.
4. Kron, G., Equivalent circuits of Electric Machinery, Wiley, 1951.
5. Liwchits, -Garik, M. Alternating current machines Van Nostrand, 1961.

ARTICLES

- 6 Harrison, The similarities of Electrical Machines when operating in the Balanced Steady State condition. International Jr. of Elect. Engineering Education V 3, n1 p. 49, May 1965.
7. Robinson , R.B., Inductance Coefficients of Rotating machines expressed in terms of winding space harmonics, Proc., Inst. Elect. Engrs, (GB) VIII, n4, p 769-74 , April 1964.
8. Stray losses in squirrel cage induction motors . Validity of reverse rotation test method. Proc. IEE(GB) V110, n10, p. 1773-7, Oct, 1963.
9. Robinson, Harmonics in a.c. Rotating machines , Proc. IEE, Pt. C, p. 380, 1962.
10. Greaheal, T.D., Determination of General Equivalent Circuit by AIEE Trans. V. 80, Pt. 3 P, 548, Oct, 1961.
11. Odok, Stray load losses and stray torques in induction machines, AIEE Trans. Pt. 3, V. 77, p. 43-53, 1958.
12. Liwchitsy Garik, M, Harmonics of the salient - Pole synchronous machines and their effects. Pt. II Synchronous torques AIEE Trans. Pt. 3, V. 76 p. 275-81, June 1957.
13. Liwchits-Garik, M, Harmonics of the salient pole synchronous machine and their effects Pt. 1st MMF harmonics produced by armature AIEE Trans. Pt. 3, V. 75, p, 35, April 1956.
14. Linkous , C.E., Effect of skew on induction motor magnetic fields

- 15(contd.) AIEE Trans. V. 74, Pt., 3 no. 19, p. 760-5, August, 1955.
15. Liwshitz-Garik, M, Computation of skin effect in bars of squirrel cage rotor AIEE Pt. 3, V. 74, p. 768-71, 1955.
16. Hearts, Saunders, Harmonics due to slots in Electric machines by AIEE Trans, Pt. (3-A) V. 73, p. 946-9, 1954.
17. Alger, P.L.; Pan, G.H; Ku, Y.H., Speed-Torque calculations for Induction motors AIEE Trans. Pt (3-A), V 73, p. 151, 1954.
18. Alger, P.L., Induced high frequency currents in squirrel cage windings AIEE Trans, V. 77, p. 724, 1957.
19. Walker, Slot ripples in Alternator EMF, waves Proc. IEE, Pt. 2, V. 96, p. 81, 1949.
20. Lloyd, T.G.; Chang, Reactance of squirrel cage motors AIEE Trans Pt. 3, V. 66, p. 1349-55, 1947.
21. Liwshitz - Garik, Differential leakage with respect to fundamental and harmonic waves AIEE Trans. Pt, 3 V 63 p. 1139, 1944.
22. Graham, Q, Dead points in induction machines AIEE Trans, Pt, 3, V 59, p. 637-42, 1940.
23. Hasuni, Y, Synchronous crawling of induction motor, ETJ Pt. 3, V2, p 14-16, 1938.
24. Bahl, R.D., Skewed slots in Induction motors, Elect. Engineering V 50, p. 941-42, 1931.
25. Kron, G., Induction motor slot combinations AIEE Trans, Pt. 3, V 50, page 757, 1931.
26. Dreese, E.E., Synchronous motor effects in Induction machine, AIEE Trans, Pt. 3, V. 49, p. 1033, 1930.
27. Walker, J.H., Noise in Salient Pole machines, AEI Engg., n 12, p. 428-35, Dec., '61.
28. Walker, J.H., Open circuit noise in synchronous machines IEE Proc., Pt. A, n 36, p. 505-12, Dec, 1960.
29. AIEE Trans, Pt, 3, V. 77 no. 40 p. 1615, Feb, 1959.
30. Muster, D.F., Wolfert, G.L., Single Phase Induction motor noise - due to dissimetry Harmonics, AIEE Trans, Pt., 3 V 74, n. 22, p. 1365, Feb, 1955.

31. Wall, R.L., Sonance design of large induction motors AIEE Trans, Pt 3, V. 74, n 21 p. 1189-92, Dec, 1955.
32. Erdelyi, E., Predetermination of sound pressure levels of magnetic noise of polyphase induction motors. AIEE Trans, pt. 3, v. 74, n 21, p. 1269-80, Dec, 1955.
33. Alger P.L., The magnetic noise of Polyphase induction motors AIEE trans, Pt. 3, V. 73, n 11, p. 118-23, April, 1954.
34. Morrill, J, Harmonic theory of noise in induction motors, AIEE Trans, V. 59, p. 474-80, August 1940.
35. Ray, B.B., Noise measurement . The case of Rotating electrical machinery Electrician V. 115, p. 219-222, August 23, 1935.
36. Church B.G., King A.J., The measurement of Noise with special reference to Engineering Noise Problem. by IEE Journal V 75 p, 401-, 1934.
37. Hilderbrand, Y.L., Quiet induction motors, AIEE Trans, p. 848, 1930.
38. Chapman , F.T., The production of noise and vibration by certain squirrel cage induction motors, Jr, IEE , V. 61, p. 39-48, 1923.